ESTIMATION AND FATE OF NEW PRODUCTION IN THE MARINE ENVIRONMENT

A Dissertation

by

ALLISON SKINNER MCINNES

Submitted to the Office of Graduate and Professional Studies of
Texas A&M University
in partial fulfillment of the requirements for the degree of

DOCTOR OF PHILOSOPHY

Chair of Committee,	Antonietta Quigg
Committee Members,	Gilbert T. Rowe
	George A. Jackson
	Anja Schulze
Head of Department,	Debbie J. Thomas

May 2014

Major Subject: Oceanography

Copyright 2014 Allison Skinner McInnes

ABSTRACT

The fate of carbon in the ocean determines both the amount of CO_2 that can be sequestered and the amount of sustainable biomass. Compartmentalization into new and regenerated production allows a first order estimate of carbon available to the local community versus the amount exported. The goal of this project was to study sources and sinks of production in order to test the general hypothesis that new production is underestimated in the marine environment. Specifically we looked at pulsed new nutrients and the effect on the ecosystem, the effect of currents on our measurements and estimates of export (equivalent to new production), and finally development of a new method which will allow *in situ* determination of new production in the majority of the global ocean.

Specifically, the role of a Pacific herring spawn was investigated as an important stimulant to ecosystem wide carbon and nitrogen cycling in Simpson Bay, Alaska. A consistent pattern was observed each year: a large bloom in June corresponded to the timing of the herring spawn and low nutrients, low phytoplankton diversity, and high POC concentrations; elucidating a previously unidentified pulse of new nutrients to the system.

Estimates of carbon export are affected by the physical environment. The model presented and validated herein is used to improve our understanding of C export by including the effect of horizontal transport. We show that measurements of export to shallow water traps are less impacted by currents than deep traps. Spatial extent of

variable primary production necessary to affect deep water traps is greater, as such, over half of the traps analyzed in this study are affected by up-current productivity regimes.

A method to simultaneously quantify the C and N fixing community in the same sample was developed, eliminating many assumptions introduced when using different techniques and incubations. Cultured and environmental samples were successfully hybridized using TSA-FISH. Strong correlations between positively tagged community abundance and $^{14}C/^{15}N$ measurements are presented. The findings of this work support the general hypothesis that new production is under-accounted for in marine systems.

ACKNOWLEDGEMENTS

First, I would like to thank my chair, advisor, and mentor, Antonietta Quigg who trusted in my abilities and ideas. I would like to thank my committee members, Gilbert T. Rowe, George Jackson, and Anja Schulze, for their investment in me as a scientist through patience, guidance and support throughout the course of this research.

I was generously funded by NOAA, Sea Grant, Texas Water Development Board, Texas Institute of Oceanography, NSF, and the Texas A&M University Dissertation Fellowship.

The studies herein have corresponding manuscripts and I would like to acknowledge my co-authors on those manuscripts; without whom the work would not be as polished or strong. For chapter II, I would like to thank Clifton C. Nunnally for collecting additional data in Alaska. Further I would like to thank Gilbert T. Rowe and Randall W. Davis for their curiosity and initial push to learn more about the phytoplankton community in Simpson Bay, Alaska. I would especially like to thank Randall W. Davis for generously allowing me to stay at the field camp in Alice Cove. Further I would like to thank Kathryn Wheatly, Ryan Wolt, Ian Davis, Michelle Cortez, Olivia Lee, and Sylvia Osterrieder for their extensive help in the field. Funding for the study in Alaska was provided by travel grants from Erma and Luke Mooney, the Marine Biology Department at Texas A&M University at Galveston, and the Oceanography Department at Texas A&M University provided funds for travel to and from the field site.

For Chapter III, I would like to acknowledge my co-authors on the corresponding manuscript for the meta-analysis: Sam Dorado who confirmed and beautified my initial multivariate statistics, and Anya M. Waite who helped me to strengthen the manuscript. I would also like to thank George Jackson for discussions and for reading a very early form of this manuscript and pushing me forward. Further we had a lot of input from Zoe Finkel, Andrew Irwin and Peter Santschi who also critiqued early versions of this idea. I was supported by a NOAA grant early on and then during the final writing stages by a Texas A&M University Dissertation Fellowship.

For Chapter IV, I would like to thank Alicia Shepard for giving me the courage to jump into microbial work and for being my "blue water buddy," with whom I could bounce around ideas and trouble shoot the inevitable bugs that arise when employing molecular methods and flow cytometry. I would like to thank John Norman (Beckman Coulter) who was extremely helpful in setting up and trouble-shooting the flow cytometer. I acknowledge the facilities, scientific and technical assistance of the National Imaging Facility at the Centre for Microscopy, Characterization & Analysis, at The University of Western Australia, a facility funded by the University, State and Commonwealth Governments. I would also like to thank Mona Hochman of the Seafood Safety Lab for providing negative control cultures. I was also supported by the NSF East Asia and Pacific Summer Institute Fellowship in conjunction with the Australian Academy of Science during sample collection in the eastern Indian Ocean.

Finally, I would like to thank my husband, whose many iterations of edits for the chapters herein made each much stronger and more fluid. Thank you also for your patience and love through the entire process.

TABLE OF CONTENTS

LIST OF FIGURES

LIST OF TABLES

Page

CHAPTER I

INTRODUCTION AND LITERATURE REVIEW

Carbon (C) is the currency of the ocean; its importance is measured either through fisheries (average catch of 68 Mt yr^{-1} equating to primary production of 3.5 Gt C yr^{-1}; (Chassot et al. 2010), or carbon dioxide (CO_2) sequestration (~48% of anthropogenic CO_2 are sequestered by the oceans; (Sabine et al. 2004; Falkowski et al. 2003). The central bank of this currency is controlled by phytoplankton; primary production converts atmospheric CO_2 into organic carbon—the critical first step in making it biologically available or in sequestration.

There are three fundamental carbon ‗pumps' that act in the marine environment to entrain CO_2 from the atmosphere into the ocean: the solubility pump (driven by the partial pressure differential of CO_2 between the surface ocean and the atmosphere), the carbonate pump (export of $CaCO_3$ from the surface to the ocean interior), and the ―soft tissue" pump (driven by the food-web structure in the surface ocean) (Volk and Hoffert 1985; Longhurst and Harrison 1989). Sarmiento et al. (1995) refined this by combining the soft tissue and carbonate pumps into the ―biological pump" denoting all carbon captured via biological processes. Because phytoplankton respond rapidly to changes in the environment, the biological pump is crucial to understanding carbon export on time scales relevant to society (Longhurst and Harrison 1989).

The range in the estimates for the amount of CO_2 uptake by the oceanic pumps is greatest for the biological pump, 2-55 Pg C yr^{-1} (Dunne et al. 2005; Behrenfeld et al.

2006). The range highlights the uncertainty in our knowledge of this oceanic sink. The general understanding of the biological pump at present is that 4-36% of primary production is exported from the photic zone, of that, 0.4% is collected in bottom sediment traps at ~4500 m, and as little as 0.004% buried in the sediments (Gardner 1997).

The efficiency of the biological pump is mediated by a number of interacting factors which can generally be divided into production, sinking, and decomposition. Initial net primary production dictates the starting value of particulate organic carbon (POC) to be processed, either remineralized or exported. The initial phytoplankton community composition will strongly influence the particle type, sinking velocity (Finkel 2007; Guidi et al. 2009), and lability (susceptibility of remineralization/consumption) of POC. Modification of sinking POC through the water column via aggregation/disggregation (Burd and Jackson 2009), repackaging into fecal material (Wilson et al. 2008), and ballasting (inclusion of various minerals into particulates, Armstrong et al. 2002; Francois et al. 2002) affects sinking velocities and thus the amount of time particles are subject to processes controlling remineralization. Decomposition (refractory DOC production or incorporation into biomass) is the only factor that directly reduces the POC flux to depth (Jackson and Burd 2002). This factor is driven by settling velocity (De La Rocha 2007), surface and mesopelagic food web composition (Legendre and Rivkin 2002; Buesseler et al 2007) and food chain length (more trophic levels correspond to more loss) as well as microbial degradation (Azam

1998). All of these factors affect "the Martin curve" which is used by modelers to describe the attenuation of POC through the water column (Martin et al 1987).

Due to the inherent complexity of the biological pump it is difficult to determine the amount of primary production that is utilized/entrained in the pelagic food web and that which is available for export to the deep sea. Compartmentalization of production based on the source of nitrogen provides a framework for conceptualizing the potential fates of fixed carbon. Primary production can be 'classified' by the corresponding source of nitrogen (Dugdale and Goering 1967). Production fueled by external sources (new) can be exported; production using recycled N remains in the system. The sum of new production and regenerated production equals total production. Thus, the f-ratio (the fraction of primary production from new inputs of nitrogen) of Eppley and Peterson (1979) was an early effort to estimate export production (difficult to measure) from measurements of new production (measurable).

The research discussed herein will attempt to understand the efficiency of the biological pump; **the general hypothesis of this work is that new production is under accounted for in marine systems.** We address this by elucidating the fate and effects of new nutrients to the food web, enhance our understanding of the export of C from the surface ocean by inclusion of the effect of horizontal transport of C, and develop a method to simultaneously estimate total and new production in a sample allowing determination of the fates of fixed C.

In **Chapter II**, annual spawning events of various organisms provide important pulses of particulate and dissolved organic nutrients to ecosystems; by definition these

inputs are ―new" to the system. Ecosystems that receive natural resource subsidies (new nutrients) often exhibit elevated biomass (Polis 1997); and these resource pulses have legacy effects that can persist from months to years after the initial pulse (Yang et al. 2008). Thus, resource pulses may be an important contributing factor to sustained abundance and diversity of this ecosystem. We investigated the role of Pacific herring (*Clupea pallasii*) spawn as a similarly important stimulant to ecosystem wide carbon and nitrogen cycling in Simpson Bay, a shallow fjord in Prince William Sound (PWS), Alaska. Dissolved nutrients, phytoplankton community composition (pigments), particulate organic carbon and nitrogen (POC/N), and export to locally-deep water (total particulate reaching 20 m and 40 m) were measured during the summers of 2008-2010. In addition, natural abundance stable isotopes ($\delta^{13}C$ and $\delta^{15}N$) were measured in the particulate matter and select resident fauna in 2010. A consistent pattern was observed each year: a large *Noctiluca* sp. bloom in June (low nutrients, low phytoplankton diversity, and high POC concentrations) corresponded to the timing of the herring spawn. Our results indicate that marine derived nutrients, introduced into the local environment by the herring spawn and entrained by a *Noctiluca* sp. bloom, represent an important pulse of nutrients in Simpson Bay. These previously overlooked effects of resource pulses may be an important contributing factor to the sustained abundance of higher trophic levels in this ecosystem.

In **Chapter III**, classification of new and regenerated production allows estimates for quantification of export and sustained production. Currently our calculations of export do not match our estimates based on new production. Accurate

estimates of particle flux are essential for global biogeochemical models. There are multiple ways to estimate or directly measure this flux; the fundamental assumption in all approaches is that particles move vertically. Here we present a simple model that can be used to estimate the potential horizontal movement of particles as they settle through the water column, improving our understanding of sources, fates, and percentages of particle flux. We demonstrate the validity of this model using two global publicly available data sets. In order for currents to modify export, primary productivity must be spatially variable. We demonstrate that shallow water traps are less affected than deep traps, due to the short time that particles remain in suspension. However, in areas of fast currents and highly variable primary production, such as the Arabian Sea during the SW monsoon, export flux can be modified even in shallow traps. The spatial extent of variable primary production necessary to affect deep water traps is greater, thus over half of the traps analyzed in this study are affected by up-current productivity regimes. This discrepancy has many implications including estimation of deep sea faunal biomass, diversity, and distribution. Further, this provides a mechanism to explain the now understood greater efficiency of the oceanic biological pump in sequestering atmospheric carbon.

In **Chapter IV**, understanding the connectivity of oceanic carbon and nitrogen cycles, specifically carbon and nitrogen fixation, is essential in elucidating the fate and distribution of carbon in the ocean. Traditional techniques measure either organism abundance or biochemical rates. As such, measurements are performed on separate samples, at different time scales and using different technologies. This study developed a

method to simultaneously quantify the microbial population (including autotrophs and heterotrophs) while estimating rates of fixation across time and space for both carbon and nitrogen fixation. Tyramide signal amplification (TSA) fluorescence *in situ* hybridization (FISH) of mRNA for functionally specific oligonucleotide probes *rbcL* (RUBISCO, primary production) and *nifH* (nitrogenase, nitrogen fixation) was optimized and combined with flow cytometry. Cultured samples representing a diversity of phytoplankton (cyanobacteria, coccolithophores, chlorophytes, diatoms and dinoflagellates), as well as environmental samples from the open ocean (Gulf of Mexico, USA) and south eastern Indian Ocean (Australia) and a coastal system (Galveston Bay, Texas, USA) were successfully hybridized in the optimization of this method. Strong correlations between positively tagged community abundance and $^{14}C/^{15}N$ measurements are presented. I propose that these methods can be used to estimate C and N fixation in environmental communities. Utilization of mRNA TSA-FISH to detect multiple active microbial functions within the same sample will offer increased understanding of the connectivity between important biogeochemical cycles in the ocean.

CHAPTER II

ECOSYSTEM RESPONSE TO A PULSE OF MARINE DERIVED NUTRIENTS

Introduction

Prince William Sound (PWS), Alaska, has many commercially important fisheries (including five species of salmon, Pacific halibut, Pacific cod and several shellfish species), abundant marine mammal populations (including humpback, sei, fin, minke, and killer whales, sea otters, harbor seals, and Steller sea lions), and a great diversity of birds (220 species; Alaska Department of Fish and Game; http://www.adfg.alaska.gov/index.cfm?adfg=animals.main). The biological mechanisms that support these populations are not completely understood. This uncertainty is further complicated because nutrient and plankton dynamics are tightly coupled to the physical conditions in this area (Eslinger et al. 2001; Childers 2005; Quigg et al. 2013), which is downwelling dominated (Childers 2005). The system is well mixed in the fall and winter, replenishing the surface water with nutrients. The water column begins to stratify in the spring as a result of inflow of freshwater and surface warming. Short, intense spring blooms occur during calmer spring seasons; stormier springs lead to increased mixing and delayed stratification, resulting in a longer, less intense bloom, with much of the primary production transferred up the food chain (Eslinger et al. 2001).

Ecosystems that receive natural resource subsidies often exhibit elevated biomass (Polis et al. 1997); resource pulses have legacy effects that can persist from months to years after the initial pulse (Yang et al. 2008). Thus, resource pulses may be an

important contributing factor to sustained abundance and diversity of this ecosystem. Traditionally, allochthonous nutrient subsidies were thought to travel unidirectionally from upstream rivers to marine environments (Leroux and Loreau 2008) via runoff and/or fluvial systems. However, many recent studies have shown allochthonous subsides in the reverse direction - from open ocean to coastal systems (Helfield and Naiman 2001; Varpe et al. 2005; Leroux and Loreau 2008; Petticrew et al. 2011). The effect of these pulses relates to the amount of nutrient input relative to the area of the aquatic system receiving them, and the permeability of the ecosystem subsidized (Polis et al. 1997). For example, many salmon in small streams have a large effect that spreads into the riparian forests that surround these streams (Helfield and Naiman 2001; Chaloner et al. 2002; Hicks et al. 2005; Chaloner et al. 2007). Additionally, ecosystems with large areas, with less defined boundaries, have also been shown to benefit from seemingly small pulsed subsidies (eg. coral reef spawn Wild et al. 2008; Eyre et al. 2008; Guld et al. 2008).

Many resource subsidies have been identified in the PWS system. In particular, spawning salmon contribute to stream, river, and surrounding forest ecosystem productivity (Bilby et al. 1996; Wipfli et al. 1998; Hicks et al. 2005; Reisinger et al. 2013). Pacific herring spawn and spawning aggregations have been shown to be important to many vertebrate species, including the resident sea otter population in Simpson bay (Lee et al. 2009). More than 30 bird species have also been documented as predators of spawning herring and herring eggs (Roper et al. 1999; Willson and Womble 2006). Consumers that are capable of rapid growth and are the direct beneficiaries of the

pulse-supplied nutrients show the most rapid and the greatest numerical response, whereas those with slower growth rates and more trophic steps away from the level of the pulse show smaller changes with increased time lag (Chaloner 2007; Anderson et al. 2008; Yang et al. 2008; Weber and Brown 2013), making identification and quantification of pulse impacts difficult. While much research has been conducted on the ecosystem of this region, a paucity of literature is available on phytoplankton community and dynamics, which may be the immediate beneficiaries of many of these subsidies and show the largest and most rapid responses (Yang et al. 2010).

This study investigated the summer phytoplankton community composition and production in an effort to understand the base of the food web that supports the high biological productivity in this system beyond the spring bloom. We determined the intra-seasonal variability in the phytoplankton community (using 16 pigments as biomarkers), dissolved inorganic nutrients, particulate organic carbon and nitrogen (POC/N), and export (total particulate reaching 20 m and 40 m) in the summers of 2008-2010, plus faunal samples for stable isotope ($\delta^{13}C$ and $\delta^{15}N$) analysis in 2010.

Methods

Study Area. Simpson Bay (Figure 2.1) is a shallow fjord in eastern PWS that consists of three distinct basins (Figure 2.1) based on geomorphology and freshwater inflows (Noll et al. 2009). North Bay is 4 km long by 0.70-1.3 km wide with a maximum depth of 85 m. The hydrography of North Bay is substantially influenced by freshwater inflows (watershed: basin surface area ratio of 20:1). West Bay is the largest (4 km long

by 2 km wide) as well as the shallowest (25-55 m) of the three sub-bay systems. West Bay exchanges directly with PWS and has the smallest input of freshwater (from shoreline creeks) with a watershed/basin surface area ratio of 1:1. East Bay also exchanges directly with PWS; it is 4 km long and 2 km wide at the head, narrowing to 1 km wide at the mouth and has a watershed/basin surface area ratio of 7:1. Differences in watershed/basin surface area ratios directly impact freshwater input, sediment load, and organic matter input.

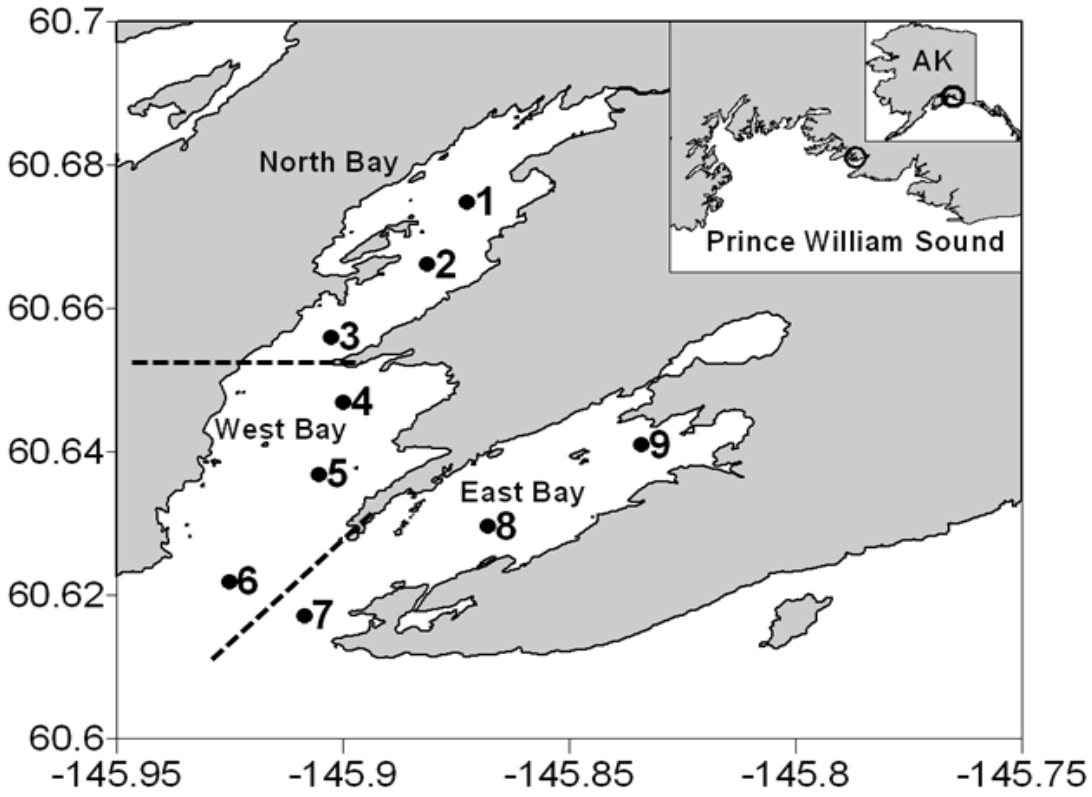

Figure 2.1: Map of study area with station locations. Insert of location within Prince William Sound and the state of Alaska. Locations of all sampling stations throughout the three summers are shown by numbers 1-9. Sub-bay divisions determined by watershed to basin surface area ratio are also marked on the map.

Sampling in 2008 & 2009. Sampling was designed to examine intra-seasonal (June, July and August) variability in phytoplankton community composition between the three sub-bays of Simpson‘s Bay. Water samples were collected at the surface and 10 m at nine stations (3 in each sub-bay; Figure 2.1). Samples were processed for chlorophyll (chl) *a*, pigment analysis, dissolved nutrients, particulate organic carbon (POC), particulate organic nitrogen (PON), particulate carbon (PC), and particulate nitrogen (PN). Samples were collected for microscopic confirmation of the reoccurring *Noctiluca* sp. bloom each summer.

Vertical Export. Sediment traps (1 m tall, 8 cm center diameter with a honeycomb baffle at the top to reduce loss from resuspension) were suspended 20 m and 40 m below surface. Traps were deployed once each month (one set in each bay) for 48 hrs (Figure 2.1). After recovery, material in the traps was allowed to settle for 4-6 hrs before the top water was poured off (via a hole in the trap) leaving the concentrated sample (1.5 L) in the bottom. Samples were filtered for chl *a*, pigments, total suspended solids (TSS), and POC, PON, PC and PN. Hereafter we refer to the average amount of material collected in sediment traps divided by area of trap opening and the number of days deployed as export.

Sampling in 2010. The 2010 summer sampling sought to determine pathways of carbon through the lower portions of the food web in Simpson Bay. Water samples were collected before, during and after the annual summer *Noctiluca* sp. bloom and analyzed for pigment composition, chl *a*, stable isotopes ($\delta^{13}C$ and $\delta^{15}N$) and dissolved nutrients.

Size fractionated plankton samples were collected using a 64 μm mesh plankton net then fractioned using a 118 μm mesh sieve; material remaining on the sieve were transferred/filtered onto 25 mm precombusted (500ºC, 5 hrs) Whatman GF/F (> 118μm sample). Material that passed through the sieve was transferred onto a separate 25 mm precombusted Whatman GF/F (< 118μm sample).

Butter clams (*Saxidomus giganteus*), Pacific blue mussels (*Mytilus trossolus*), juvenile herring, and herring roe were collected for stable isotope ($\delta^{13}C$ and $\delta^{15}N$) analyses. Clams were collected from mean tide line < 25 cm deep. Shells were removed and the samples were rinsed with filtered sea water (< 0.7 μm), then frozen. Mussels were collected from rockweed (*Fucus gardneri*) in the intertidal zone and were processed in the same manner as the clams. Herring muscle tissue was collected from beached fish, filleted, rinsed with filtered sea water and frozen. Herring roe attached to eel grass in the subtidal zone was removed and placed on 118 μm mesh sieve and rinsed with filtered sea water. All samples were stored frozen in the field until transported to the lab where they were stored at -80ºC until analysis.

Particulate Carbon and Nitrogen Analyses. Samples for particulate organic C and N were collected on filters (13mm Gelman filters, precombusted at 600ºC for 4 hrs) using gentle vacuum filtration and frozen prior to analysis on a Perkin-Elmer 2400 CHNS analyzer. Filters were dried for 24 hrs at 60 ºC, then acidified by placing samples in a desiccator with 8N HCl for 24 hrs, and subsequently dried for another 24 hrs. Dried, acidified samples were weighed (precision to 0.01 mg), packed in tin capsules, and run. Calibration curves were prepared prior to starting a batch of samples, and an acetanilide

standard (C 71.09%, N 10.36%) was run after every 10 samples to monitor machine drift ($StdDev_C$ <1.5%, $StdDev_N$ <0.25).

Pigment Analysis using High Performance Liquid Chromatography (HPLC). Prior to solvent extraction, filters were lyophilized (-50 °C, 0.57 mbar, 12h; Labconco FreeZone 2.5). Pigments were extracted using 90% acetone (500µl) at -20 °C for 18-20 h. Synthetic carotenoid β-apo-8‘-carotenal was added (Sigma, cat. No. 10810; 50 µl) as an internal standard. After extraction the sample was filtered through a 0.45 µl PTFE filter (Gelman Acrodisc) to remove particules. Prior to analysis, an ion-pairing solution (1.00 M ammonium acetate) was added to the sample vial in a ratio of 4 parts extract to 1 part ammonium acetate. Two different reverse-phase HPLC C_{18} columns were connected in series. A single monomeric guard column (Rainin Microsorb, 0.46 x 1.5 cm, 3 µm packing) was followed by a momomeric reverse-phase C_{18} column (Varian Microsorb-MV 100 – 3, 0.46x10 cm, 3 µm packing) and a polymeric reverse-phase C_{18} column (Vydac 201TP54, 0.46 x 25cm, 5 µm packing).

Photopigment peaks were quantified at 440 nm (Jeffrey et al. 1997) and identified based on retention time and spectral matches with liquid standard pigment spectra (DHI, Hørsholm, Denmark). Peak areas were quantified using Shimadzu Client/Server 7.2.1 SP1 software. A total of 16 pigments were identified in each sample: chlorophyll c_3, chlorophyll c_1& c_2, peridinin, fucoxanthin, 19‘-hexanoloxyfucoxanthin, neoxanthin, violaxanthin, diadinoxanthin, alloxanthin, diatoxanthin, lutein, zeaxanthin, chlorophyll *b*, ββ-carotene, prasinoxanthin, and chlorophyll *a*.

We used peridinin as a proxy of relative abundance for dinoflagellates, alloxanthin for cryptophytes, lutein for chlorophytes, and prasinoxanthin for prasinophytes, as these pigments are only found in these respective groups (Jeffrey et al. 1997; Dorado et al. 2012). Similarly, fucoxanthin was used as a proxy for diatoms and zeaxanthin for cyanobacteria; these pigments are not specific to these groups but have been used as their proxies in other studies (Andersen et al. 1996; Murrell and Lores 2004; Dorado et al. 2012). Pigment data were standardized to chl *a* and then to total pigment (equal to a Wisconsin double standardization). From these data a Shannon Diversity Index and Pielou's evenness were calculated using the R computing environment (version 2.17.2, www.r-project.org/) and vegan library (1.17-9).

Dissolved Inorganic Nutrients. Filtrate from pigment analysis samples was used to rinse the filter tower twice prior to collection of samples for nutrient analysis. Filtrate was collected in acid-washed 60 ml Nalgene bottles and frozen. Dissolved inorganic nutrients (NH_4^+, NO_3^-, NO_2^-, and PO_4^{3-}) were analyzed by the Geochemical and Environmental Research Group at Texas A&M University, College Station. Dissolved inorganic nitrogen (DIN) concentrations were calculated as the sum of NH_4, NO_3, and NO_2.

Stable Isotopes. All faunal and size fractioned POM samples were dried at 60ºC, coarsely ground and split. Half of each sample was ground to a fine powder using a mortar and pestle for $\delta^{15}N$ analysis. The other half of the sample was processed using a Dionex accelerated solvent extractor (ASE) to remove lipids (Barrow et al. 2008) then acidified in 8N HCl fumes for >7 days to remove calcium carbonate (Armitage and

Fourqurean 2009). Acidified samples were dried again at 60 ºC, then weighed and packaged into tin boats with the optimal N load of 50 µg. Samples were analyzed at the University of California (Davis) Stable Isotope Facility.

Statistics. SPSS (version 16.0) was used to perform statistical analyses. Data were analyzed for normality using the Kolmogorov-Smirnov statistic; none were normally distributed (alpha < 0.05). Kruskal-Wallis H tests were performed throughout. If months were significantly different then Mann-Whitney U tests were performed on variables of consecutive months to determine statistical similarities (using a Bonferroni correction, alpha=0.017) to minimize Type 1 error. Samples collected in North Bay were drastically different from those collected in East and West Bays. Because the goal was to elucidate effects of marine derived nutrients on this system, North Bay was removed from further statistical analyses due to the strong influence of freshwater inflows to this sub-bay. In order to analyze the inter-annual and intra-seasonal variability, rather than spatial difference, samples collected from the surface and 10 m for both East and West Bays were pooled to represent each sampling month.

Results

Phytoplankton Variability. Chl *a* (total biomass proxy) showed no significant (p>0.05) inter-annual or intra-seasonal variability (Table 2.1). Highest Chl *a* values occurred in June of each year, decreased in July and rose again in August (Figure 2.2a). In 2010, measurements focused on the *Noctiluca* sp. bloom in June (Figure 2.2a);

maximum Chl *a* concentrations were measured mid-month increasing twofold from the two weeks prior.

June samples each year had the highest concentrations of all pigments, but the least diversity of accessory pigments (Table 2.1). Of the 16 accessory pigments measured, we found fucoxanthin (diatoms/dinoflagellate), peridinin (dinoflagellates), and alloxanthin (cryptophytes) were the dominant accessory pigments throughout the three summers (Figure 2.3). These, in conjunction with zeaxanthin (cyanobacteria), lutein (chlorophytes) and prasinoxanthin (prasinophytes), offered a clear description of the community dynamics (Table 2.1). The nine remaining pigments were grouped together as ―other" in Fig. 3. Zeaxanthin was absent in all June samples, with the exception of the final sample collected on June 25, 2010, that was taken during the decline of the bloom.

Table 2.1. Median (MD) water column and export values for parameters measured throughout the three summers. Numbers in parenthesis are number of samples contributing to median value and were used for Mann-Whitney U tests. Bold values are significant (alpha < 0.017). Values for p and U after August relate to the comparison with June. All pigments are reported in the same units (ug l^{-1}). Pigment and water column POC and PON values are median values from 0 and 10 m for both the East and West arms of Simpson Bay. Export values are median values from traps at 20 m and 40 m. Pigments are abbreviated as follows: chl a = chlorophyll a; peri = peridinin; fuco = fucoxanthin; pras = prasinoxanthin; zea = zeaxanthin.

	June			**July**			**August**		
2008	MD	p	U	MD	p	U	MD	p	U
chl *a*	1.37 (12)	0.093	94.0	1.08 (24)	0.159	102.0	1.30 (12)	0.603	63.0
peri	0.05 (12)	**0.002**	52.0	0.02 (24)	**0.001**	45.0	0.06 (12)	0.386	57.0
fuco	0.45 (12)	**0.015**	72.0	0.17 (24)	0.568	127.0	0.16 (12)	**0.013**	29.0
allo	0.03 (12)	0.146	100.0	0.04 (24)	0.048	85.0	0.06 (12)	**0.015**	30.0
prasino	0.01 (12)	**0.000**	28.0	0.02 (24)	0.199	105.0	0.02 (12)	**0.005**	23.0
zea	0.00 (12)	**0.000**	0.0	0.03 (24)	**0.004**	59.0	0.06 (12)	**0.000**	5.0
lutein	7 E-5 (12)	**0.004**	59.0	3 E-3 (24)	0.420	120.0	5 E-3 (12)	**0.000**	8.0
other	1.13 (12)	**0.007**	64.0	0.68 (24)	0.251	109.0	0.88 (12)	0.273	53.0
Diversity	1.34 (12)	**0.000**	7.0	1.90(24)	0.379	117.0	1.93 (12)	**0.000**	6.0
water column (µmol l^{-1})									
POC	57.89 (12)	**0.000**	0.0	15.11 (12)	**0.001**	11.0	28.14 (6)	**0.003**	4.0
PON	3.33 (12)	**0.000**	18.0	0.80 (24)	**0.000**	8.0	3.15 (6)	0.512	29.0
POC:PON	13.97 (12)	0.670	103.5	13.99 (19)	0.025	22.0	8.99 (6)	**0.001**	0.0
export (mg m^{-2} d^{-1})									
POC	5.18 (6)	**0.011**	9.0	2.47 (12)	0.025	12.0	1.46 (6)	**0.004**	0.0
PON	0.50 (6)	0.039	14.0	0.18 (12)	0.241	23.5	0.14 (6)	**0.016**	3.0
POC:PON	13.88 (6)	0.841	31.0	13.41 (11)	0.391	20.0	11.66 (5)	0.170	7.5
2009	**June**			**July**			**August**		
chl *a*	1.00 (12)	0.119	45.0				0.63 (12)		
peri	0.05 (12)	**0.011**	28.0				0.02 (12)		
fuco	0.01 (12)	0.326	55.0				0.01 (12)		
allo	0.02 (12)	0.603	63.0				0.02 (12)		
prasino	0.01 (12)	0.773	67.0				0.01 (12)		
zea	0.00 (12)	0.103	50.5				0.00 (12)		
lutein	0.00 (12)	**0.012**	34.0				2 E-3 (12)		
other	1.42 (12)	**0.000**	3.0				0.38 (12)		
Diversity	1.06 (12)	**0.000**	6.0				1.58 (12)		
water column (µmol l^{-1})									
POC	41.53 (12)	**0.000**	0.0				10.56 (12)		
PON	3.58 (12)	**0.000**	0.0				1.05 (10)		
POC:PON	11.18 (12)	0.552	51.0				10.53 (10)		

Table 2.1: Continued

	3-Jun			**15-Jun**			**25-Jun**		
2010	MD	p	U	MD	p	U	MD	p	U
chl *a*	0.75 (5)	0.175	6.0	1.44 (5)	0.465	9.0	1.40 (5)	0.465	9.0
peri	0.02 (5)	0.075	4.0	0.08 (5)	**0.009**	0.0	0.01 (5)	0.459	9.0
fuco	0.17 (5)	0.465	9.0	0.27 (5)	0.917	12.0	0.32 (5)	0.754	11.0
allo	0.02 (5)	0.917	12.0	0.02 (5)	0.251	7.0	0.06 (5)	0.251	7.0
prasino	0.00 (5)	0.169	6.0	0.01 (5)	0.602	10.0	0.02 (5)	0.072	4.0
zea	0.00 (5)	**0.009**	0.0	0.02 (5)	0.465	9.0	0.03 (5)	**0.009**	0.0
lutein	0.00 (5)	**0.007**	0.0	10 E-3 (5)	0.917	12.0	10 E-3 (5)	**0.013**	1.0
other	0.49 (5)	0.117	5.0	1.29 (5)	0.117	5.0	0.65 (5)	0.347	8.0
Diversity	1.59 (5)	0.076	4.0	1.80 (5)	0.465	9.0	1.78 (5)	**0.009**	0.0

Peridinin concentrations (Fig 2b) were significantly (p=0.002) greater in June than July in 2008 (Table 2.1). August 2008 concentrations were significantly higher (p=0.001) than July but were not significantly different than June (p>0.05). June 2009 peridinin concentrations were greater than those in July 2009 and similar to those measured in June 2008, demonstrating a consistent pattern of high peridinin concentrations in early summer. During the summer of 2010 peridinin showed a significant increase (nearly 5 times) from June 3rd to 15th (Figure 2.2b). These concentrations were significantly lower (p=0.009) ten days later (Figure 2.3).

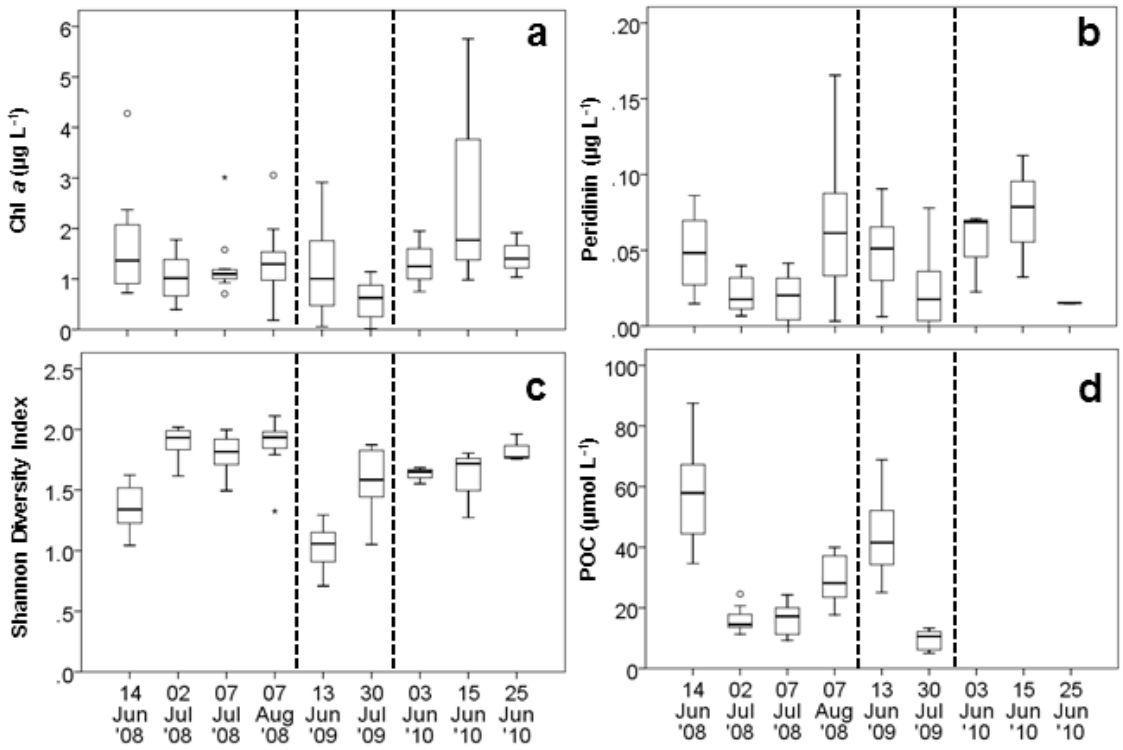

Figure 2.2: Time series of a) chl *a* (phytoplankton biomass proxy) b) peridinin (dinoflagellate biomass proxy) c) Shannon diversity index and d) POC through the three summers. Very little intra-seasonal or inter-annual variability is evident in chl *a* concentrations; however a clear pattern of increased peridinin and POC corresponds to a decrease in diversity during June of each year.

Fucoxanthin was also significantly greater in June 2008 than July or August (Table 2.1; Figure 2.3). In 2009 fucoxanthin did not change between the two sampling efforts and was much lower than values measured in 2008. In 2010 fucoxanthin nearly doubled between the 3rd to the 15th of June, increasing again to the 25th (Figure 2.3), however none of these changes were significant ($p>0.05$). Lutein was the least abundant of the indicator pigments but increased through the summer, every summer. June 2008 concentrations were significantly lower than both July and August ($p<0.001$). June 2009

lutein concentrations were significantly lower than August (p=0.012). Interestingly lutein increased significantly (*p*=0.007) from before the bloom to the peak of the bloom in June 2010 (Table 2.1). Alloxanthin increased through the summer for all summers measured, however this pigment concentration was always low and never changed significantly (Table 2.1; Figure 2.3). Prasinoxanthin and zeaxanthin trended similarly throughout all summers with values remaining below 0.05 µg l^{-1}.

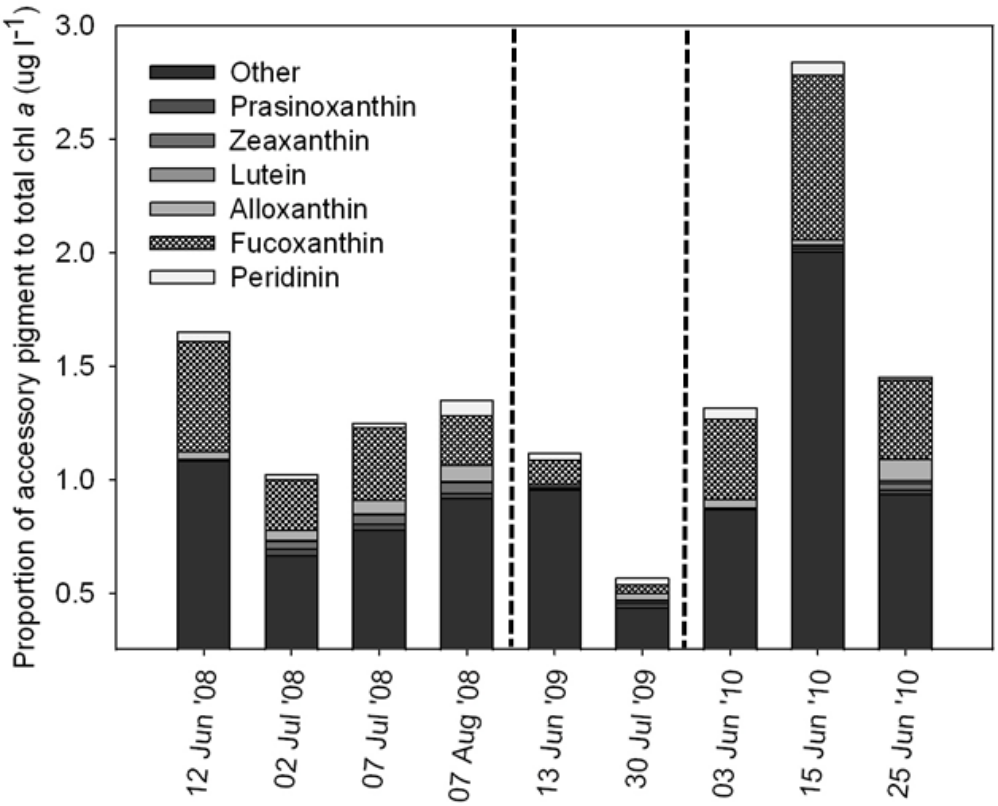

Figure 2.3: Accessory/marker pigments, shown as % contribution (calculation equivalent to Wisconsin Double Standardization) to total chl *a*. Bar height is equal to the amount of chl *a* in the sample.

Shannon Diversity indices (Figure 2.2c) were lowest in June of each year, consistent with the dominance of a single group of phytoplankton. June 2008 index was significantly less ($p<0.001$) than that for July which was not significantly different than August ($p>0.05$; Table 2.1). This pattern was observed again in 2009 (Figure 2.2c). The Shannon diversity index for June 2009 was significantly less than August ($p<0.001$). Shannon indices for June 2010 were not significantly different between sampling dates during the bloom ($p>0.05$). However, an increase in diversity was observed through the decline of the bloom. Fig. 4c shows the decrease in diversity corresponding to highest levels of POC. Highest water column carbon content occurred simultaneously with the least diversity of phytoplankton, supporting the observation of a monospecific *Noctiluca* sp. bloom.

POC concentrations (Figure 2.2d) were significantly greater (nearly 3 times) in June 2008 than July which was the lowest measured in the summer (Table 2.1). The same pattern was observed in 2009 whereby June POC concentrations were significantly greater than POC concentrations measured in August ($p<0.001$).

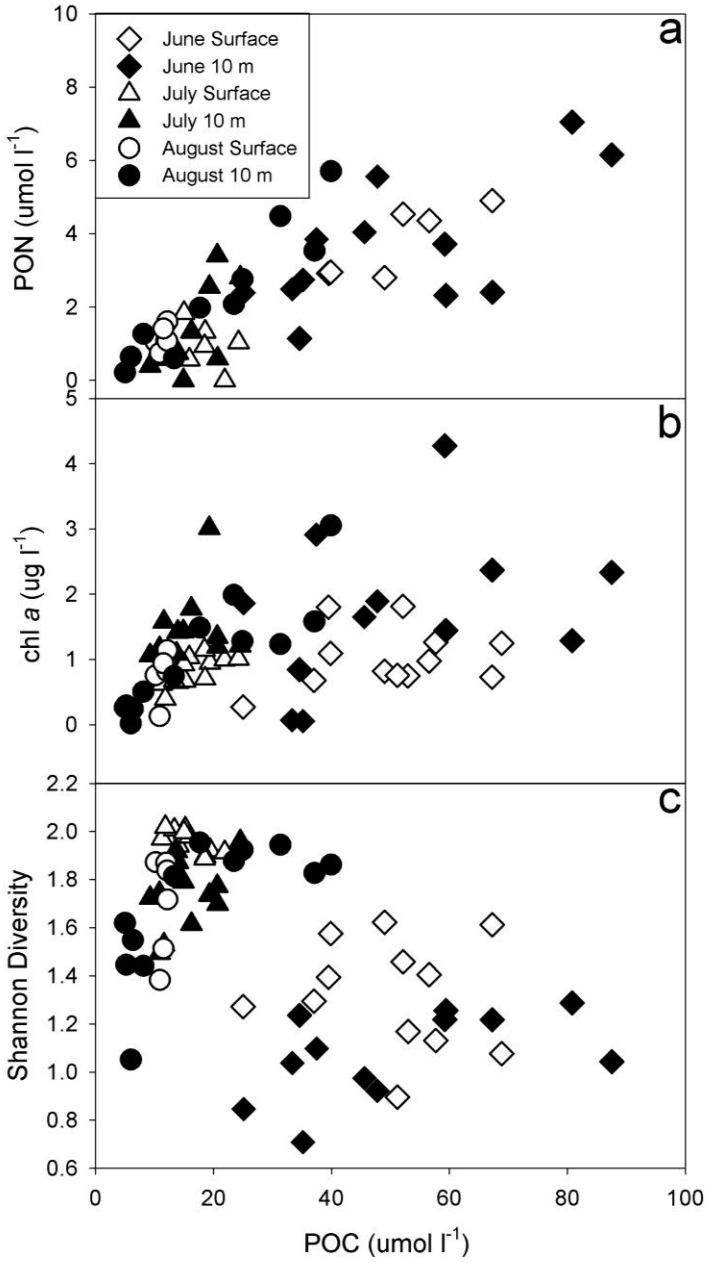

Figure 2.4: Community indicators measured in surface (0 and 10m) waters during the summers of 2008-2010. The POC:PON ratio (a) decreased through the summer The POC:Chl *a* ratio (b) also decreased through the summer, indicating a switch from a more heterotrophic community to a more autotrophic community. The Shannon diversity index versus POC (c) reveals lowest diversity indices correspond to the highest POC concentrations, capturing the bloom of *Noctiluca* sp.observed during the summer in PWS. Open symbols represent surface samples (0 m), closed symbols represent samples collected at 10 m; diamonds = June, triangles = July, circles = August.

Bloom Impacts – Water Column (0-10m). The highest POC and PON concentrations were measured in June each year, corresponding to the herring spawn and the *Noctiluca* sp. bloom (Figure 2.2d). The increase in POC does not directly correlate with autotrophic biomass; Chl *a*:POC ratios increased through each summer due to the decrease in POC concentrations (Figure 2.4b). The low Chl *a*:POC ratios each June were consistent with a heterotrophic bloom. Therefore, the effect of the bloom on the phytoplankton community is clearer when parameters are compared directly with POC (Figure 2.4). The increases in water column POC and PON were not the same as demonstrated by the slope < 1 in Figure 2.4a; there was a greater increase in POC than PON. POC:PON was greater in June 2008 than July but not significantly (p>0.05; Table 2.1). This ratio declined again in August though the change was not significant. The Shannon Diversity Index decreased with increasing POC (Figure 2.4c). Samples collected with the highest POC concentrations also represented those with the lowest diversity. As the summer progressed POC decreased and diversity increased.

Nutrient concentrations (Figure 2.5) of ≤ 1 μmol l^{-1} DIN or ≤ 0.2 μmol l^{-1} P_i are indicative of oligotrophic waters while nutrient ratios of DIN:P_i < 10 and DIN: P_i > 30 can be used to indicate N versus P_i limitation, respectively (Dortch and Whitledge 1992; Sylvan et al. 2006; Quigg et al. 2011). For the period of this study, DIN was generally < 5 μmol l^{-1} DIN in surface waters (Figure 2.5), with occasional values up to 9 μmol l^{-1}; P_i was more variable but remained < 1.2 μmol l^{-1} at nearly all the stations, with the exception of those nearest North Bay. P_i was frequently < 0.50 μmol l^{-1} except in July. The combination of low DIN and relatively high P_i resulted in the low DIN:P_i ratios,

suggesting N limitation of the phytoplankton community in this system each year, particularly in June.

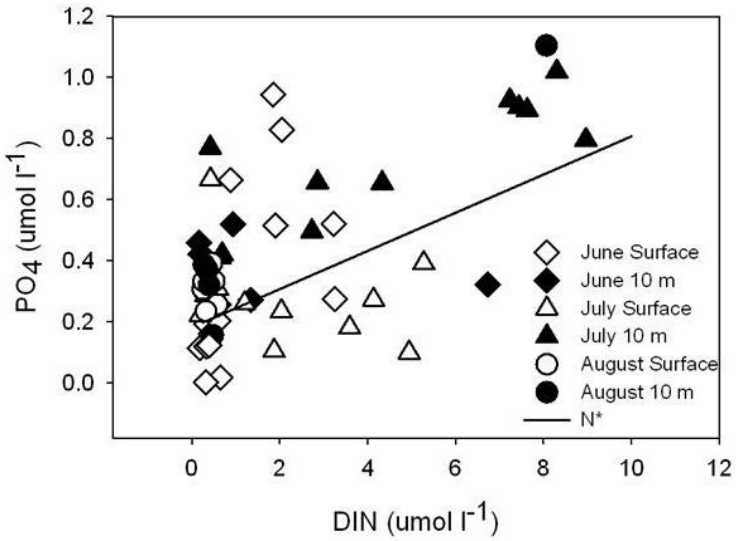

Figure 2.5: Dissolved inorganic nitrogen (sum of NO_3, NO_2, NH_4) versus phosphate (μmol l^{-1}); black line = N* as calculated from Gruber and Sarmiento (1997). Values above the line are indicative of photosynthesis whereas values below the line are indicative of new sources of nitrogen, either through herring spawn or nitrification. Open symbols represent surface samples (0 m); closed symbols collected at 10 m; diamonds = June, triangles = July, circles = August.

Bloom Impacts – Export from the Water Column (0-10m) to Sediment Traps (20-40m).

Sediment traps were deployed regularly from June-August in 2008, and are thus the most descriptive of intra-seasonal variability of C and N export. POC_{Trap} exported in June was significantly greater, nearly 2-4 times, than in either July or August (Table 2.1); PON_{Trap} exported was also greater in June than July or August, though not significantly. These trends paralleled those observed in the water column described above. Qualitatively POC_{WC}:PON_{WC} (ratio of POC:PON measured in the water column

at 0 and 10m) measured immediately prior to deploying sediment traps was 13.97 compared to 13.88 POC_{Trap}:PON_{Trap} (median ratio measured in traps at 20m and 40m) in June (Table 2.1). In June the ratio of POC:PON did not change significantly in the water column or in the export. However, in August the POC:PON measured in the water column decreased to 8.99 ($p>0.05$). POC_{Trap}:PON_{Trap} also decreased but not at the same magnitude, suggesting there was elevated N recycling in the water column or excess C exported.

Bloom Impacts – Food Web. Natural abundance stable isotope values for POM collected in July 2010 were not significantly different spatially (δ^{13} $p = 0.496$, $n = 10$; $\delta^{15}N$ $p = 0.169$, $n = 10$) or by size fraction (δ^{13} $p = 0.602$, $n = 10$; $\delta^{15}N$ $p = 0.602$, $n = 10$) (Md $\delta^{13}C$ = -19.58 ‰; Md $\delta^{15}N$ = 7.83 ‰) (Figure 2.6; Table 2.2). The isotopic signature of herring ($\delta^{13}C$ -17.53 ‰, $\delta^{15}N$ 13.55 ‰) was approximately two trophic levels above that of the POM (difference is 2.06 ‰ $\delta^{13}C$ and 5.79 ‰ $\delta^{15}N$) (Fig. 6). Values for *Noctiluca* sp. were $\delta^{13}C$ -17.70 ‰ and $\delta^{15}N$ 5.74 ‰, demonstrating a shift of inputs to the food web (higher $\delta^{13}C$ and lower $\delta^{15}N$ than the POM collected prior to the spawn/bloom; Fig. 4). Mussels and clams collected after the *Noctiluca* sp. bloom have C values ($\delta^{13}C$ -17.73 ‰) similar to those of *Noctiluca* sp., and enriched N values ($\delta^{15}N$ 8.29 ‰) common to the trophic difference.

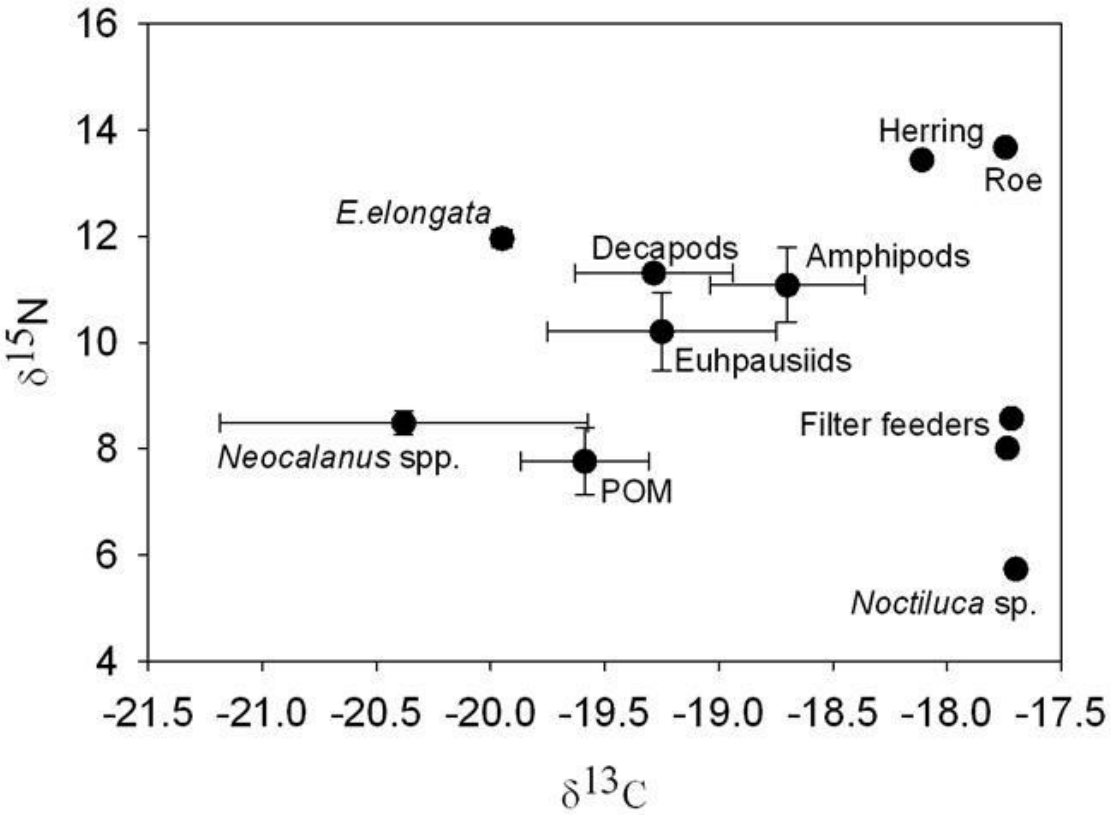

Figure 2.6: Property property plot of natural abundance stable isotopes collected during this study combined with values from Kline Jr. (1999) for Amphipods, Decapods, Euphausiids, *E. elongata*, and *Neocalanus* spp..

Table 2.2: Natural abundance C and N stable isotope values for key organisms in the Simpson Bay system measured during this study and compared with previously measured values. Values are averages where more than one sample was collected and the values in parentheses are the range. * indicates values reported for *Neocalanus* spp. (primary consumer) similar trophic relationship to the *Noctiluca* sp. reported in this study. Genera of filter feeders examined by Powers et al. (2005) were *Mytilus trossulus* and *Mya arenaria*. † indicates estimated value for Pacific herring consuming only prey from PWS and bays – measured values show usage of Gulf of Alaska food sources as well and range from -20.5 to -18.5.

POM		Noctiluca		Herring/Roe		Muscles/Clams		Reference
C	N	C	N	C	N	C	N	
-19.59 (0.90)	7.76 (2.05)	-17.70	5.74	17.64 (0.21)	13.61 (0.12)	-17.73 (0.01)	8.29 (0.56)	This study
-19 to -24	4 to 8							Fry 2006
		-17.2 to -17.5 GOA*	8.4 to 9.5 GOA*					Kline Jr. 2009
		-18.5 to -19.8 PWS*	9.5 to 8.8 PWS*					
		-20.8*	8.4*	-22.6 (±0.67)	12.7 (±0.24)			Kline Jr. 1999
				-19 to -17†				Kline Jr. & Campbell, 2010
				-17.5	13.5			Hobson et al. 1994
						-16.85, -16.94	9.43, 9.59	Powers et al. 2005

Discussion

A bloom of the heterotrophic dinoflagellate *Noctiluca* sp. occurred in June of 2008-2010 in Simpson Bay, PWS, potentially in response to the pulse of marine derived nitrogen from a herring spawn. Significant intra-seasonal variability was observed: peridinin, POC, and PON were higher in June than July or August. Diversity and DIN were significantly lower in June, but there was no trend in chl *a*. The lack of a peak in chl *a* during the June bloom is consistent with heterotrophic dinoflagellate bloom rather than an autotrophic algal bloom like those typically observed early in April (Eslinger et al. 2001). The disconnect between the Chl *a* and POC in our study points to a dominance

of a phytoplankton with either low Chl *a* concentrations or a species that is facultatively heterotrophic, such as the dinoflagellate *Noctiluca* sp., that can use other dissolved organics for nutrition. Thus, understanding the phytoplankton community and discerning possible blooms of heterotrophic algae would be enhanced by more comprehensive pigment analyses, as opposed to measuring chl *a* alone

The impacts of this annual bloom in June are reflected in the export of particulate organic matter from the surface, particularly in June 2008. Two-to-three times more POC was measured in the sediment traps (20 m and 40 m) in June than either July or August (Table 2.1). Most of the carbon exported in June was organic and likely from the bloom observed during this period. Qualitatively, the POC:PON ratios measured in the water column and in the sediment traps decreased through the summer. POC:PON ratios measured in water column (WC) relative to those measured in the traps (Trap) for June were nearly equal, indicating rapid export. Measured export was lowest in July; also, both WC and Trap ratios decreased indicating relatively less C export or increased N export. Interestingly, in August the ratio of POC:PON in the water column versus trap switched with a higher ratio measured in the trap, indicating a relative decrease in the amount of N reaching the traps and a relative increase in the water column, pointing to a recycling of N in the system. Thus, the nutrients from the spawn entrained in the system during the *Noctiluca* sp. bloom may still be an important source of nutrients for the food web of Simpson Bay for as long as two months.

Further evidence of nutrient recycling comes from dissolved nutrient concentrations. Using the tracer N* described by Gruber and Sarmiento (1997) (black

line in Fig. 5), new inputs of N were evident in the surface waters in June and in July. Positive N* values indicate either nitrification, N_2 fixation, or some other increase in N (below the black line in Figure 2.5), whereas negative N* values point to either denitrification or photosynthesis. We measured positive N* values in the surface waters of Simpson Bay in June and July (samples above the black line in Figure 5). Positive N* values correlated with increased N from the spawning event in June; we postulate that the even higher values in July demonstrate nitrification, a process of recycling N from the spawn in the surface waters during this time. Negative N* values were observed primarily in August.

In addition, natural abundance stable isotope samples collected in this system showed that the bloom was accompanied by shifts in the sources of carbon and the composition of the phytoplankton community (Figure 2.6). This shift from -19.59 ‰ (POM) to -17.70 ‰ (*Noctiluca* sp.) is indicative of a shift to more marine source of carbon (Fry 2006). Correspondingly, the shift in $\delta^{15}N$ from 7.76 ‰ to 5.74 ‰ suggests there was also a change to a marine source of nitrogen. Similar decreases in $\delta^{15}N$ values have been documented between neritic and oceanic POM (Dorado et al. 2012). The shift to a lower trophic level (depleted $\delta^{15}N$ values in *Noctiluca* sp.) is particularly interesting as *Noctiluca* sp. are known facultative heterotrophs and they appear at a lower trophic status than the POM. This may be indicative of the *Noctiluca* sp. feeding on heterotrophic bacterial biomass which increased as a result of the herring spawn.

We have described a pulse of marine derived nutrients from herring spawn having a direct effect on the phytoplankton community composition and abundance.

Previous studies have shown these pulses to be important to higher trophic organisms in other ecosystems (Roper et al. 1999; Willson and Womble 2006). Schools of adult Pacific herring migrate into PWS in mid-spring (Norcross et al. 2001) and spawn in large aggregations along the coast. A spawning event generally lasts 5-21 days, and the eggs hatch 22-24 days later (Norcross et al. 2001). In 2007 an aggregation of sea otters in Simpson Bay was observed consuming herring roe on kelp between 11 June – 3 July (Lee et al. 2009), confirming an additional, apparently small, summer spawning event in the study area (as eggs hatch within 1.5-3 weeks (Wilson and Womble 2006). While the summer spawn of herring is smaller than the spring event, it may still contribute substantial amounts of nutrients to the bays where it occurs (including Simpson Bay), as was observed in the current study. The pulse of nutrients alleviates the nitrogen limitation of primary productivity typically observed in fjords in PWS in the summer (Eslinger et al. 2001; Quigg et al. 2013). This study demonstrates that resource pulses can stimulate the system at trophic levels above and below the level of input. Further research is required to explicitly quantify the energy and nutrient input to Simpson Bay and PWS. These previously overlooked effects of resource pulses may be an important contributing factor to the sustained abundance of this ecosystem.

CHAPTER III

ADDRESSING ASSUMPTIONS REGARDING THE OCEANIC C-CYCLE: LATERAL TRANSPORT OF PARTICLES THROUGH THE WATER COLUMN

Introduction

Currently there is extensive focus on the global carbon (C) cycle, primarily to understand how this cycle modifies and is modified by global climate change. While it is well known that human driven perturbations have had a large impact on our planet, the extent to which the environment is able to cope with these fluctuations is not completely understood. The oceans are linked with the atmosphere in regulating heat, fresh water, atmospheric gases, and other substances by redistribution or sequestration. Of particular interest is the connection between the atmosphere (reservoir 784 Pg C), oceanic biota (reservoir 1-2 Pg C), dissolved organic carbon (DOC; reservoir 662 Pg C) and the deep ocean sediment (reservoir 1000 Pg C, to 1 m depth), also known as the biological C pump (Emerson and Hedges 2008; Jiao et al. 2010). This pump represents the conduit from the surface ocean to the deep ocean where C is stored long term. The components, mechanisms, and efficiency of this pump remain unclear.

Most studies on elemental cycling focus on C, and relate the cycling of other elements to the C-cycle. Phytoplankton, being the primary fixers of inorganic C to organic C, are studied in their uptake, utilization, and transfer of these organic compounds to bacteria (microbial loop, Azam 1998; Jiao et al. 2010) and other trophic levels (Volk and Hoffert 1985; Longhurst and Harrison 1989). Carbon, nitrogen, and

phosphorus (C, N, P) cycle through the phytoplankton community with a global average stoichiometric ratio of 106:16:1 (Redfield 1958). Determination of the amount of C sequestered by the ocean is therefore often estimated via study of the other essential elements, mainly N. Movement of C is estimated based on classification as either regenerated or new production determined by the source of N (Dugdale and Goering 1967). Due to the inherent complexity of the biological pump it is difficult to determine the amount of primary production that is: 1) utilized/entrained in the pelagic food web, 2) converted into DOC by bacteria (Jiao et al. 2010), and 3) exported to the deep sea. We will focus on the later parameter in this study.

The f-ratio of Eppley and Peterson (1979) was an early effort to estimate export (difficult to measure) from measurements of new production (measurable). Subsequently, different ratios and techniques have been described in an effort to quantify new production including: $^{15}NO_3$ assimilation (Neess et al. 1962; Montoya et al. 1996; Mohr et al. 2010), sediment traps (Honjo et al. 2008), NO_3^- flux to the photic zone (Hales et al. 2005), O_2 utilization (Jenkins 1988), $^{238}U/^{234}Th$ (Buesseler et al. 1992; Santschi et al. 2006), and the depletion of winter NO_3^- (Millero 1996). These techniques have proven useful in improving our knowledge of the flux of C from the euphotic zone.

Assumptions and biases exist in these export measurements/estimations. The f-ratio utilizes the compartmentalization of production into new and regenerated pools to estimate export production (Eppley and Peterson 1979). It has been assumed that the contribution of new nitrogen from nitrogen fixation is negligible and thus this method is not very accurate when used in subtropical and tropical oceans (60% of the world‘s

ocean) as nitrogen fixation has now been shown to be very prominent in these waters (Karl et al. 1997; Montoya et al. 2004; Groβkopf et al. 2012). Further, experimental addition of ^{15}N labeled NO_3 can change the N concentration in an assay to such a degree that the measurements are not accurate (see Falkowski et al. 2003). Other potential problems include the changes in the community during incubations, which in turn impacts both the ^{15}N uptake and ^{14}C measurements (Fernandez et al. 2003; Aranguren-Grassis et al. 2012).

The e-ratio is a description of the amount of primary production exported (measured with sediment traps and compared to various primary productivity estimates) in an attempt to better constrain estimates of C sequestration (Murray et al. 1996). Sediment traps are generally regarded as measuring the ‗minimum' export because of shear (movement of water across the surface of the trap thus excluding particles), exclusion (particles not entering the trap due to the physics of a particle displacing the water already filling the trap), preservation (biases depending on the type of preservative or lack of preservative), and swimmers (entering and leaving the trap after consumption of some particulate or entering and staying when they would not normally have done so) (Gardner 1997; Buesseler et al. 2007). However, traps arguably remain our best form of measurement of exported particulate matter. Buesseler et al. (2001) and Falkowski et al. (2003) have suggested sediment traps can be calibrated using the ^{234}Th method, thus increasing their accuracy.

Another ratio, ThE ratio, uses the disequilibrium between the naturally occurring radio isotopes ^{234}Th and ^{238}U. Because ^{238}U degrades into the short lived ^{234}Th that

readily adheres to particles, the difference between the two isotopes is used to estimate particulate export (Buesseler et al. 1992; Falkowski et al. 2003; Santschi et al. 2006). Estimates of the C concentration in the sinking particles must be made in order to then estimate the amount of C drawdown (Buesseler et al. 1992), and further, particles measured for ^{234}Th:POC must be representative of the majority of the flux particles, often a problem for the most rapidly sinking particles (Waite and Hill 2006). Because of the short half-life of ^{234}Th this ratio is only good for shallow (100 – 250 m) water fluxes (Buesseler et al. 1998, 2006).

The oxygen utilization rate ratio (OUR ratio) measures the consumption of oxygen below the photic zone as an estimate of surface production exported (Feely et al. 2004; Falkowski et al. 2003). Because most of the organic material that is exported is remineralized by bacteria (del Giorgio et al 1997; Azam 1998; Jiao et al. 2010), consuming O_2, the difference between the amount of oxygen present and the amount originally present during formation of the water mass from ventilation yields an estimate of the amount of organic matter that was exported (Falkowski et al. 2003). This method represents a very long term estimate (equivalent to the turn over time of the oceans; Feely et al. 2004). Further, not all organic matter is remineralized in the water column, and some is exported to the sediments where the remaining POC is either remineralized or buried. The OUR method focuses on the consumption of organic matter below a specified isopycnal, thus it is important to be as close to the bottom of the euphotic zone as possible even though the isopycnals might not necessarily align exactly with this

depth. It is also likely that some remineralization will above and thus occur before the depth where measurements were made (Falkowski et al. 2003).

Because the C cycle has been the center of much debate in the past decade, many efforts have been made to determine the various factors that control C export in order to improve our understanding of the ocean‘s role in sequestration of anthropogenic C and accurate representation of the oceans in global C-cycle models. These efforts have greatly expanded our understanding of the effects of temperature (Laws et al. 2000) on surface (Guidi et al. 2009) and mesopelagic (Robinson et al. 2010) community composition and biomass in relation to particle attenuation, size and composition (Richardson and Jackson 2007).

Despite the strides made by biological and chemical oceanographers in improving our understanding of the C cycle, our estimates of export production versus actual export remains imbalanced. Robert Ballard attributes his finding of the RMS Titanic, in part, to incorporating the effect of the local currents on the sinking pieces of the vessel; he also discusses the size fractionated trail of debris (Ballard 1995). The argument of incorporating horizontal advection of particles entering sediment traps due to currents is not new (Deuser et al. 1988; Siegel et al. 1990; Siegel et al. 2008). It has also been shown that particles entering a sediment trap at any depth rarely enter the trap at an angle of greater than 10° (Gardner 1980; Siegel and Deuser 1997). Theoretical and site specific considerations of overlying current regimes on the effects of sinking particles have been made (Deuser et al. 1988; Siegel et al. 1990; Siegel and Deuser

1997; Siegel et al. 2008). However, a global analysis of implications to carbon export estimates, and thus climate change, have not been addressed.

The objective of this paper is to determine the accuracy of present estimates of global C export using published data from sediment traps. We hypothesize that incorporation of current regimes over the spatial distribution of sediment traps can explain the variability recorded in these measurements. To test this hypothesis, we developed a simple numerical model to estimate horizontal distance traveled by sinking particles, based on current velocity and sinking rates. We used this model to understand the effects of currents on estimated and measured export for two publically available datasets (Buesseler 2011; Honjo et al. 2008) with details on shallow and deep water traps.

Methods

Settling velocity and size of fecal pellets (Smayda 1971), aggregates (Pilskaln et al. 1998), and single cells (Eppley et al. 1967) were compiled and normalized to an environment with a temperature of 20 °C and salinity of 35 (global surface averages, Falkowski and Raven 2007), with corresponding density and viscosity calculated using Seawater lab functions for MatLab (http://www.cmar.csiro.au/datacentre/ext_docs/seawater.htm). McDonnell and Buesseler (2010) report settling velocities of particles measured in the open ocean corresponding to these ranges. Using vector addition and the laws of similar triangles, an estimated horizontal distance carried was calculated, using a hypothetical current velocity of 2 km

day^{-1} (the global median value for current velocities; NASA OM 2011, Table A1, Figure A1).

Two publicly available data sets were used: (1) the JGOFS data set which uses the ThE ratio and shallow trap measurements of POC export to between 50 and 200 m (Buesseler 2011), and (2) the mesopelagic/bathypelagic (m/b) data set that used sediment traps to measure C export to the m/b boundary at approximately 2000 m (see Honjo et al. 2008). JGOFS data (station, latitude, longitude, depth, POC flux, primary production, and ThE ratio) were compiled from the US JGOFS Synthesis and Modeling Project for ^{234}Th based POC export (Buesseler 2011). Corresponding surface current and temperature data were compiled from NOAA Ocean Motion (using location and date closest to the JGOFS sampling) (NASA OM 2011). Deep flux (m/b) data including: station, latitude, longitude, depth, POC flux to 2000 m, estimated export production (EP) using remote sensing ecosystem model (Laws et al. 2000), and primary production were compiled from Honjo et al. (2008). For the purpose of our analysis, these will be referred to as ―shallow" and ―deep" water traps respectively.

Multivariate analyses were performed using the ―vegan" (Oksanen et al. 2011) and ―sigclust" (Whitaker and Christman 2010) packages in R 2.15 (R Development Core Team 2012). For the JGOFS series, only stations where all the environmental data (depth, POC flux, primary production, and ThE ratio, surface current velocity and temperature) were available were used. All data sets were log transformed, centered (subtracted by sample mean) and normalized (divided by standard deviation) before subjected to analyses. To assess the relationship between export and environmental

parameters, JGOFS export data were visualized in ordination space using principal components analysis (PCA) and coupled to environmental vector fitting. The m/b data set did not have all of the relevant environmental parameters so they were not included in the PCA.

In order to assess the similarity in export between sites, significant cluster analysis was run on both the JGOFS and m/b data sets using the ward minimum variance method. Small branches were grouped and major site assemblages were determined according to resultant of the dendrograms. Permutational multivariate analysis of variance (PERMANOVA) was then run (using the vegan package) on the major site assemblages to ensure the data between groups was significantly different.

Results & Discussion

Principal components analysis of data compiled from US JGOFS ~~–s~~hallow" traps show that variability of Export POC, ThE ratio and primary productivity is significantly driven by the environmental parameters of surface temperature and depth ($p<0.001$; Figure 3.1A). These relationships are well described in the literature but were included to validate the explainable variability in the datasets discussed below. It is predictable that depth will play the dominant role in driving this variability of shallow traps as all of the environmental parameters (e.g., POC flux, primary production) decrease with depth. The trend of temperature variance has also been previously discussed by Laws et al. (2000). Temperature is a good indicator of C in the ocean given phytoplankton community compositional changes with surface temperature – larger more dense

diatoms thrive in colder waters, smaller phytoplankton dominate warmer habitats (Finkel 2007) (these trends may also be proportional to nutrients – Irwin et al. 2006). Current velocities are not a significant driver of the variability in shallow trap measurements (Fig 3.1B) as a group. There may still be locations where PP variability and current velocities are great enough to affect POC measurements.

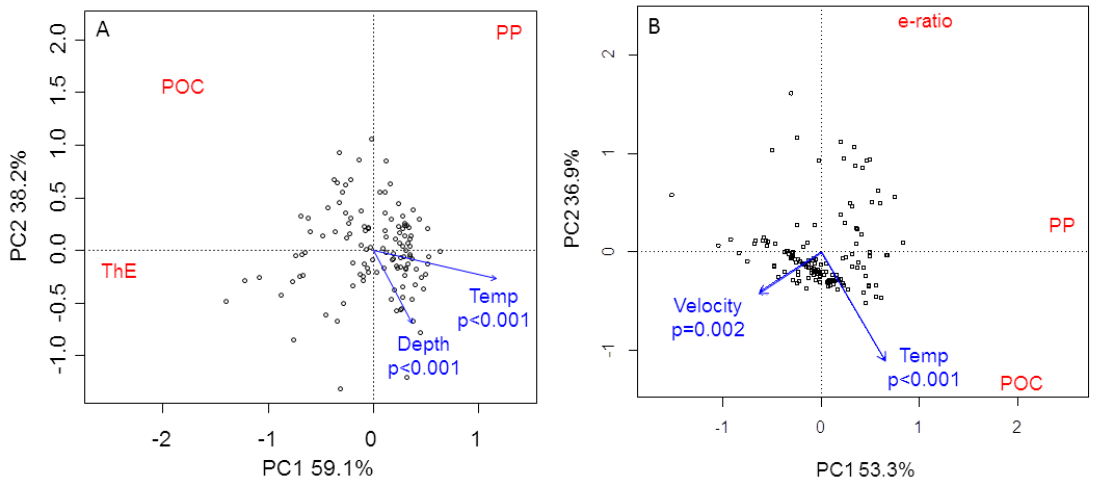

Figure 3.1: Principal components analysis showing variability in sediment traps compiled from (A) JGOFS ^{234}Th based POC export (Buesseler 2011) and (B) normalized (to m/b boundary) deep trap POC export measurements compiled by Honjo et al (2008). Separation in A is based on POC flux, primary production, and ThE ratio tested environmental vectors include surface current velocity and temperature and trap depth. Surface temperature (Temp) and Depth are significant contributors to the variability shown (vectors indicates magnitude and directionality of influence). Separation in B is based on POC flux measured in traps, primary production and the e-ratio. Significant environmental variables explaining some of the variability within this data set include temperature and current velocity.

Principal component analysis of the measurements for deep traps (from Honjo et al. 2008) shows that variability in measurements of PP, e-ratio, and POC are significantly driven by current velocity and temperature (compiled from Lumpkin and

Johnson 2013). The e-ratio and POC flux are similarly driven by PP however the remaining variability changes along the temperature gradient, pointing to a more complex relationship between export and temperature. Further, both the e-ratio and POC flux decrease with increasing current velocities. In fast regimes less POC is collected in traps.

We found the relationship between the variability of the data (Export POC, ThE ratio, primary production) and the environmental vectors (temperature and depth) to be nonlinear (Figure 3.1A). Therefore, another as yet to be defined variable must also be contributing to the variability in the Buesseler (2011) data set. Based on theoretical considerations (Deuser et al. 1988; Siegel and Deuser 1997; Siegel et al. 2008), this variable is most likely to be current velocity. If we assume that currents drive the remaining variability, it is then feasible to describe four different categories: sites where local primary productivity is high and up-current productivity is also high (HH), sites where local primary productivity is low and up-current productivity is also low (LL), sites where local primary productivity is lower than up-current values and the resultant export ratio would be high (LH), and sites where local primary productivity is higher than up-current, resulting in a low export ratio (HL). After defining these categories, we reanalyzed the data to determine the variability in export POC, PP, and ThE ratio with reference to current velocity.

Model Development. Phytoplankton, aggregates, and fecal pellets have very different sinking rates; they range from 0.17 – 240 m day^{-1} (Eppley et al. 1967; Smayda 1971; Pilskaln et al. 1998; Appendix A Table 1). Through simple vector addition of

sinking velocity and the dominant current velocity, it is possible to estimate the horizontal distance traveled by individual particles (Figure 3.2). Assuming an average ocean depth of 4000 m and no action by the microbial zooplankton communities, particles could remain in the water column from 16 to 400 d (sinking velocities of 250 m d^{-1} to 10 m d^{-1}). If horizontal movement is accounted for, the particles collected in sediment traps could originate in surface waters as far away as 10,000 km (Figure 3.2). The distance travelled depends both on the size and density of the particle. Fecal pellets tend to travel the least distance while aggregates and single phytoplankton cells travel the greatest distances (Figure 3.2).

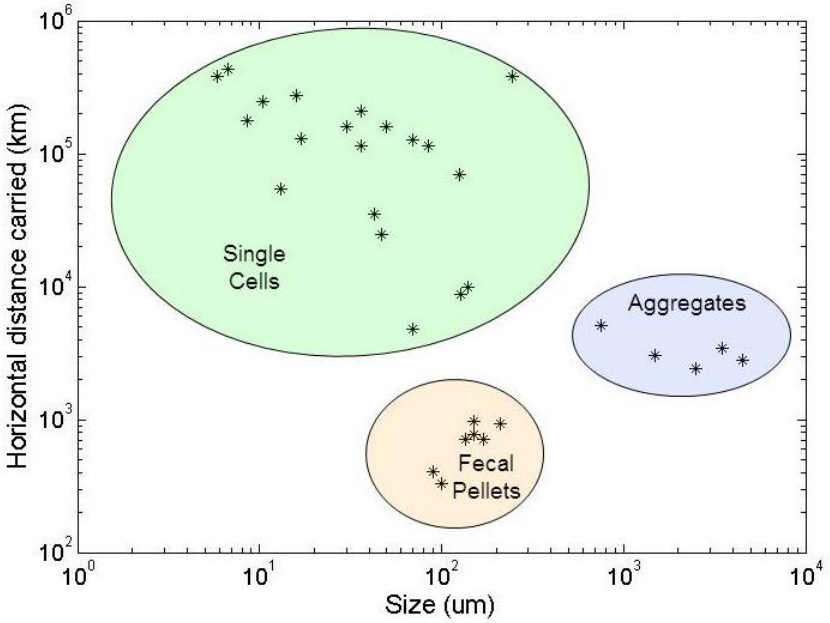

Figure 3.2: Calculated hypothetical horizontal distance carried for sinking particles (NOTE log log plot). It is density, more so than size, that determines distance carried because aggregates, being less dense but bigger than fecal pellets, sink more slowly and potentially travel further.

Because surface productivity is not uniform throughout the world ocean, we explore here the need to account for dominant currents when attempting to quantify particulate export from the surface ocean. A regression line through the log log plot of the calculated horizontal distance carried (km) and the normalized settling velocities (m day^{-1}) yields a simple equation (Appendix A Figure 1) that can be used to estimate the distance carried based on the settling velocity of particles (Table 3.1). Because the angle is so small (the hypotenuse of the triangle very nearly equates to the current velocity) the current can be substituted, yielding the simplified equation (1):

$$\text{current velocity (m d}^{-1}\text{)} * \text{depth (km)} * [\text{settling velocity (m d}^{-1}\text{)}]^{-1} = \text{horizontal distance carried (km)}$$

Using average current velocities for the major global surface currents (Table 3.1), we can gain insight into the regions and parameters which will likely be most influential in the horizontal transport of particles. Current velocity, depth of influence for surface currents (between 300-100 m, Pickard and Emery 1990) and the settling velocity have equal influence on the horizontal distance carried; but because current velocity and the depth of influence often co-vary, the effects of currents are compounded in regions where they have the potential to influence export.

Table 3.1: Compilation of current velocities and the calculated horizontal distance transported (using equation 1 – see text). The minimum distances are calculated using rapidly sinking particles (250 m day^{-1}) corresponding to fecal pellets, maximum distances are calculated using slowly sinking particles (10 m day^{-1}) corresponding to the fastest sinking individual particles and slowly sinking aggregates. The large range in the second column is due to different depth of influence from the currents (i.e. lowest impact arises from the fastest sinking particles combined with the shallowest depth of influence and the largest impact occurs in areas with the slowest sinking particles and the deepest depth of influence).

Current	Current Velocity (cm sec^{-1})	Horizontal distance transported (km) to 150 m	to 300-1000 m	Reference
East Greenland	30-35	15-450	30-3025	Lumpkin and Johnson 2013
West Greenland	45-50	20-650	50-4320	Lumpkin and Johnson 2013
Labrador	15-30	10-390	15-2590	Lumpkin and Johnson 2013
Atlantic North Eq	22	10-290	25-1900	Richardson and Reverdin 1987
Atlantic Eq CC	20-40	10-520	20-3455	Richardson and Reverdin 1987
Atlantic South Eq	27	15-350	30-2335	Richardson and Reverdin 1987
Guiana	41-123	20-1600	45-10630	Febres-Ortega and Herrera 1976
Caribbean	30-70	15-910	31-6050	Lumpkin and Johnson 2013
Gulf Stream	70-200	35-2600	70-17280	Lumpkin and Johnson 2013
Canary	10-15	5-195	10-1295	Lumpkin and Johnson 2013
Agulhas	60-200	30-2600	60-17280	Lumpkin and Johnson 2013
Benguela	17	10-220	20-60	Shannon 1985
North Brazilian	80-140	40-1800	85-12095	Lumpkin and Johnson 2013
Malvinas	30-50	15-650	31-4320	Lumpkin and Johnson 2013
Pacific North Eq	20	10-260	20-1730	Lumpkin and Johnson 2013
Pac North Eq CC	90	50-1200	95-7775	Johnson et al. 2001
Pac South Eq	25-30	15-390	25-2590	Lumpkin and Johnson 2013
Kuroshio	70-132	35-1700	75-11405	Chao et al. 2009
Kuroshio extension	90-120	50-1500	95-10370	Nonaka et al. 2012
Oyashio	40	20-520	40-3455	Sakamoto et al 2010
California	25-50	15-650	25-4320	Lynn and Simpson 1987
Humbolt	10-15	5-190	10-1295	Fuenzalida et al. 2008
East Australia	90	50-1200	95-7775	Lumpkin and Johnson 2013
Somali	50-150	25-1900	50-12960	Flagg and Kim 1998
Leeuwin	20-100	10-1300	20-8640	Lumpkin and Johnson 2013

Rapidly sinking particles (i.e. fecal pellets) will not be transported far average ~500 km (Table 3.1; Fig. 3.2). Faster sinking particles are advected less and would thus be the primary component of export POC measured directly below the surface. This tight coupling between the surface and deep sea due to the rapid sinking rates is well documented (Trull et al. 2008). The role of slowly sinking particles is less constrained. Slower sinking particles have the potential to be transported vast distances (Table 3.1; Fig. 3.2). In areas where aggregates are the dominant export particle, currents will more effectively transport these particles horizontally as their sinking speeds are slower. Further, some aggregates have been shown to become neutrally buoyant (Alldredge and Crocker 1995); this condition would exacerbate the effect of currents on export. It is possible that the export contribution of locally formed slower sinking particles is not measured in traps directly beneath, and may be, consequently, largely disregarded.

Elucidating sinking and distribution of aggregates is very important as direct sedimentation of aggregated phytoplankton is the largest component of export to the abyss (Turner 2002). It has also been argued that fecal pellets are the dominant component of POC flux (Trull et al. 2008). Aggregate versus fecal pellet contribution may, in fact, vary according to surface phytoplankton community composition (Guidi et al 2009). Due to the relatively slow settling velocity of aggregates it is assumed that they would be subject to proportionally increased remineralization/repackaging, however studies have shown that they are very labile (Alonso-Gonzalez et al. 2010); indicating that either aggregates are locally formed or that they are somehow less susceptible to

remineralizitation. If aggregates measured are formed locally (from the depth where they are measured) the matter still, at some point, originated at the surface.

The disparate effects of currents on the different types of particles affects our estimates of export. It may be that regions where fluxes are dominated by fecal pellets are indicative of the primary productivity at the surface, however in regions where aggregates and slower sinking particles dominate, currents influence on export is more important.

Meta-Analysis (JGOFS – Shallow Export). Cluster analysis of the JGOFS data (Buesseler 2011) yields 4 distinct groups (Figure 3.3). The median PP, POC flux and ThE% values for each of these groups is given in Table 3.2. When ranked by these median values, the groups can be sorted into the corresponding categories: Group 1 (red) has high PP and low export (HL) while Group 2 (orange) has low PP and high export (LH). Group 3 (yellow) is representative of groups with high PP and high export (HH), and Group 4 (green) represents low PP and low export (LL). Shallow water trap distribution (shown as circles on Figure 3.3) categorized into these four groups illustrates the areas where specific patterns associated with currents would be a primary driver in the variability of export fluxes.

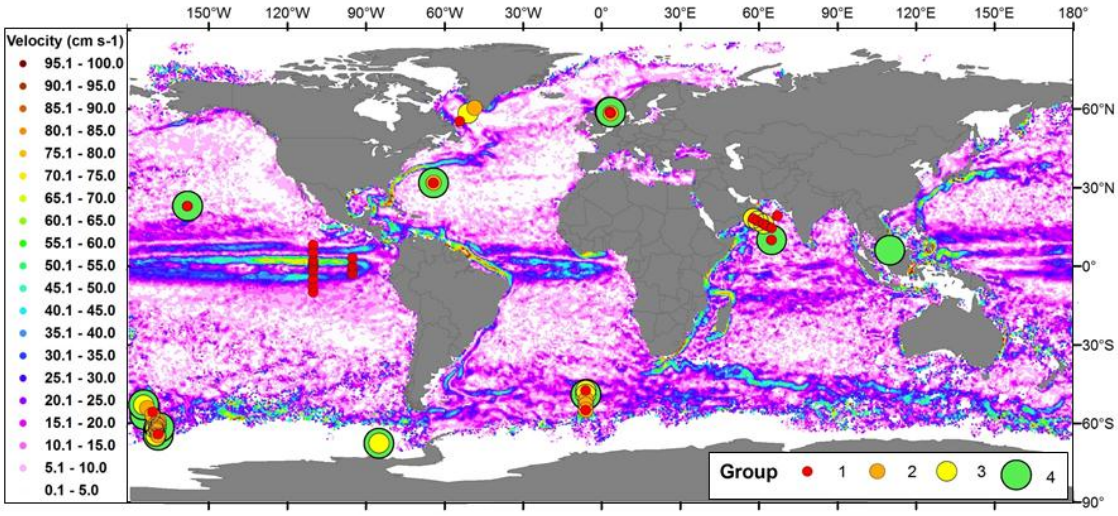

Figure 3.3: Global distribution of JGOFS samples (Buesseler 2011), overlain on annual mean surface current velocity (Lumpkin and Johnson 2013). Groups are those defined above: Group 1 consists of samples with High PP and low ThE (HL), Group 2 has low PP and high ThE (LH), Group 3 has high production and high export (HH) and Group 4 has low production and low export (LL).

Table 3.2: Summary data for the groups defined from meta-analysis of JGOFS sediment trap data (Buesseler 2011). Median primary production (PP, mmol m^{-2} yr^{-1}), POC flux estimated using ^{234}Th at the base of the photic zone (mmol m^{-2} yr^{-1}), ThE ratio (POC flux/PP) expressed as a percentage of surface production for groups in Figure 3. Hypothetical categories: local primary productivity is high and up-current productivity is also high (HH), sites where local primary productivity is low and up-current productivity is also low (LL), sites where local primary productivity is lower than up-current values and the resultant export ratio would be high (LH), and sites where local primary productivity is higher than up-current, resulting in a low export ratio (HL).

Group	1	2	3	4
PP	68.00 (±28.0)	20.30 (±13.30)	110.30 (±42.16)	47.46 (±13.37)
POC flux	2.72 (±1.78)	15.17 (±6.42)	21.83 (±7.32)	7.27 (±3.56)
ThE %	4.08 (±2.23)	54.77 (±24.8)	22.42 (±12.01)	16.46 (±4.63)
# traps	61	19	14	24
Theoretical Category	HH	LL	LH	HL

In order for currents to affect estimates of export to shallow traps, surface production would necessarily be highly spatially variable and currents would have to be very fast. The best example of this is from the traps in the Arabian Sea, where seasonal and spatial variations in primary production are well documented (Barber et al. 2001; Quigg et al. 2013b). The variability within the sediment trap sites from the Arabian Sea is primarily driven by differences in export (export and ThE ratio changes; Figure 3.3; Table 3.2), correlating with different seasons (not shown), and can be explained by examining the site placement relative to both production and surface current changes regarding the annual monsoon season. The switch from Group 3 (HH) to Group 1 (HL) (see overlap in Figure 3.3) in this region corresponds with the southwest monsoon (higher export in the summer with onshore winds, upwelling, and deepening of the mixed layer). There are two possible ways to obtain a higher ThE: increase export or decrease PP. Sediment trap samples collected in the winter have low ThE ratios, low POC export and fairly high PP, and fall into Group 1 (HL). Samples taken in the summer fall into Group 3 (HH), a season of upwelling due to the direction of the winds and currents (Flagg and Kim 1998). As a result of this upwelling, the summer ratio of PP to export is much higher, indicating that some of the POC in the traps may have come from upwelling regions up-current. Summer samples show a 38% increase in PP from the winter months; however these traps also have 87% increase in POC (81% increase in ThE) representing an additional 49% increase in export not accounted for by the increase in PP (calculated from Buesseler 2011). A potential source, the Somali Boundary Current (associated with the SW monsoon) has an average speed of 150 cm s^{-1} (Flagg

and Kim 1998). Using our model, particles collected in these Arabian Sea traps (at 100m depth) could originate between 51-760 km up-current (based on sinking speeds of faster sinking fecal pellets and slower sinking aggregates), which is within range of the increased surface production up-current (Figure 3.3).

Not all of the variability in export can be explained by accounting for currents, as evident at the long term monitoring stations: the Bermuda Atlantic Time-series Station (BATS) and the ALOHA North Pacific Station Time-series Station (Figure 3.3). Groups 1 - 4 overlap in the North Atlantic while Groups 1 & 4 overlap in the central North Pacific). Previous studies have demonstrated the variability in export POC in traps at the BATS corresponds to the passing of mesoscale eddies and/or with winter mixing (Sweeney et al. 2003). These seasonal influences are also evident in our findings by the overlapping of the different groups in the same sediment trap location (Figure 3.3). The ALOHA station traps also exhibited seasonality in export between summer (July-Oct; Group 4) and winter-spring (Nov-May; Group 1). Although the median PP values differ between the ranked groupings, the PP at station ALOHA is not highly variable (Group 1 PP_{mdn} = 49.95 mmol C m^{-2} d^{-1}; Group 4 PP_{mdn} = 43.29 mmol C m^{-2} d^{-1}). The difference between seasons at this site is driven by export (Table 3.2; Buessler 2011) which is likely explained by the predictable summer export pulses from the surface waters around ALOHA. These export pulses have been attributed to seasonal blooms of diatoms with symbiotic diazotrophs, increasing export in August to three times greater than that in the winter months (Karl et al. 2012).

All traps in the equatorial Pacific fall into Group 1 (Figure 3.3), representing relatively high productivity and low export (HL), with no temporal or spatial variability. Using equation 1 and considering the slowest sinking particles (Appendix A Table 1), the estimates of PP above the trap should be representative of local export, as the furthest calculated influence is only 1200 m up-current, in the North Equatorial counter current (Table 3.1). Satellite imagery and models show little spatial variation of PP within this area of influence (Laws et al. 2011). Thus, the relatively high PP in this region versus the relatively low export is not likely explained by currents. If the phytoplankton in this region typically form aggregates it may be possible that the production is carried further down current than our estimates (Table 3.1), especially if they were to become neutrally buoyant. This, however, would further depend on having only a very small zooplankton community which could repackage the aggregates into faster sinking particles. It is more likely that the microbial community in the warm waters of the tropics is rapidly converting PP into DOC (Carlson et al. 1994; Azam 1998; Jiao et al. 2010).

Meta-Analysis (Mesopelagic Bathypelagic Boundary). The average percent PP exported to the m/b boundary, according to the deep water trap data compiled and normalized by Honjo et al. (2008) is 1%. These data separate into seven distinct groups ($p = 0.001$; Figure 4). When ranked by their median values for PP, estimated export (EP; Laws et al. 2000), and POC export at the m/b boundary, these groups fall into the four hypothetical categories described above. Groups 1 and 7 (LH, yellow triangle and square respectively) are representative of traps with relatively low PP and high POC flux

(Figure 3.4; Table 3.3). Because surface productivity is high, our model estimates of EP for these categories over-predict the measured export.

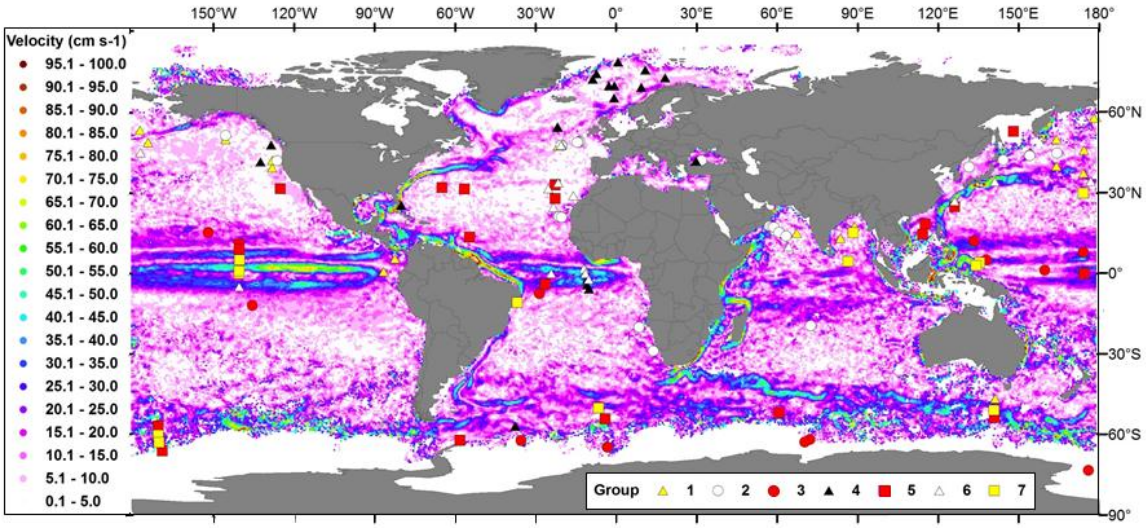

Figure 3.4: Global distribution of Honjo et al. (2008) samples, overlain on annual mean surface current velocity (Lumpkin and Johnson 2013). Groups defined in Table 3.

Group 2 in Figure 3.4 is representative of traps with high local PP and high POC flux (HH, Table 3.3; white circles). PP measured ranks highest (25.9 mol m^{-2} yr^{-1}) and measured POC flux is highest (0.24 mol m^{-2} yr^{-1}), with the second highest EP (4.70 mol m^{-2} yr^{-1}) (see Table 3.3). Similarly, Group 6 ranks near the top for both PP and POC flux (HH in Table 3.3; white triangles in Figure 3.4). Due to the similarities between local and up-current production, current velocity and horizontal advection likely do not affect these estimates of export as strongly, and these estimates may be representative of the percentage of export in high productivity regions. Groups 3 and 5 are representative of traps with low PP corresponding to low POC flux (LL, Table 3.3; red circles and squares

Figure 3.4). Similarly to Groups 2 and 6, these estimates may be representative of the percentage of POC flux but for traps with low/medium productivity.

Table 3.3: Summary data for the groups defined from meta-analysis of sediment trap data originally compiled by Honjo et al. (2008). Median primary production (PP, mol m^{-2} yr^{-1}), export production (EP, mol m^{-2} yr^{-1}), ef-ratio (EP/PP), flux measured in sediment traps normalized to the m/b boundary (mol m^{-2} yr^{-1}), calculated percentage of PP measured at m/b boundary for groups in Figure 3.4. Hypothetical categories: local primary productivity is high and up-current productivity is also high (HH), sites where local primary productivity is low and up-current productivity is also low (LL), sites where local primary productivity is lower than up-current values and the resultant export ratio would be high (LH), and sites where local primary productivity is higher than up-current, resulting in a low export ratio (HL)

Group	1	2	3	4	5	6	7
PP	15.00 (±3.68)	25.90 (±12.73)	4.40 (±1.82)	20.20 (±6.28)	8.20 (±1.97)	12.40 (±3.69)	7.20 (±1.70)
EP	2.00 (±1.47)	4.70 (±3.84)	0.70 (±0.32)	7.60 (±5.24)	1.20 (±1.05)	1.70 (±0.36)	1.05 (±0.30)
ef-ratio	0.13 (±0.08)	0.18 (±0.12)	0.16 (±0.02)	0.36 (±0.20)	0.15 (±0.10)	0.13 (±0.01)	0.14 (±0.02)
POC flux	0.17 (±0.06)	0.24 (±0.12)	0.03 (±0.01)	0.06 (±0.03)	0.06 (±0.01)	0.10 (±0.01)	0.15 (±0.04)
$\%PP_{exp}$ (export/PP*100)	1.14 (±0.69)	1.11 (±0.62)	0.64 (±0.50)	0.31 (±0.13)	0.68 (±0.33)	0.84 (±0.23)	1.68 (±0.74)
# traps	19	27	13	21	21	17	14
Theoretical Category	LH	HH	LL	HL	LL	HH	LH

Group 4 is representative of traps with high PP and correspondingly high EP with low POC flux measured in traps (HL, Table 3.4; black, Figure 3.4). Nine of the 21 traps that fall into this group are found in the Greenland and Norwegian seas, a highly dynamic region known for deep water formation and large increases in PP during the spring (von Bodungen et al. 1995). Group 4 has the second highest median PP (20.2 mol

m-2 yr-1), the highest EP out of the euphotic zone (7.6 mol m^{-2} yr^{-1}), and the second lowest POC flux (0.06 mol m^{-2} yr^{-1}; Table 3.3). It is important to note that the EP is for the euphotic zone whereas POC flux is measured much deeper at the m/b boundary, and much production may be lost in the mesophotic zone (Buesseler et al. 2007). However there may also be loss due to strong sub-surface current regimes in this area.

Table 3.4: Export Ratios calculated from the literature, and the median value for the data sets presented herein. The Export value is calculated using the reported ratio and global production of 52.1 Gt C yr^{-1}.

Ref	Ratio	depth	method	Export Gt C yr^{-1}
JGOFS	0.085	Euphotic	ThE - traps	4.44
m/b Honjo 2008	.15	Euphotic	Model Laws 2000	7.82
	.01	M/B boundary	Sed Traps	0.52
Laws 2011	0.18-0.30	euphotic	Model	9 - 16
Dunne 2005	0.04-0.72	euphotic	Model	2 – 38
Falkowski 2003	0.31	0 – 100 m	Model Laws 2000	16
	0.33	0.1 – 1 km	Model Laws 2000	17
	0.18	>1 km	Model Laws 2000	9

The distribution of groups globally may be influenced by a multitude of factors; analysis of these distributions yields insight into the precision of our global flux estimates/measurements. These data represent yearly averages of fluxes and thus some of the variability in currents is smoothed out. Also because of the long deployments of the sediment traps, the likelihood that wandering currents may impact export measurements is increased, but these influences will vary regionally. Slow, shallow eastern boundary currents, such as the California Current system will have less of an effect on the measurement of particulate in traps. The changes in traps will also be more

variable within a smaller area due to the compression of current influences (25-650 km based on average current depth influence of 300 m and velocity of 25 cm s^{-1}). The two traps at the northern end of this dynamic region are in group 4 (HL; Figure 3.4 black triangles). Productivity in this region is known to be high; however the up-current productivity is very low. Slower current regimes will have a lesser effect on the horizontal transport of particles, including a contraction of spatial variability. Traps found midway down the coast of this region are categorized as LH (offshore) and HH (nearshore) clearly collecting more than their up-current counterparts. Finally, the trap furthest south (pink square) is in Group 5 (LL), and is not affected by the increased production in this upwelling regime.

The equatorial Pacific represents an area with very shallow (~200 m, Johnson et al 2001), slow currents (20-30 cm s^{-1}, Johnson et al 2001) representing an area where currents will likely have little influence (15-350 km). The array of traps transecting the equatorial region, group according to the different currents present (North Equatorial Current, Equatorial Counter Current, South Equatorial Current). The presence of Group 7 (LH, yellow square) is interesting because the currents are not likely causing the disparity in PP and Flux, suggesting the flux is sourced directly above the traps. The high export measured may be indicative of the export in this region or perhaps the role of microbes in equatorial waters is overestimated.

Typically western boundary currents are deep, fast and slender, producing mesoscale eddies as they leave the coast. Currents in these regions will likely have the greatest effect on export measurements (Eq 1). The Kuroshio Current can be up to 1 km

deep with an average velocity of 130 cm s^{-1}. Using our model the distance particles can be carried range from 450-11230 km. Traps in this region near the coast fall into Group 6 (HH) but those in the Kuroshio extension change to Group 1 & 7 (LH). These traps are within the specified distance likely to be affected by currents (Table 1).

Clearly, current velocity is capable of driving large changes in fluxes hitherto attributed only to other mechanisms which include sediment trap inaccuracies (Michaels et al. 1994), organic matter remineralization (Feely et al. 2004), mesopelagic attenuation (Buesseler et al. 2007; Lomas et al. 2010), and phytoplankton community structure (Laws et al. 2000; Dunne et al. 2005; Guidi et al. 2009).

Summary

Low PP with high POC flux indicates that traps are collecting a greater percentage than we would estimate without horizontal transport, suggesting increased input from up-current. High PP with low POC flux indicates a larger percentage may be missed than we would expect. When using surface productivity to estimate export, low PP and high POC flux leads to an underestimation. When using traps, high PP and low POC flux leads to underestimation because it implies that some matter is being advected. Our analysis of export to the m/b boundary shows large discrepancies in actual/predicted export with ~31% traps "over collecting" and ~20% of the traps "under collecting" compared to local surface production and modeled estimates. Over half of the export measurements (traps) analyzed in this study inaccurately represent POC flux. Studies have attributed these inconsistencies to sediment trap inaccuracies (Michaels et al.

1994), organic matter remineralization by bacteria (del Giorgio et al. 1997; Azam 1998; Jiao et al. 2010), and meso-pelagic attenuation (Buesseler et al. 2007; Lomas et al. 2010). While these may represent significant losses to the amount of particulate matter exported, this study has demonstrated that the influence of currents should also be considered in determining the export flux, and thereby both vertical and horizontal processes.

Current velocities significantly influence POC measurements in deep sediment traps (Fig. 3.1B). As current velocities increase measured POC flux decreases. Using this simple model, velocities greater than 25 cm s^{-1} can transport fast (250 m d^{-1}) sinking particles beyond 300 km. Thus it is likely that traps in current regimes above this velocity are under-collecting POC and thus lowering our estimates of POC exported from the surface. Approximately one-fifth (22 out of 132) traps are located in current regimes with velocities greater than 25 cm s^{-1}, we are likely missing a large amount of flux to the deep sea.

By using equation (1) to estimate horizontal advection of particulates (Table 3.1) it is clear that currents can play an important role in trap measurement variability. Even the fastest sinking particles in fast currents can be transported ~250 km and potentially across entire oceans. It is likely that during these vast transports much repackaging (Turner 2002) could occur and thus particles will be exported from the surface much sooner than our model estimates. Notably, when evaluating the global distribution of these measurements and traps, the central parts of the ocean gyres are excluded. These vast areas are known to collect large quantities of ~~"t~~rash" (Lumpkin and Johnson 2013).

Waite et al (2014) also show particle concentration and sorting in mesoscale eddies. It is possible that the subdued current velocities in the central parts of ocean gyres, or other mechanisms, similar to those described in Waite et al. (2014), would encourage sedimentation and thus represent areas of the highest export of particulate matter as well as —trash."

The measured export ratios for the two data sets from the euphotic zone are at the low end of the model estimates. It is important to note that small changes in the export ratio represent large changes in export (Table 3.4): an increase in the export ratio from 0.2 to 0.3 nearly doubles the export of particulate matter from surface waters. Actual export (traps) and estimated export (models) do not co-vary, despite the global averages being fairly similar (Table 3.4). Regions where low export is predicted by existing models correspond to some of the largest measured export numbers. Further, it is becoming more and more clear that the contribution of new production (roughly equal to export production Eppley and Peterson 1979) from N_2-fixation is much greater than previously estimated (Subramaniam et al. 2001; Falcón et al. 2004; Capone et al. 2005). The primary regions of N_2-fixation are warm, low nutrient waters of the ocean gyres (Monteiro et al. 2011).

If we accept that currents drive some of the documented variability in sediment trap measurements, then equation 1 represents a fair estimate of their impact. The velocity of the current has a large impact on the horizontal distance particles can be transported while also modifying the range over which they will settle out of the overlying water column. This could have profound implications for estimates of C-

export from the surface ocean as well as our understanding of subsurface ecosystem structure, biomass and function. Future challenges will involve applying currents which are appropriate to different depths in the water column rather than a global average; this would enhance the models applicability to shallow versus deep traps.

CHAPTER IV

CARBON AND NITROGEN FIXATION: SIMULTANEOUS QUANTIFICATION OF ACTIVE COMMUNITIES AND ESTIMATION OF RATES USING FLUORESCENCE IN SITU HYBRIDIZATION AND FLOW CYTOMETRY

Introduction

Carbon (C) is the currency of the ocean; its importance is measured either through carbon dioxide (CO_2) sequestration (~48% of anthropogenic CO_2 are sequestered by the oceans; Sabine et al. 2004; Falkowski et al. 2003) or fisheries (average catch of 68 Mt yr^{-1} equating to primary production of 3.5 Gt C yr^{-1}; Chassot et al. 2010). Primary production converts atmospheric CO_2 into organic carbon, the critical first step in making inorganic carbon biologically available. Multiple methods exist for quantification and/or classification of phototrophs including chlorophyll *a* measurements, pigment analysis using high performance liquid chromatography (Jeffrey et al. 1997) and flow cytometry (Marie et al. 1997; Lomas et al. 2011). Methods to measure rates of primary production include light/dark bottles (Gaarder and Gran 1927), ^{14}C uptake (Steeman-Nielsen 1952), stable isotopes of oxygen (^{16}O, ^{18}O and ^{17}O - Bender et al. 1987; Luz et al. 2000) or fluorescence kinetics (Kolber and Falkowski 1993; Kolber et al. 1998).

It is generally accepted that primary production in the open ocean is limited by nitrogen (N) (Vitousek and Howarth 1991; Tyrell 1999; Howarth and Marino 2006; Moore et al. 2013). Determination of the fate of fixed C can be estimated by examination

of the source of N (Dugdale and Goering 1967). In recent decades, it is increasingly clear that the primary source of new N in the oligotrophic ocean is microbially mediated biological N fixation (Gruber 2005, Gruber 2008; Fawcett et al. 2011; Moore et al. 2013). In theory, if accurate measurements of biological N fixation can be made, C sequestration and food web production can also be estimated (see Eppley and Peterson, 1979). However, similar issues exist for quantification and activity measurements of the microbial community involved in biological N fixation that exist for the photosynthetic community. Disparate techniques are used for quantification (DAPI and other nucleic acid stains) and determination of the rates of targeted processes including acetylene reduction reactions (Hardy et al. 1968) or $^{15}N_2$ uptake (Neess et al. 1962; Montoya et al. 1996; Mohr et al. 2010).

Thus far, quantification of different carbon or nitrogen fixing populations and estimates of their respective fixation rates have used fundamentally different techniques. Consequently, the goal of understanding the connectivity of these two cycles is replete with assumptions. To improve our understanding, microbial biologists need to not only determine composition of the microbial community (DNA) but to include activity (rRNA), and recently, specific activity (mRNA) within these populations. Fluorescence in situ hybridization (FISH) has been extensively employed to determine abundance and general activity (using rRNA probes) of prokaryotes in aquatic environments (Kirchman 2008). Transcript abundance (mRNA) of RUBISCO (Paul 1996; John et al. 2007; Corredor et al. 2004) and nitrogenase (Martin-Nieto et al. 1991) correlate with their respective rate measurements. mRNA FISH is a tool capable of community

quantification while simultaneously quantifying the number of organisms performing a specific function (Pilhofer et al 2009). Due to the low abundance of target sequences (mRNA < rRNA, Pernthaler and Amann 2004) amplification of the signal using tyramide signal amplification (TSA) is necessary. Most studies have been limited to very specific groups (Lefort and Gasol 2013; Lee et al. 2012), this study aims to target processes that span taxonomic and genetic variability. By incorporating universal multiple oligonucleodite probes complimentary to multiple functions actively expressed in the sample population we can begin to understand the connectivity of these processes in a less theoretical way.

The aim of this study was to develop a concise method employing TSA-FISH with general oligonucleotide probes complimentary to *rbcL* (RUBISCO, primary production) and *nifH* (nitrogenase, nitrogen fixation) mRNA transcripts allowing simultaneous quantification of C and N fixing communities as well as estimation of C and N fixation rates within those communities. Application of this method eliminates many assumptions and allows a more direct understanding of the connectivity of these two dynamic cycles.

Methods

Probe Design. In this study, our aim was to target community function, instead of tagging a unique species. The challenges this presents are twofold. First, finding a conserved target region in the gene sequences across a diversity of organisms, and second, allowing enough generality in hybridization optimization to tag all functioning

representatives. We addressed the first issue during probe design (Tables B1 & B2). We compiled 113/124 (*rbcL/nifH*) sequences including 7/4 Phyla representing 17/15 orders and 26/37 genera from GenBank (http://www.ncbi.nlm.nih.gov/nucleotide/). These were aligned using MEGA5/ClustalW (gap opening penalty of 15, gap extension penalty of 6.6, http://www.megasoftware.net/). The most conserved region was chosen and further analyzed using OligoCalc (v3.26) to ensure no hairpin formation potential, 3‘ complementarity, or self-annealing (http://www.basic.northwestern.edu/biotools/OligoCalc.html). Comparisons of these probe sequences were performed against the GenBank database to verify specificity to primary producers and nitrogen fixing organisms. NON338, a sequence commonly employed as a negative control, was used in this study (Wallner et al. 1993; Lee et al. 2012).

To eliminate background fluorescence from nonspecific binding of the amplification reagent used in visualization, horseradish peroxidase was directly attached (van de Corput et al. 1998) to the 5‘ end of the oligonucleotide probes (reverse compliment of the target sequence, Tables B1 & B2) (Life Technologies Invitrogen custom oligonucleotide probes). Because we tagged both prokaryotes and eukaryotes, a traditional positive control was not used. Instead, we verified target presence with SYBR Green I nucleic acid stain (1:10000, Molecular Probes). After initial determination of accurate *rbcL* probe hybridization to *Synechococcus sp*. (not shown), this culture and probe was run as a positive control verifying chemical and probe functionality.

Cultured Strains, Environmental Samples, and Cell Fixation. In order to ensure accuracy while maintaining generality, *rbcL* probe specificity was determined using cultured phytoplankton that span the evolutionary spectrum, including: cyanobacteria (*Synechococcus* sp.), dinoflagellates (*Thoracosphaera hemii*), diatoms (*Thalassiosira oceanica* and *Amphora coffeaeiformis*), coccolithophores (*Emiliana huxleyi*), and green algae (*Dunaliella tertiolecta*) (Table 4.1). Cultures were grown at optimal temperatures according to Provasoli-Guillard National Center for Culture of Marine Phytoplankton (https://ncma.bigelow.org/) in f/2 media (Guillard and Ryther 1962) on a 12:12 light:dark cycle at 19^0C or 24^0C and ~130-150 μmol photons m^{-2} s^{-1}. Media recipes on the culture collection website were followed, with Gulf of Mexico seawater used as the base for the f/2 media. The bacterium *Escherichia coli*, grown in LB broth (LB Broth Base Tablets 50 ml, TRU MEASURE, Sigma Aldrich L7275-100TAB) at 35^0C, was used as a negative control.

Table 4.1. Cultures used to test hybridization of *rbcL* probe. Strain and group of cultures tested, including temperature used for culture growth.

Strain	Source	Group (Class)	Temp ºC
Synechococcus elongatus	CCMP 1379	Cyanobacteria (Oscillatoriophycideae)	24
Emiliania huxleyi	CCMP 372	Coccolithophore (Coccolithophyceae)	24
Amphora coffeaeformis	CCMP 128	Diatom (Bacillariophyceae)	24
Thoracosphaera heimii	CCMP 1069	Dinoflagellate (Dinophyceae)	24
Dunaliella tertiolecta	CCMP 364	Green Algae (Chlorophyceae)	19
Thalassiosira oceanica	CCMP 1004	Diatom (Coscinodiscophyceae)	24
Escherichia coli	ATCC 11775	Gamma proteobacteria	37

Environmental samples were collected to test hybridization of probes for both *rbcL* and *nifH*. Samples were collected in the Gulf of Mexico (between 26-27^{0}N, 86-92^{0}W, June 2011) across warm and cold core eddy features where biological nitrogen fixation has been documented (Dorado et al. 2012). Samples were also collected from Galveston Bay (Texas, USA; 29º34 N, 94º50 W) representing an environment where biological nitrogen fixation is unlikely. Water samples were concentrated using gentle vacuum filtration (<2 mmHg) onto a Whatman Nucleopore polycarbonate track-etched membrane 0.2 µm filter (09-300-61). Membrane filters were placed in a microcentrifuge tube with phosphate buffered saline (PBS, autoclaved and 0.2µm filtered; 750 µl) and cells were vortexed off the filters so they could be analyzed using flow cytometry (Sekar et al. 2004). Samples were preserved with molecular grade paraformaldehyde (PFA, 4x final concentration) overnight at 4^{0}C (Yan et al. 2010). Cells were then collected via centrifugation (13000 rpm, 5 min) and PFA was removed; cells were re-suspended in absolute ethanol and stored at -80 ^{0}C.

Diel Cycle Sample Collection. Primary production and nitrogen fixation rates vary on a diel cycle (Berman-Frank et al. 2007; Mohr et al. 2010). Laboratory cultures of *Synechococcus sp*, *T. hemii*, and *T. oceanica* were grown in triplicate batch cultures using the same media and growth conditions described above. Samples were harvested every 3 hours over a 24 hr cycle and processed for ^{14}C uptake using the method of Lewis and Smith (1983); additional aliquots were preserved for mRNA FISH. Samples were inoculated with ^{14}C sodium bicarbonate (final conc. 1µCi mL^{-1}) for 20 min. at 16 light intensities (0- 1800 µmol photons m^{-2} s^{-1}) at 24^{0}C in a photosynthetron. Triplicate blanks

and total counts (to determine specific activity) were prepared. Incubations were terminated with buffered formalin (50 μL) and all samples acidified for 24 hrs. Radioactivity was measured using a Beckman LS8100 scintillation counter.

To elucidate the importance of accounting for diel periodicity in primary production, the median value for replicate samples from the TSA FISH analysis were interpolated (linear) over the 24 hr cycle. These data were then integrated over various time periods (12 hrs light and entire 24 hrs) to compare with standard protocols (JGOFS; Knapp et al 1996). The amplitude (minimum PP subtracted from maximum PP) was computed to demonstrate the intensity of the diel variation.

Environmental samples for analysis of *nifH* mRNA expression versus ^{15}N uptake were collected in the eastern Indian Ocean during two cruises in August and September of 2012 (Figure B1). Aliquots for mRNA FISH were collected every 3 hours, while ^{15}N uptake measurements were made every 6 hours over a 24 hr cycle. Four acid-washed, polycarbonate, incubation bottles rinsed 3 times with seawater immediately prior to collection were filled with sample water. Parafilm was used to ensure no gas bubbles were trapped in the threads of the septum bottle caps. The direct addition of $^{15}N_2$ tracer-enriched seawater was used to estimate N_2 fixation rates (Mohr et al. 2010; Groβkopf et al. 2012). The $^{15}N_2$ tracer-enriched artificial seawater was prepared by degassing and filtering (0.2 μm Sterivex filter) YBCII media (Chen et al. 1996) and stored in 3 L gas tight Tedlar bags then spiked with 1 mL $^{15}N_2$ (98 atom%; Aldrich) gas per 100 mL YBCII media. Incubations were initiated by introducing $^{15}N_2$ tracer-enriched seawater aliquots of 2.6 % of the total incubation volume. Bottles were gently rocked ~50 times to

enhance gas equilibration in the seawater. Bottles were incubated for 6 hours in an on deck incubator covered with neutral density screening to simulate in situ light intensities and under ambient sea surface temperatures. Subsequent time points were spiked with enriched YBCII at the end of the previous incubation. Experiments were stopped by collecting the suspended particles from each bottle by gentle vacuum filtration (pressure drop < 2 mmHg) through a 25-mm precombusted GF/F filter. Filters were frozen in liquid nitrogen and immediately stored in a -80 ºC freezer while at sea. During subsequent laboratory analysis, filters were acidified and dried overnight at 60 °C. Further determination of total N and $\delta^{15}N$ was carried out using a continuous flow system consisting of a SERCON 20-22 mass spectrometer connected with an Automated Nitrogen Carbon Analyzer (Sercon, UK). Samples for natural particulate organic nitrogen (PON) abundance determinations were obtained by gentle vacuum filtering of 4 L water samples onto precombusted GF/F filters. Absolute N uptake rates (ρ in nmol N L^{-1} h^{-1}) were calculated following Dugdale and Goering (1967). Detailed explanation on uptake rates calculations can be found in the Protocols for the Joint Global Ocean Flux Study (Knap et al. 1996).

Fluorescence *in situ* Hybridization for Flow Cytometry. The hybridization and detection protocol used herein is based on Pernthaler and Amann (2004), with some modifications. Preserved laboratory and environmental samples were collected via centrifugation (13000 rpm for 5 min) and ethanol removed. Cells were re-suspended in 1x phosphate buffered saline (PBS; 0.14M NaCl, 2.7 mM KCl, 10.1mM Na_2HPO_4, 1.8 mM KH_2PO_4), and centrifuged again to remove PBS (this process will hereafter be

referred to as a wash/washed step). Endogenose peroxidase activity and RNAses were quenched/removed by incubation of samples in 0.1% diethylpyrocarbonate (DEPC) for 12 min at room temperature (RT, Pilhofer et al. 2009) followed by a wash to remove DEPC. Cells were permeabilized by incubation in 5 mg ml^{-1} lysozyme for 1 hr at 35 ^{0}C, followed by a wash in 1x PBS, and re-suspended in 1% sodium dodecyl sulfate (SDS) for 1 hr at room temperature (RT, Pernthaler et al. 2004). Post permeabilization, the cells were incubated in 0.01% H_2O_2 for 10 min at RT to quench any newly exposed peroxidases.

Specificity of the oligonucleotide probes was optimized using various formamide concentrations (Hougaard et al. 1997) because the horseradish peroxidase (HRP) attached to the 5‘ end of the probes is unstable above 35^{0}C (Pernthaler et al. 2001). It should be noted that the equation used to determine specificity of oligonucleotide probes, at its most stringent, allows for 20% mismatch (Hougaard et al. 1997). Cell suspensions were incubated at 35 ^{0}C for 1hr in hybridization buffer, containing 1-150 µl formamide, 30 µl 20x sodium citrate buffer (SSC, Amresco), 60 µl 10% w/v dextran sulfate, 30 µl 10% w/v blocking solution (component D, Invitrogen TSA Kit #6, T-20916), 15 µl 4 mg ml-1 yeast RNA, 6 µl 10 mg ml-1 sheared salmon sperm DNA, and 9-159 µl autoclaved MilliQ water. Oligonucleotide probes were diluted in hybridization buffer and incubated at 35 ^{0}C for 5 min, then added to cell suspensions (final concentration between 100-500 ng µl-1) and incubated for 24 hrs at 35 ^{0}C.

Cell suspensions were washed with MilliQ, then with wash buffer (0.2x SSC, 0.01% w/v SDS) at 35 ^{0}C for 30 min. Probes were detected using 1:100 Alexa 647

labeled tyramide (Invitrogen TSA Kit #6) in amplification buffer (0.1% blocking solution, 1% dextran sulfate 2M NaCl, 0.0015% fresh H_2O_2) for 30 min at RT. Cells were washed and re-suspended in PBS and counter stained with 30 mM tripotassium citrate and SYBR Green I nucleic acid stain (Invitrogen, Catalogue #S7563) 1:10000 then incubated for 15 min at 35 ^{0}C.

Flow Cytometry. Samples were enumerated using a Beckman Coulter Gallios flow cytometer equipped with 488 nm and 638 nm lasers. Fluorescence was measured using bandpass filters corresponding to emissions for SYBR (filter: 525/30) and Alexa 647 (filter: 695/30). Measurements for forward scatter (FS, roughly equivalent to size), and side scatter (SS, indicator of granularity) were also collected (Hyka et al. 2012). The concentration of 15 µm beads (Coulter CC Size standard L15; 6602797) was determined using a haemocytometer. These were added to samples prior to flow cytometric analysis so that accurate sample volumes could be determined. Raw data was processed using Kaluza (V6). Living cells were distinguished from other particulates using FS versus SYBR fluorescence plots. These events were then plotted using FS versus red fluorescence (Alexa 647). Gates were drawn on control plots to ensure that unhybridized cells were not counted. These gates were transferred to sample plots (with corresponding formamide concentrations). Positive results, if present, in the negative controls were subtracted from the corresponding samples.

Results & Discussion

Method Optimization. Successful *in situ* hybridization of mRNA depends on optimization of a number of steps including permeabilization and probe specificity, as well as minimization of background fluorescence and non-specific binding (Table 4.2). The first obstacle in probing a great diversity of organisms is the accompanying variety of cell walls and tests in the target population, making permeabilization optimization difficult. Previous studies have used minimal treatments to avoid cell loss (Table 4.2). These treatments were attempted initially, but binding did not occur in our samples (data not shown). When permeabilization was increased (incubation in 5 mg ml^{-1} lysozyme for 1 hr at 35^0C, washed, and incubated in 1% SDS for 1 hr at RT) probes bound to targets. This permeabilization treatment was successful for all cultures and environmental samples, including phytoplankton with coccoliths (*E. huxleyi*), theca (*T. heimii*) or silicified frustles (*A. coffeaeformis, T. oceanica*) (Table 4.1; Figure 4.2). However, the effect on cell density varied between them, as evidenced by visualization of the pellet after treatment. *T. hemii* showed the greatest change in visual loss of the pellet; however cells were successfully hybridized, indicating that the target cells themselves were not lost.

Minimizing background fluorescence is difficult when targeting photosynthetic organisms given the intrinsic fluorescence of the target cells. Storage in absolute ethanol and subsequent permeabilization steps reduced intrinsic fluorescence. In addition, the sensitivity of the photomultiplier tubes in the flow cytometer were adjusted so that intrinsic fluorescence was accounted for with unhybridized controls. Quenching of

endogenous peroxidase activity is essential in reducing background fluorescence by limiting binding of tyramide-fluorophore to non-target areas. Optimization of this step was essential as the chemicals used can reduce targets as well as target integrity, and insufficient quenching can lead to difficulties differentiating between positive target and background fluorescence (see Figure 4.1). Hence, we tested nine concentrations of H_2O_2 (0-1% for 10 min at RT) on *Synnechococcus sp*. and found maximum differentiation of positive target to background fluorescence was achieved at 0.01% H_2O_2 (Fig. 4.1). Separation of the microbial community from background fluorescence was enhanced using SYBR Green I as a counter-stain. SYBR has a strong affinity to double stranded DNA and binds to single stranded DNA and RNA at lower affinities (Marie et al. 1997) allowing differentiation of cells to background particulate. SYBR positive cells (were selected and subsequently analyzed for red fluorescence (Alexa 647). Red positive events are cells that have been successfully hybridized with mRNA tags. Thus, the total microbial community (SYBR positive cells) and the proportion showing positive target fluorescence (Red positive cells) could be quantified.

Table 4.2. Steps and methods involved in optimization of FISH.

Process		Reference
Fixation	2% PFA 30 min RT	Pernthaler and Amann 2004 Pilhofer et al. 2009
	0.1% PFA	
	2-4% PFA 1-24 hrs	Pernthaler et al. 2001
	5-10% Formalin Overnight	Yan et al. 2010
	4% PFA 12-24 hrs 4^0C	This Study
Storage	Collect and resuspend cells/pellet in molecular grade 100% EtOH and store at -80ºC	
Permeabilization	[5mg ml^{-1}] lysozyme 30 min RT	Pernthaler and Amann 2004 Pilhofer et al. 2009
	96% EtOH	Lee et al. 2012
	7% Tween20	
	0.1% DEPC 12 min RT	Pernthaler et al. 2002
	Or 0.5% SDS 10-15 min	
	[5mg ml-1] lysozyme 30 min RT	This study
	1% SDS 1 hr RT	
Quenching	0.1% DEPC 12 min RT	Pernthaler and Amann 2004 Pilhofer et al. 2009
	1-3% H2O2 60 min RT (kit)	Lee et al. 2012
	0.1% DEPC 12 min RT	This study
	0.01% H_2O_2 10 min RT	
Probe concentration	250 ng μl^{-1} 24 hrs	Pernthaler and Amann 2004 Pilhofer et al. 2009
	25 ng μl^{-1} 2.5 hrs	Lee et al. 2012
	50 ng μl^{-1}	Pernthaler et al. 2004
	Probe vs cell conc. important beyond just adding probe	This study
Fluorophore concentration	0.25-0.5 µg ml^{-1} 5 min RT	Pernthaler and Amann 2008 Pilhofer et al. 2009
	1:50	Lee et al. 2012
	1:100 5-10 min RT	kit
	1:100 30 min RT	This study

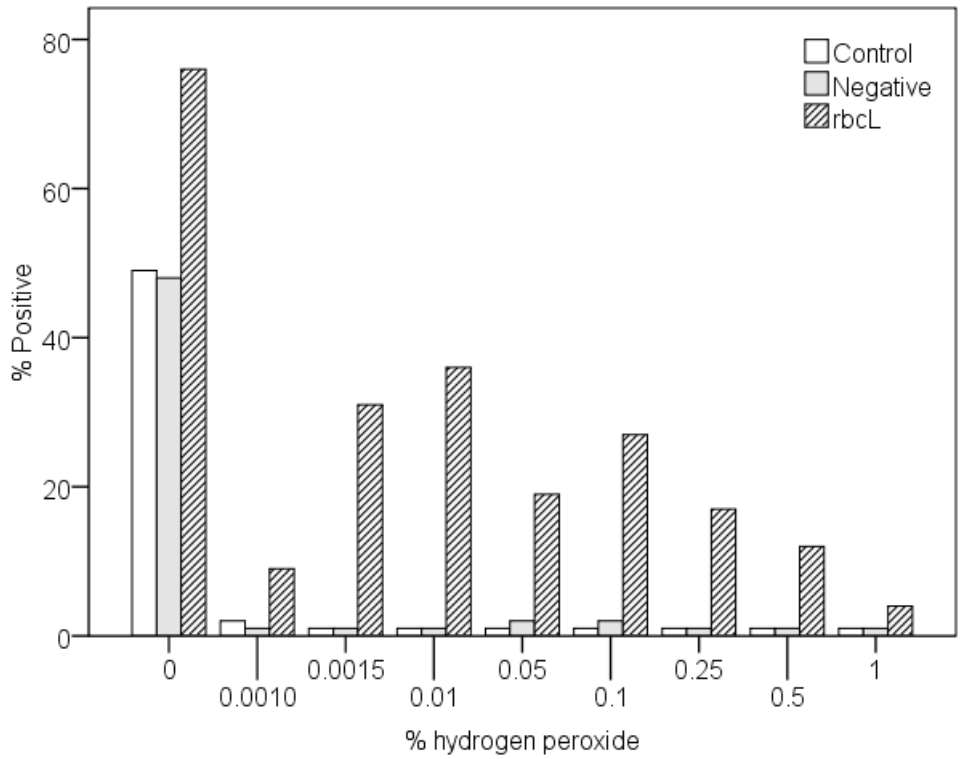

Figure 4.1. Optimum quenching conditions for TSA FISH. Quenching test performed on *Synechococcus sp*. Bar values are percent positive cells. All quenching treatments were performed on the same sample using 25% formamide for the *rbcL* probe and 40% formamide for the negative probe (equivalent specificities adjusted for GC%) and 250 ng μl^{-1} of oligonucleotide probe. Greatest relative fluorescence intensity was achieved with no quenching, but visual separation of *rbc*L hybridized probes was not possible from negative probe hybridized. Maximum differentiation and positive hybridization (> 35%) is achieved at 0.01% H_2O_2.

Because hybridization temperature and probe concentration both affect hybridization, a matrix of formamide concentrations (used to account for a fixed hybridization temperature) and probe concentrations was performed on five different samples for *rbcL*: *Synechococcus sp*., *T. hemii*, *T. oceanica*, Gulf of Mexico (open ocean), and Galveston Bay (coastal) (Figure 4.2). Formamide concentrations of 25% (equating to a minimum homology of 73% between probe and target) yielded maximum

hybridization for all of the samples (Figure 4.2). The effect of probe concentration varied between samples and appeared to be primarily a function of cell concentration (data not shown). It is important to create a ―probe driver situation", which occurs when all target sequences are hybridized and excess probe is removed in subsequent washes (Pernthaler and Amann 2004). Hybridization specificity was purposefully less stringent here than previous studies (Pernthaler and Amann 2004; Lee et al. 2012; Biegala et al. 2003) in order to be general enough to capture processes across taxonomically distinct groups. Therefore, the need for negative controls was paramount. *E. coli* (negative control) did not hybridize using the methods described in this study. Further, the cultures used for verification of the positive detection using the *rbcL* probe were monospecific, but not axenic; and the bacterial population present was not tagged (Fig. 4.3). Additionally, negative control probes were simultaneously applied to corresponding samples to ensure there was no non-specific binding of the oligonucleotide probes (<3% dependent upon probe concentration) (Fig. 4.3).

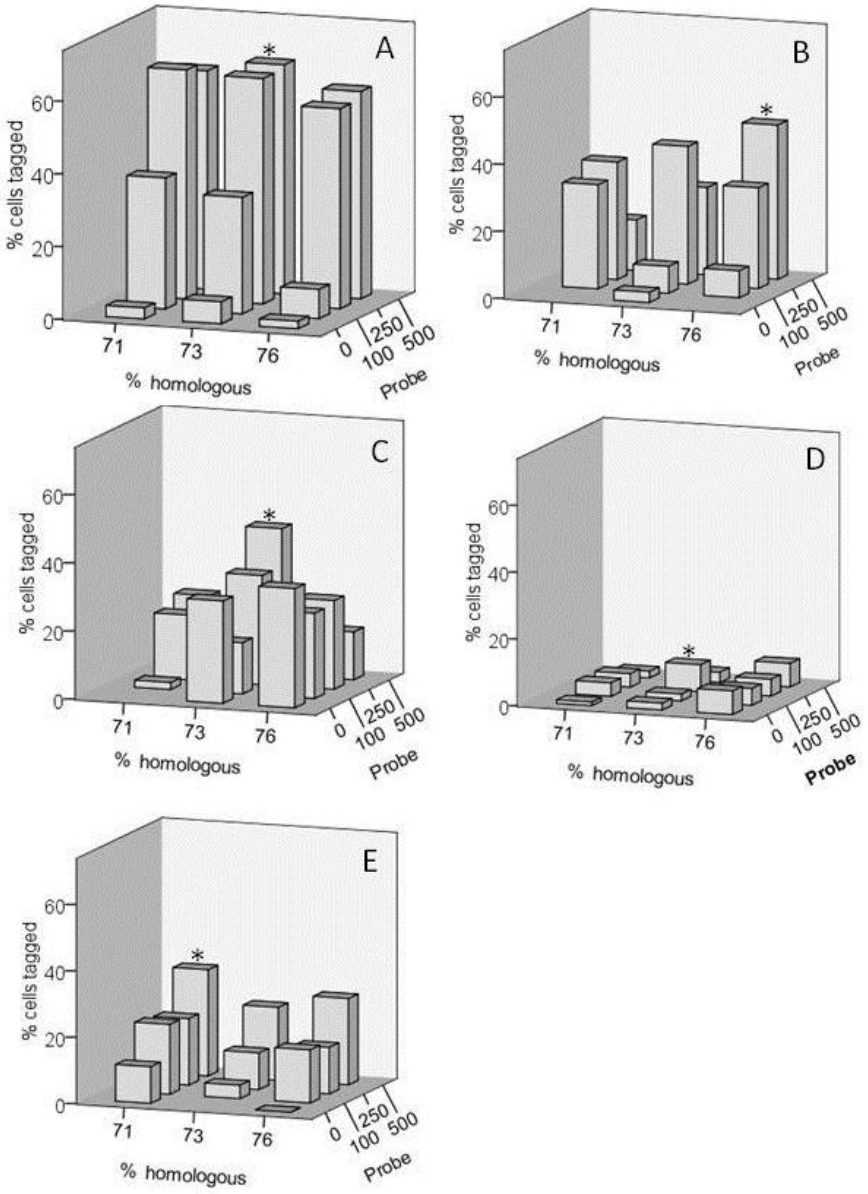

Figure 4.2. Percent hybridization of *rbcL* probe using cultures and environmental samples. Results of the matrix of formamide concentration (columns) vs. probe concentration (rows) for the *rbcL* oligonucleotide probe for (A) *Synechococcus sp*., (B) *T. hemii*, (C) *T. ocean,* (D) blue water Gulf of Mexico, and (E) coastal Galveston Bay, Texas. Colors are % positive probe hybridized minus % negative probe hybridized. The asterix represents the combination that yielded the highest percentage hybridization for each sample. Patterns are similar across the range of culture and environmental samples, that is, maximum differentiation is achieved using 25% formamide (equating to a minimum homology of 73% between probe and target). The concentration of probe added needs to exceed the number of targets, thus maximum hybridization is achieved at high probe concentrations. * represent treatment with maximum hybridization.

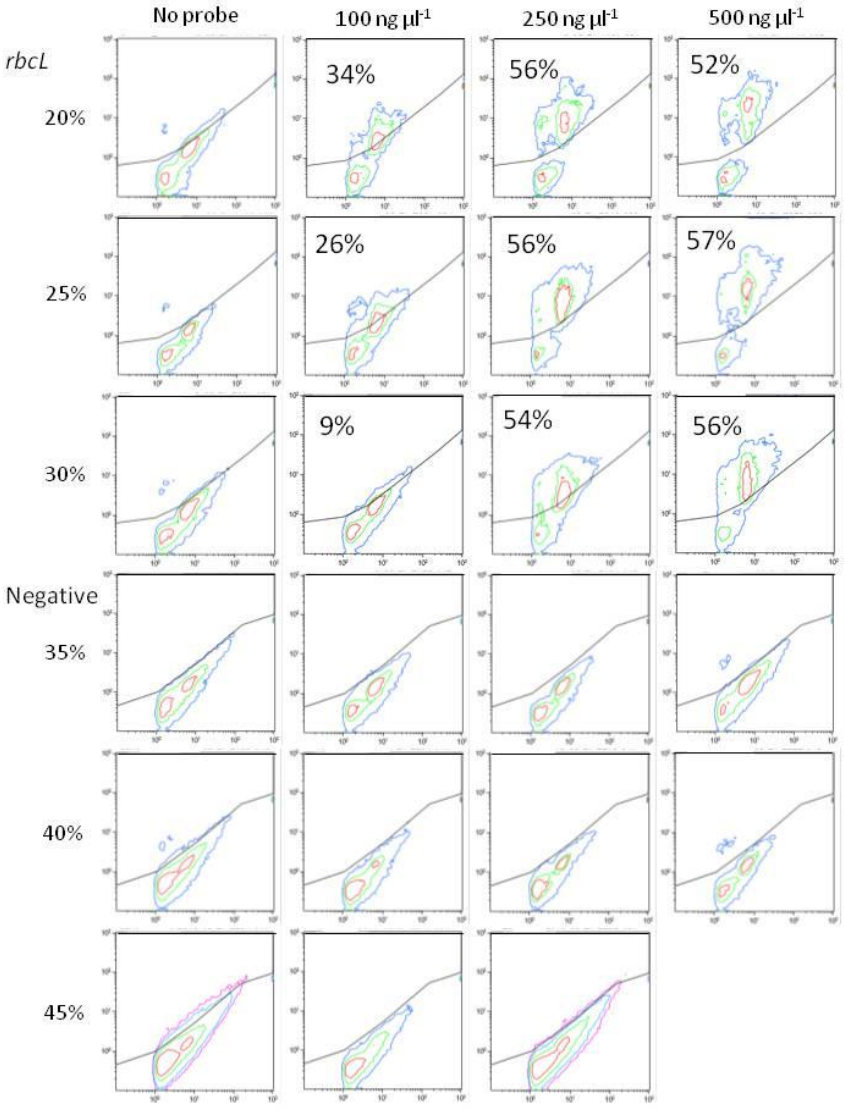

Figure 4.3. Results of matrix concentration tests on *Synechococcus sp*. for *rbcL* and negative control probes. A gate was drawn on controls (no probe) so that a minimum number of cells were counted as positive. This gate was then applied to all remaining treatments. Very few events were counted as positive in any of the negative controls (lower 12 panels); those present (< 3%) were subtracted. The percentages include the small microbial community present in the culture. Increasing specificity through increasing formamide concentration decreases target hybridization, especially at low probe concentrations (upper 12 panels). These panels also make clear the importance of creating a probe driver situation, while there is apparent tagging at the lowest probe concentrations the differentiation between hybridized and unhybridized cells is less, and minimally different from the control. Axes are arbitrary units, showing only relative changes in y = red fluorescence and x = size.

Similar matrix combinations were run for *nifH* oligonucleotide probe on samples where biological nitrogen fixation should be occurring (open ocean Gulf of Mexico) and on samples where there should be no biological nitrogen fixation (coastal Galveston Bay) (Figure 4.4). Successful detection of active biological nitrogen fixation was achieved using a general *nifH* oligonucleotide probe (Figure 4.4). Biological nitrogen fixation has been documented in the Gulf of Mexico across warm and cold core eddy features (Dorado et al. 2012). Multiple samples were collected from these same transects and combined from across the warm and cold core eddy features in order to have enough homogenous sample to test with various treatments. The *nifH* oligonucleotide probe used in this study successfully hybridized to targets from the open ocean Gulf of Mexico samples (Figure 4.4). Hybridization was attempted using a negative control oligonucleotide probe on all of the same treatments (variation in formamide and probe concentration) with less than 10% positive results (data not shown). Optimal results (highest positive hybridization using the *nifH* probe with minimum hybridization using the negative probe) were achieved at a 35% formamide concentration. Galveston Bay samples showed minimal hybridization (<4%) by comparison to the 10-22% hybridization in the open ocean Gulf of Mexico samples, indicating specificity of the *nifH* probe to *nifH* mRNA transcripts (Fig. 4.4) Optimal formamide concentration for the *nifH* oligonucleotide probe is 35%.

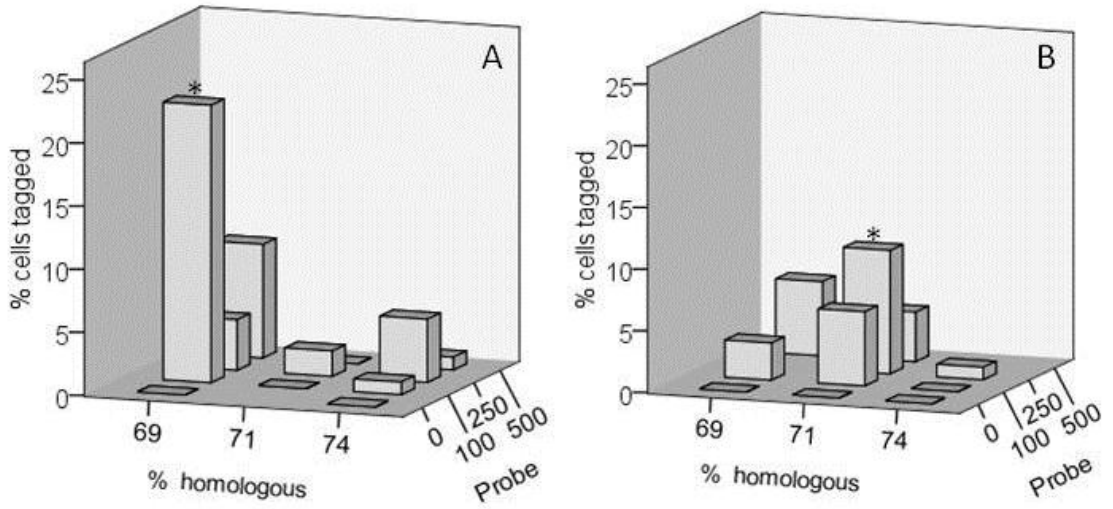

Figure 4.4. Percent hybridization of environmental samples using *nifH* probe. Results of the matrix of formamide concentration vs. probe concentration for the *nifH* oligonucleotide probe for (A) blue water Gulf of Mexico and (B) coastal Galveston Bay, Texas. Colors are % community hybridized with the *nifH* probe minus the % hybridized using the negative probe. The asterix represents the combination that yielded the highest percentage for each sample. Successful hybridization to *nifH* mRNA sequences in the blue water Gulf of Mexico sample occurred only low amounts of hybridization were detected in coastal Galveston Bay. This pattern is consistent with predictions based on the literature (see text). Maximum hybridization is achieved at lower % homology (35% formamide ~ minimum homology of 69%) than the rbcL probe; this may be due to the fewer number of variable bases in the *nifH* probe. * represent treatment with maximum hybridization.

Using these controls, it is evident that the probe and optimization outlined herein represents an accurate tool to quantify the active biological nitrogen fixation community in environmental samples. These findings indicate the *nifH* oligonucleotide probe is sensitive enough to detect nitrogen fixation in oligotrophic waters but not overly responsive that non-specific binding occurs (e.g., in coastal waters where nitrogen fixation does not occur). Under the optimal conditions described, the increase in fluorescence above background allowed differentiation of mRNA targets. In Figure 4.3,

we show the results of matrix concentration tests on *Synechococcus sp*. for *rbcL* and the corresponding negative control probes. To account for intrinsic fluorescence and non-specific binding of the fluorophore, control samples (with no probe added) were run for all formamide concentrations (first column in Figure 4.3). Control samples showed very limited hybridization, indicating that removal of intrinsic fluorescence and quenching of endogenous peroxidase activity were effective (Figure 4.3, column 1). Hybridization with the NON388 showed limited hybridization (<5%, lower 12 panels in Figure 4.3). Hybridization increased with increasing probe concentration, and decreased with increasing formamide concentration (increasing specificity, upper 12 panels in Figure 4.3). The increase in fluorescence of positively hybridized targets is sufficient to easily differentiate these from background fluorescence.

Detection of Active Primary Producers and Nitrogen Fixers Using TSA-FISH. Cultured phytoplankton, representing a diversity of photosynthetic organisms, were successfully tagged using a general *rbcL* oligonucleotide probe (Figure 4.5); this technique was also shown to be successful in samples from both coastal and open ocean environments (Figure 4.2). The cultures were chosen to represent the diverse evolutionary history of phytoplankton (Table 4.1), and were all small enough to be analyzed using flow cytometry (< 50 μm). The variation in the total number of target cells detected (35-70%, Figure 4.5) may be due to initial differences in the percentage of the population represented by phytoplankton to other microbes, or to differential peaks in transcription of target mRNA due to the time of day the cells were harvested (typically mid-morning). It is known that environmental diel expression of *rbcL* peaks

between 2-6 hours after the start of the light cycle (Wyman et al. 1999; Prichard et al. 1997; Warwrik et al. 2002).

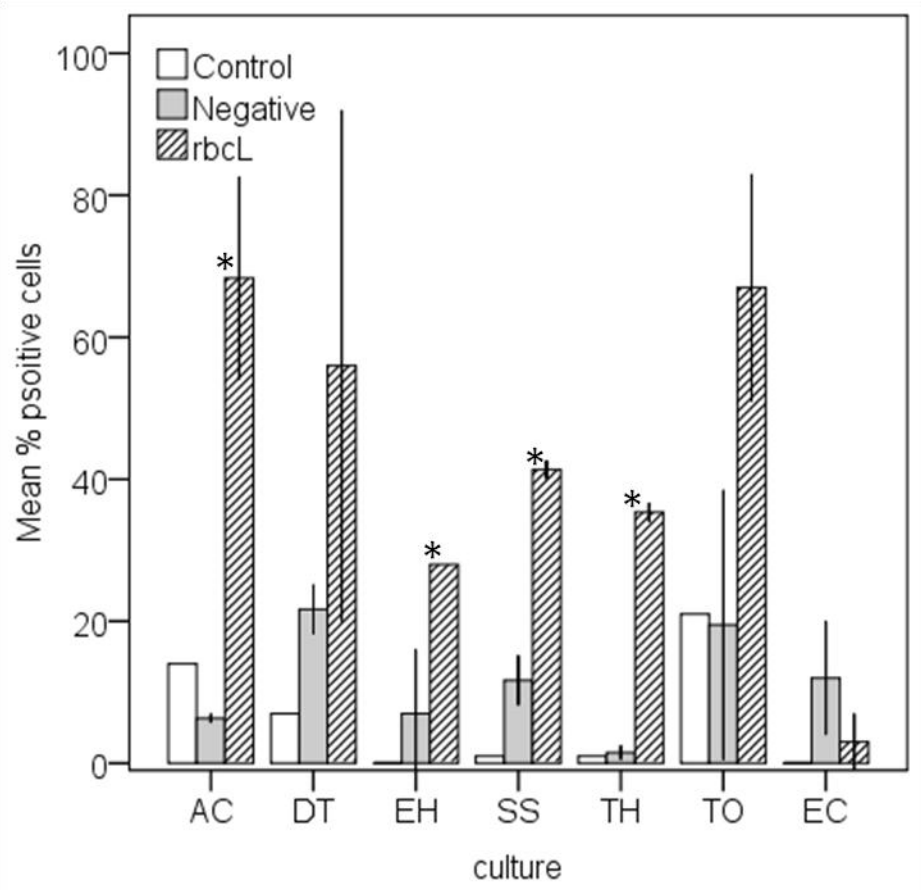

Figure 4.5. Hybridization of phytoplankton cultures using universal *rbcL* probe. Seven cultures were hybridized with *rbcL* and Negative probes: *Amphora coffeaeformis* (AC), *Dunaliella tertiolecta* (DT), *Emiliania huxleyi* (EH), *Synnechococcus sp.* (SS), *Thoracosphaera heimii* (TH), *Thalassiosira oceanica* (TO), *Escherichia coli* (EC). Samples were run using 25% formamide for the *rbcL* (striped bars) probe and 40% formamide for the Negative probe (grey bars) representing roughly equivalent specificities. Error bars (±2 SE) represent triplicate samples (except *D. tertiolecta, T. oceanica and E. coli*, n = 2). White bars represent the intrinsic fluorescence of the samples (no probe added; controls). Some pigments remained, particularly in the diatoms. * represents samples with significant differences between positive and negative probes.

All differences in positive versus negative probe samples were significant (<0.05; Figure 4.5) except for *D. tertiolecta* (p=0.20, independent samples t-test) and *T. oceanica* (p=0.06, independent samples t-test). One of the triplicate samples of *D. tertiolecta* did not hybridize, yet the other two were significantly higher than the negative probe. *T. oceanica* showed a limited difference in positive versus negative hybridization. This may be due to limited signal as a result of low number of target cells present. *E. coli* (negative control) showed no hybridization using the *rbcL* probe (Figure 4.5), supporting accuracy in the specificity of the *rbcL* probe to transcripts of *rbcL* mRNA. The high degree of hybridization across a diversity of cultured organisms reveals that this technique may be successfully employed for a wide variety of samples. Samples from coastal waters (Galveston Bay) and open ocean waters (Gulf of Mexico) were also used to test the effectiveness of the general *rbcL* probe to quantify active primary producers in environmental samples - both samples were successfully tagged (Figure 4.2).

Due to the many steps involved in this method, some cell loss is inevitable. However, as long as the proportions of the community are retained throughout, this method can determine the percent of the microbial community expressing *rbcL* and *nifH* genes. Up to half of the microbial community may be autotrophic (Partensky et al. 1999; Karner et al. 2001). We found ~30% of the microbial population sampled in Galveston Bay and ~10% of the microbial population from the Gulf of Mexico samples were hybridized using the *rbcL* probe (Figure 4.3). The similarity of these numbers to population percentages (~ 24-40% in Galveston Bay, picoautotrophs, < 20 μm –

unpublished data); ~20-50% eastern Indian Ocean unpublished data) suggests conservation of the relative community composition in environmental samples. Diversity and presence of *nifH* gene expression in environmental samples have been reported for environments around the world (Church et al. 2005; Zehr et al. 2003). However, reported proportions of diazotrophic microbial community and abundance measurements are limited. Unicellular cyanobacteria expressing *nifH* genes can represent up to 10% of the microbial community composition (Zehr et al. 2001), but this number does not account for potential heterotrophic nitrogen fixers. We found 10-25% of the microbial population sampled in the Gulf of Mexico hybridized using the *nifH* probe. Though similar, these numbers point to the sensitivity of this method for enumeration of the entire biological nitrogen fixing community.

Expression and Rates. From the photosynthesis versus irradiance curves prepared for the cultures, we calculated P_{max} , that is, the maximum ^{14}C uptake from the plateau region at maximum photon fluxes. The differential expression and fixation of carbon is clearly depicted in the cultured samples as shown in Fig. 6 for the cyanobacterium *Synechococcus sp.*, the dinoflagellate *T. hemii* and the diatom *T. oceanica.*

Synechococcus rbcL transcription peaked 6 hours prior to the start of and again 3 hours into the light cycle (Figure 6A) similar patterns were observed by Paul et al. (2000). Maximum C fixation was observed sequentially after the peaks in *rbc*L activity. A dip in C fixation occurred mid-morning, perhaps due to increased requirements for RUBISCO, as suggested by the increase in *rbcL* transcription at this time (Figure 6A).

The maximum ^{14}C fixation rate measured in the middle of the day for *Synechococcus sp.* was 1500 mg C m^{-3} hr^{-1}. T. *heimii* transcribes *rbcL* to a greater extent throughout the night compared to activity during the day (Figure 6B). Three hours prior to the end of the night cycle, highest ^{14}C fixation rates of 45 mg C m^{-3} hr^{-1} were measured. Rates of ^{14}C fixation were 10 times lower during the day (~4 mg C m^{-3} hr^{-1}) than maximum rates at night (~ 40 mg C m^{-3} hr^{-1}); peaks during the dark period are not unusual (John et al. 2012). *T. oceanica rbc*L expression and ^{14}C fixation were tightly coupled throughout the light and dark cycles (Figure 6C) with maximum values measured during the day and lowest values measured during the night, similar to findings by Corredor et al. (2004). Greatest diatom ^{14}C fixation rates (~220 mg C m^{-3} hr^{-1}) were five-times higher than those measured in *T. heimii* but significantly lower than in those measured in *Synechococcus sp.*.

The importance of incorporation of diel periodicity has been demonstrated previously in cultured phytoplankton including representatives of diatoms, dinoflagellates, chlorophytes, chrysophytes and cyanobacteria (Harding et al. 1981) and environmental samples (Harding et al. 1982). Diel variability, expressed as the amplitude of the cycle, range from 4-6 in environmental samples (Harding et al. 1981; Harding et al. 1982; Yoshikawa and Furuya 2006). Similar amplitudes in periodicity are demonstrated here: *Synechococcus* sp. 2-6 (mean 4), *T. hemii* 3-29 (mean 13), *T. ocean* 2-15 (mean 6.5). Typical protocols for incubations suggest incubating through the light cycle (Knapp et al. 1996). Integrated values for the entire diel cycle in this study are nearly twice as high than values integrated for the light period alone (~46% PP missed

for *Synechococcus* sp., ~60% PP missed for *T. hemii*, ~44% missed for *T. ocean*) similar to values previously reported (Harding et al. 1982; Yoshikawa and Furuya 2006). Both the diel variability and potential underestimation of PP are greatest for *T. hemii*. Interestingly, the variability is lowest for *Synechococcus* sp., however nearly half of the total PP would be missed if standard practices were continued due to the large amount of PP occurring at night. Correspondingly, rate measurements are overestimated when measurements only occur in the daylight for *Synechococcus* sp. and *T. ocean*. *T. hemii* rates are underestimated, as the peak in carbon fixation occurs at night. Phytoplankton community composition likely plays an important role in variability in the diel cycle, as demonstrated by the different diel patterns presented here (Fig. 4.6).

Highest positive *nifH* community expression was 10,500 cells ml^{-1} (mean 600 cells ml^{-1}) whilst highest biological nitrogen fixation (BNF) rates were 16.37 nmol $l^{-1}hr^{-1}$ (mean 3.5 nmol l^{-1} hr^{-1}). The differential strategies of N fixation among diazotrophs has been well documented (Berman-Frank et al. 2007). The pattern observed in the eastern Indian Ocean (Figure 4.7) mimics that of free-living single celled diazotrophs (*Cyanothece* sp., Berman-Frank et al. 2007). This includes a peak in *nifH* expression (left y-axis) and N fixation (right y-axis) at night and lowest values for both during the day. Observation of this pattern in environmental samples is particularly interesting because it points to the possibility that the single celled diazotrophic community (a large percentage of the microbial population in this region) is either being temporally separated on an organismal level, or the O_2 generation (resultant of C fixation) on a community level inhibits N fixation at a community level. Either scenario demonstrates

the need to measure the interconnectivity of these two cycles on a fine temporal scale using the same methods. Such temporal separation of C and N fixation has been observed (Berman-Frank et al. 2007).

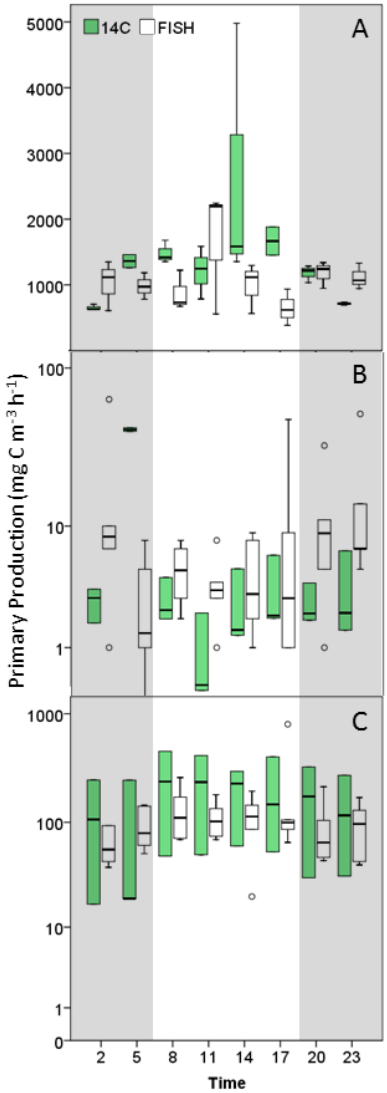

Figure 4.6. Diel cycle of *rbcL* (solid black squares) and PP (circles and dashed line) from triplicate laboratory samples. A = *Synechococcus* sp. B = *Thoracosphaera hemii* C = *Thalassiosira oceanica*. Lines represent the mean of the triplicate samples (solid line *rbcL* expression, dashed line C fixation). Note the different strategies, *rbcL* mRNA expression leads C uptake in *Synechococcus* cultures, follows closely with *T. oceanica* and occurs at night in *T.hemii*.

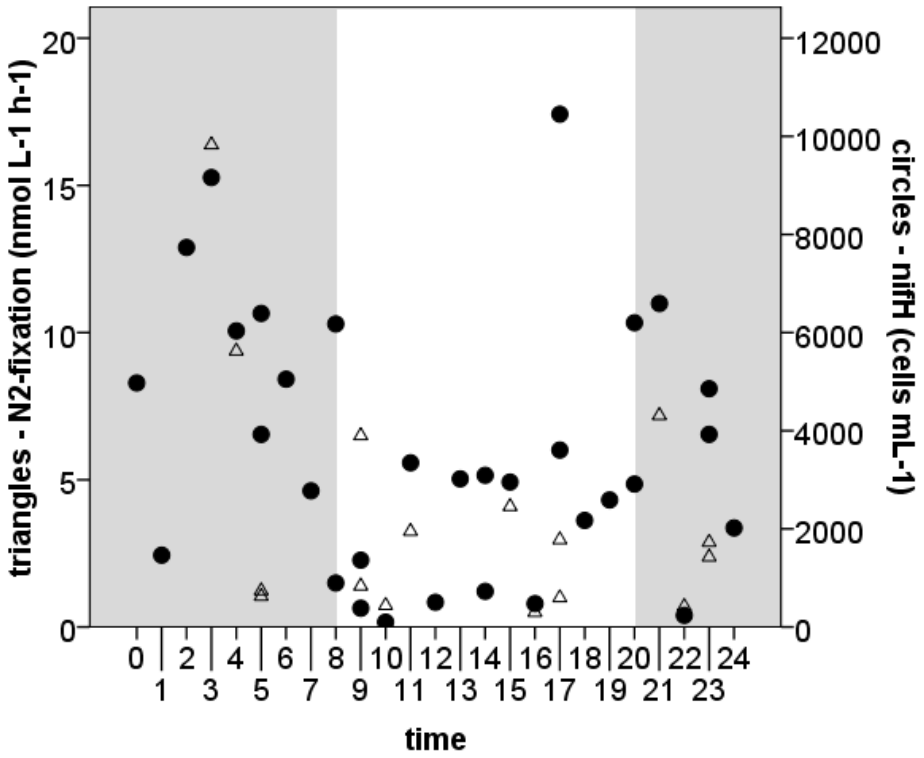

Figure 4.7. Environmental diel *nifH* expression and N_2-fixation. Note the strong diel cycle of increased expression and N fixation during dark hours, and decreased expression and measured fixation during day light hours.

Quantification of the Fraction of the Microbial Community Actively Fixing C and N. Marine primary producers range from prokaryotes to eukaryotes and span a size range covering many orders of magnitude (Kirchman 2008). In order for samples to be compared, the fluorescent biovolume (FB) was calculated for each of the cultures (removing fluorescent variability inherently associated with cell size) (Figure 4.8) using equation 1 below:

$$FB = ([Fluoro_{sample}/Fluoro_{beads}]*[FS_{sample}/FS_{beads}]*\text{positive cells/ml}) \quad (1)$$

John et al. (2012) found mRNA expression lead P_{max} by 3-9 hours. Similarly, we shifted the measured concentration (positive *rbcL* cells ml^{-1}) relative to P_{max} plus/minus

3, 6, 9, and 12 hours and compared the correlations between *rbcL* expression and max ^{14}C uptake. We found *rbc*L expression (# positive cells per ml) lead P_{max} (maximum ^{14}C uptake) across the diel light cycle by 6 hours ($r = 0.823$, $p < 0.001$; Figure 4.6). Previous studies have shown strong correlations between primary production and mRNA present in the community (Paul 1996; John et al. 2007; Corredor et al. 2004; Martin-Nieto et al. 1991), The strength of the relationship (see equation below) demonstrated in Figure 4.8 shows that it is possible to not only enumerate the cells ml^{-1} actively transcribing *rbcL*, accounting for differential expression between different components of the community (prokaryotes vs eukaryotes) but to also estimate C-fixation. Equation (2) can be used to estimate production (P_f) from fluorescent biovolume as determined by mRNA FISH:

$$P_f = (3*10^{-8})*(\text{fluorescent biovolume/ul})^{0.82} \quad (2)$$

When we applied this equation to estimate C fixation rates from samples collected in the eastern Indian Ocean, using values for fluorescent biovolume, the estimated C fixation rates range from 0.2-8 mgC $m^{-3}d^{-1}$ with a mean of 1.95 mgC $m^{-3}d^{-1}$, corresponding to rates previously reported for this region (Waite et al. 2007; Holl et al. 2007). One station (D6, Appendix B Figure 1) had anomolously high values, ranging from 4.5 to 8.5 mgC $m^{-3}d^{-1}$ through the diel cycle. When this station is removed the values for the other 7 stations have a maximum value of 2.7 and an average of 1.36 mgC $m^{-3}d^{-1}$.

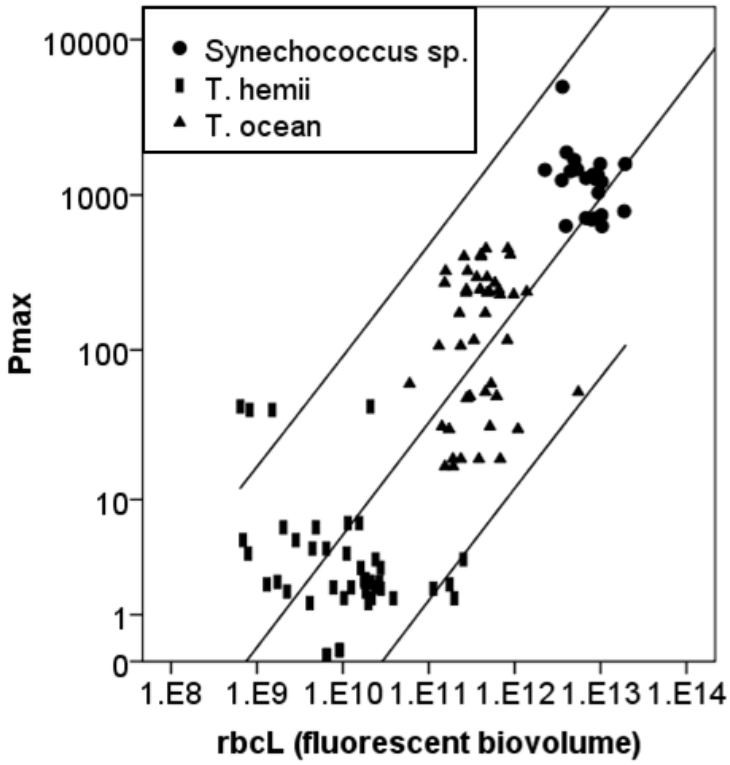

Figure 4.8: Regression of fluorescent biovolume and C fixation. C fixation follows *rbcL* expression by 6 hours, therefore to determine the relationship between C fixation and *rbcL* expression has been shifted 6 hours. Linear best fit line (with 95% CI) through the three species ($r^2 = 0.80$).

Nitrogen fixing organisms are less diverse and span a smaller size range (Church et al. 2005), though some are symbiotic with larger algae (Carpenter et al. 1999; Zehr et al. 2000). Thus changes in fluorescence intensity of a sample maybe due more to positive target concentration than to differential expression, confounding the fluorescent biovolume calculation (see equation 3). Concentration of cells per ml was significantly correlated with ^{15}N uptake ($r = 0.554$ $p = 0.026$; Fig. 4.9) when examined for a select set of stations from the eastern Indian Ocean.

$$BNF = (0.05)*(\text{positive cells/ml})^{0.5} \quad (3)$$

Using the above equation to estimate biological nitrogen fixation (BNF) in the 24 hr samples collected in the remainder of the samples, N fixation rates range from 0.5-5 nmol l^{-1} hr^{-1} with an average value of 2.76 nmol l^{-1} hr^{-1}. The biggest discrepancy is that we miss the very high value measured at a coastal station (16.4 nmol l^{-1} hr^{-1}). Interestingly mRNA FISH of *nifH* transcripts was able to differentiate communities of endosymbiotic diazotrophs (Appendix B Figure 2).

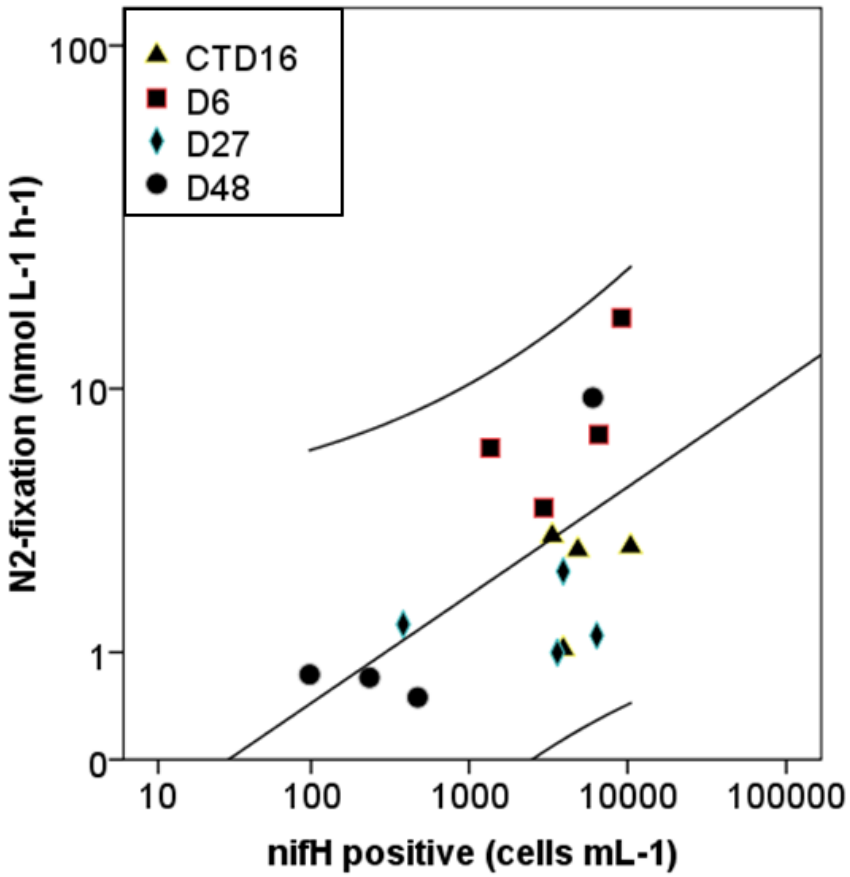

Figure 4.9: Regression of *nifH* expression versus biological nitrogen fixation in the eastern Indian Ocean. The different 24 hour stations are represented by the different colors. Linear best fit line (with 95% CI) through the four stations ($r^2 = 0.45$).

Simultaneous measurements using traditional, direct measurements of isotopic C and N incorporation are significantly correlated with fluorescently labeled cells (r^2 = 0.68 and 0.31 respectively) as shown in Figure 4.8 and 4.9 respectively. This method yields not only number of cells actively fixing C and N but can also be used to estimate rates, providing a new mechanism for elucidating the strong connectivity of the C and N cycles simultaneously and on the same sample.

Conclusions

The probes and optimization parameters outlined in this study provide an exciting new tool for elucidating the connectivity of the C and N cycles by simultaneous quantification of the fraction of the microbial community actively fixing C and N. Carbon fixation and biological nitrogen fixation are partially controlled by transcription of *rbcL* and *nifH* genes (Martin-Nieto et al. 1991; Paul 1996; John et al. 2007; Corredor et al. 2004). Therefore, mRNA TSA-FISH may offer new insights into the number of organisms actively performing these functions, as well as estimates of these two processes. This study introduces a new perspective on FISH. Instead of highly stringent, species specific conditions, it is possible to accurately detect and quantify a more evolutionarily diverse, yet functionally similar, community. The power of quantifying functional gene expression in situ combines community enumeration and estimation of important rate measurements. Flow cytometry allows more rapid quantification of positive cells than traditional epifluorescence microscopy, as well as analysis of a larger

number of events, thereby providing rapid, robust datasets. By combining detection of mRNA, using TSA-FISH, and enumeration via flow cytometry, the method optimized and outlined in this study offers robust, high sensitivity analyses of active microbial populations.

The work described herein represents an interesting insight into the diel cycles of both carbon and nitrogen fixation. Diatoms exhibit classical transcription and C-fixation; both peak during the day. However, cyanobacteria fix large amounts of C at night. At first this seems counter intuitive for photosynthesis, but actual fixation of C through action by RUBISCO is part of the dark reactions, which do not require light, only stored energy. Further, the dinoflagellates appear to have a different strategy altogether. These results indicate that 1) primary producer community composition is important in determination of net primary production and 2) a substantial portion of C fixation may occur at night. *Synechococcus* and *Prochlorococcus* dominate the open ocean environments (Partensky et al 1999). Thus, current estimates (Field et al 1998) and methods (Behrenfeld and Falkowski 1997) of net primary production which extrapolate primary production contingent upon daylight hours may be underestimating the large amount of C fixation occurring in the dark (accurate for diatoms but not for cyanobacteria).

Community composition likely plays a role in N-fixation as well (Berman-Frank et al 2007). Our data indicate a dominance of unicellular diazotrophs present in the samples tested as evidenced by the peak N-fixation occurring at night. A better understanding of diel patterns of both C and N fixation and their respective

synchronicity may offer new insights into the connectivity of the two cycles and feedbacks between the two cycles affecting global oceanic production.

CHAPTER V

SUMMARY AND CONCLUSIONS

The oceans are responsible for half of the primary production on Earth (Falkowski and Raven 2007). The components, mechanisms, and efficiency of this pump remain unclear. Compartmentalization of production into new and regenerated pools allows a first order estimation of the fates of this fixed C. However, even estimation of one component, new production, is difficult and continuously being improved. The goal of this work was to elucidate the fate of new production. **We found the general hypothesis of this work—new production is under accounted for in marine systems—to be true.**

In **Chapter II** we have described a pulse of marine derived nutrients from herring spawn having a direct effect on the phytoplankton community composition and abundance. Previous studies have shown these pulses to be important to higher trophic organisms in other ecosystems (Roper et al. 1999; Willson and Womble 2006). Schools of adult Pacific herring migrate into PWS in mid-spring (Norcross et al. 2001) and spawn in large aggregations along the coast. A spawning event generally lasts 5-21 days, and the eggs hatch 22-24 days later (Norcross et al. 2001). In 2007 an aggregation of sea otters in Simpson Bay was observed consuming herring roe on kelp between 11 June – 3 July (Lee et al. 2009), confirming an additional, apparently small, summer spawning event in the study area (as eggs hatch within 1.5-3 weeks (Willson and Womble 2006). While the summer spawn of herring is smaller than the spring event, it may still

contribute substantial amounts of nutrients to the bays where it occurs (including Simpson Bay), as was observed in the current study. The pulse of nutrients alleviates the nitrogen limitation of primary productivity typically observed in fjords in PWS in the summer (Eslinger et al. 2001; Quigg et al. 2013). This study demonstrates that resource pulses can stimulate the system at trophic levels above and below the level of input. Further research is required to explicitly quantify the energy and nutrient input to Simpson Bay and PWS. These previously overlooked effects of resource pulses may be an important contributing factor to the sustained abundance of this ecosystem.

Future studies would benefit from incorporation measurement of the microbial community. A potential mechanism for the amplification and attenuation effects of pulsed nutrients (described by Yang et al. 2010) may be a shunting of production from the microbial loop to the food web; leaving the overall balance of regenerated production to new production intact. Evidence for this relationship can be found in the patterns described by Eslinger et al. 2001—stormier springs provide more C to the foodweb. The elongated increase in new production (production from upwelled/mixed nutrients) may be ~~"~~priming the pump."

Further, bacterial production is a smaller fraction of total ecosystem metabolism in cold, high-latitude oceans compared with temperate or tropical ecosystems (Kirchman 2008), because there is a stricter dependence of bacterial metabolism on temperature compared with phytoplankton. Therefore environmental conditions have different effects on the grazing vs. the microbial food webs, thus the transfer of C through the food web and export (Falkowski and Raven 2007). Pomeroy and Deibel (1986) found that low

temperatures at high-latitudes suppress bacterial activity and results in a larger fraction of PP funneling toward higher trophic levels rather than being respired by microbial food webs (in Kirchman 2008). Whereas areas with dominant microbial loop will have less matter and energy available to higher trophic levels (Falkowski and Knoll 2011), therefore PWS will support more and higher trophic levels. This is primarily due to the fact that each trophic transfer represents large losses (80%) of matter and energy (Falkowski and Knoll 2011) thus there would be a greater loss in the microbial loop (consisting of more trophic transfers). Also larger animals require less food per unit mass therefore the same amount of primary production can support a higher biomass of large individuals due to increased metabolic efficiency (Pershing et al. 2010). This may be why PWS can support large communities of megafauna on relatively low productivity.

The increased production shunted to the food web may hold true in some cases of blue water new production. Fawcett et al. (2011) show that the eukaryotic phytoplankton in the Sargasso Sea obtain their N from upwelled (new) nitrate, a shunting of new production to a particular piece of the food web. However, if new production is equal to export production (Epply and Peterson 1979) our measurements of export production is relatively low. Discrepancies in estimated export have hitherto been attributed only to other mechanisms which include sediment trap inaccuracies (Michaels et al. 1994), organic matter remineralization (Feely et al. 2004), mesopelagic attenuation (Buesseler et al. 2007; Lomas et al. 2010), and phytoplankton community structure (Laws et al. 2000; Dunne et al. 2005; Guidi et al. 2009). In **Chapter III** we developed a simple

numerical model to estimate the horizontal distance traveled by sinking particles. Using this model we show that currents can play a dominant role in trap measurement variability. Even the fastest sinking particles in fast currents can be transported beyond the grid typically used to estimate surface production (~250 km) and potentially across entire oceans. We analyzed the distribution in statistical variability of traps for two publically available data sets (Buesseler 2011 and Honjo et al. 2008) in an effort to determine if this model may be employed to describe variability in export. For shallow traps the influence of current regime is less pronounced than for deep traps as the particles collected are in the water column for a shorter period of time. However, in areas of highly variable surface productivity and fast currents, measurements can be affected (e.g. the Arabian Sea). The spatial extent of surface production variability necessary to affect deep water traps is much larger. We show "over collection" of POC flux in traps across the equatorial Pacific. In over half of the deep water traps analyzed POC fluxes are likely affected by currents. This could have profound implications for estimates of C-export from the surface ocean as well as our understanding of subsurface ecosystem structure, biomass and function.

While our measurement of flux may be the cause of discrepancy between estimated and measured fluxes, measurement and estimation of new production and thus export production may also be skewed. In **Chapter IV** we describe development of a concise method employing TSA-FISH with general oligonucleotide probes complimentary to *rbcL* (RUBISCO, primary production) and *nifH* (nitrogenase, nitrogen fixation) mRNA transcripts allowing simultaneous quantification of C and N fixing

communities as well as estimation of C and N fixation rates within those communities. Application of this method eliminates many assumptions (necessitated by disparate techniques and incubations currently employed) and allows a more direct understanding of the connectivity of these two dynamic cycles. The probes and optimization parameters outlined in this study provide an exciting new tool for elucidating the connectivity of the C and N cycles by simultaneous quantification of the fraction of the microbial community actively fixing C and N. Carbon fixation and biological nitrogen fixation are partially controlled by transcription of *rbcL* and *nifH* genes (Martin-Nieto et al. 1991; Paul 1996; John et al. 2007; Corredor et al. 2004). Therefore, mRNA TSA-FISH may offer new insights into the number of organisms actively performing these functions, as well as estimates of these two processes. This study introduces a new perspective on FISH. Instead of highly stringent, species specific conditions, it is possible to accurately detect and quantify a more evolutionarily diverse, yet functionally similar, community. The power of quantifying functional gene expression in situ combines community enumeration and estimation of important rate measurements. Flow cytometry allows more rapid quantification of positive cells than traditional epifluorescence microscopy, as well as analysis of a larger number of events, thereby providing rapid, robust datasets. By combining detection of mRNA, using TSA-FISH, and enumeration via flow cytometry, the method optimized and outlined in this study offers robust, high sensitivity analyses of active microbial populations.

In conclusion, the findings of this thesis support the general hypothesis that new production is under-accounted for in marine systems. New pulses of nutrients (especially

N) can lead to amplification of energy and nutrients to a particular portion of the food web, in the case study performed in Prince William Sound (Alaska, USA), we showed an increase in phytoplankton biomass (typically overlooked in this region) corresponding to a small herring spawn. A concurrent marine shift in the stable isotope values was also observed. These changes led to increased export and nutrients later in the summer. In order to understand the general movement of exported C from the photic zone in oligotrophic water (30% of the world‘s ocean and growing, Beckmann and Hense 2009; Polovina et al. 2008) we developed a model to account for currents in our export estimations. We then preformed a meta-analysis of the JGOFS (Buesseler 2011) and Honjo et al. (2008) data sets revealing that currents affect our measurements and estimates in over half of the data analyzed. Our estimates of export are not only affected by the end result (sinking particle measurements) but also by our ability to simultaneously measure new and total production. Simultaneous of C and N fixation in the same sample without incubation could vastly improve our estimates of these important numbers. We developed a method using fluorescence in situ hybridization of mRNA, tagging both C and N fixing organisms. Using lab cultures and field samples from Galveston Bay (Texas, USA), the Gulf of Mexico (USA) and the eastern Indian Ocean (off the coast of Western Australia), we were able to show the utility of this new approach.

REFERENCES

Alaska Department of Fish and Game. (2013). Animals. Retrieved from http://www.adfg.alaska.gov/index.cfm?adfg=animals.main

Alldredge, Alice L., and Kenneth M. Crocker. 1995. Why do sinking mucilage aggregates accumulate in the water column? *The Science of the Total Environment* 165:15-22.

Alonso-Gonzalez, Ivan J., Javier Aristegui, Cindy Lee, Anna Sanchez-Vidal, Antoni Calafat, Joan Fabres, Pablo Sangra, Pere Masque, Alonso Hernandez-Guerra, and Veronica Benitez-Barrios. 2010. Role of slowly settling particles in the ocean carbon cycle. *Geophysical Research Letters* 37:1-5.

Andersen, Robert A., R. R. Bidigare, Maureen D. Keller, and Mikel Latasa. 1996. A comparison of HPLC pigment signatures and electron microscopic observations for oligotrophic waters of the North Atlantic and Pacific Oceans. *Deep Sea Research II* 43 (2-3):517-537.

Anderson, Wendy B., D. Alexander Wait, and Paul Stapp. 2008. Resources from another place and time: responses to pulses in a spatially subsidized system. *Ecology* 89 (3):660-670.

Aranguren-Grassis, Maria, Eva Teira, Pablo Serret, Sandra Martinez-Garcia, and C. Fernandez. 2012. Potential overestimation of bacterial respiration rates in oligotrophic plankton communities. *Marine Ecology Progress Series* 453:1-10.

Armitage, Anna R., and James W. Fourqurean. 2009. Stable isotopes reveal complex changes in trophic relationships following nutrient addition in a coastal marine ecosystem. *Estuaries and Coasts* 32 (6):1152-1164.

Armstrong, Robert A., Cindy Lee, John I. Hedges, Susumu Honjo, and Stuart G. Wakeham. 2002. A new, mechanistic model for organic carbon fluxes in the ocean based on the quantitative association of POC with ballast minerals. *Deep Sea Research II* 49:219-236.

Azam, F. 1998. Microbial control of oceanic carbon flux: the plot thickens. *Science* 280 (5364):694-696.

Ballard, Robert D. 1995. *The Discovery of the Titanic*. Toronto: Madison Press Books.

Barber, Richard T., John Marra, Robert C. Bidigare, Louis A. Codispoti, David Halpern, Zackary Johnson, Mikel Latasa, Ralf Goericke, and Sharon L. Smith. 2001. Primary productivity and its regulation in the Arabian Sea during 1995. *Deep Sea Research II* 48:1127-1172.

Barrow, Lindy M., Karen A. Bjorndal, and Kimberly J. Reich. 2008. Effects of preservation method on stable carbon and nitrogen isotope values. *Physiological and Biochemical Zoology* 81 (5):688-693.

Beckmann, Aike, and Inga Hense. 2009. A fresh look at the nutrient cycling in the oligotrophic ocean. *Biogeochemistry* 96:1-11.

Behrenfeld, Michael J., and Paul G. Falkowski. 1997. A consumer's guide to phytoplankton primary productivity models. *Limnology and Oceanography* 42 (7):1479-1491.

Behrenfeld, Michael J., Robert T. O/'Malley, David A. Siegel, Charles R. McClain, Jorge L. Sarmiento, Gene C. Feldman, Allen J. Milligan, Paul G. Falkowski, Ricardo M. Letelier, and Emmanuel S. Boss. 2006. Climate-driven trends in contemporary ocean productivity. *Nature* 444 (7120):752-755.

Bender, Michael, Karen Grande, Kenneth Johnson, John Marra, Peter J. LeB. Williams, John Seiburth, Michael Pilson, Chris Langdon, Gary Hitchcock, Joseph Orchardo, Carleton Hunt, Percy Donaghay, and Kristina Heinemann. 1987. A comparison of four methods for determining planktonic community production. *Limnology and Oceanography* 32 (5):1085-1098.

Berman-Frank, I., A. Quigg, Z. V. Finkel, A. J. Irwin, and L. Haramaty. 2007. Nitrogen-fixation strategies and Fe requirements in cyanobacteria. *Limnology and Oceanography* 52 (5):2260-2269.

Biegala, Isabelle C., Fabrice Not, Daniel Vaulot, and Nathalie Simon. 2003. Quantative assessment of picoeukaryotes in the natural environment by using taxon-specific oligonucleotide probes in association with tyramide signal amplification-fluorescence *in situ* hybridization and flow cytometry. *Applied and Environmental Microbiology* 69 (9):5519-5529.

Bilby, R. E., B. R. Fransen, and P. A. Bisson. 1996. Incorporation of nitrogen and carbon from spawning coho salmon into the trophic system of small streams: evidence from stable isotopes. *Canadian Journal of Fisheries and Aquatic Sciences* 53:164-173.

Buesseler, K. O., M. P. Bacon, J. K. Cochran, and H. D. Livingston. 1992. Carbon and nitrogen export during the JGOFS North Atlantic Bloom Experiment estimated from super ^{234}Th: ^{238}U disequilibria. *Deep-Sea Research* 39 (7):1115-1137.

Buesseler, K. O. 1998. The de-coupling of production and particulate export in the surface ocean. *Global Biogeochemical Cycles* 12 (2):297–310.

Buesseler, K. O., L. Ball, J. E. Andrews, J. K. Cochran, D. J. Hirschberg, M. P. Bacon, A. Fleer, and M. Brezezinski. 2001. Upper ocean export of particulate organic carbon and biogenic silica in the Southern Ocean along 170 W. *Deep Sea Research II* 48:4275-4297.

Buesseler, K. O., C. R. Benitez-Nelson, S. B. Moran, A. Burd, M. A. Charette, J. K. Cochran, L. Coppola, N. S. Fisher, S. W. Fowler, W. D. Gardner, L. D. Guo, O. Gustafsson, C. H. Lamborg, P. Masque, J. C. Miquel, U. Passow, P. H. Santschi, N. Savoye, G. Stewart, and T. W. Trull. 2006. An assessment of particulate organic carbon to ^{234}Th ratios in the ocean and their impact on the application of ^{234}Th as a POC flux proxy. *Marine Chemistry* 100:213-233.

Buesseler, K. O., A. N. Antia, M. Chen, S. W. Fowler, W. D. Gardner, O. Gustafsson, K. Harada, A. F. Michaels, M. R. van der Loeff, M. Sarin, D. K. Steinberg, and T. Trull. 2007. An assessment of the use of sediment traps for estimating upper ocean particle fluxes. *Journal of Marine Research* 65:345-416.

Buesseler, K. O. 2011. U.S. JGOFS Synthesis & Modeling Project - Data. U.S. JGOFS. iPub: January 2004. Last accessed *05 April 2011.* http://usjgofs.whoi.edu/mzweb/data/Buesseler/world_ocean_export.xls

Burd, Adrian B., and George A. Jackson. 2009. Particle aggregation. *Annual Review of Marine Science* 1:65-90.

Capone, Douglas G., James A. Burns, Joseph P. Montoya, Ajit Subramaniam, Claire Mahaffey, Troy Gunderson, Anthony F. Michaels, and Edward J. Carpenter. 2005. Nitrogen fixation by *Trichodesmium* spp.: An important source of new nitrogen to the tropical and subtropical North Atlantic Ocean. *Global Biogeochemical Cycles* 19:GB2024.

Carlson, C. A., H. W. Ducklow, and A. F. Michaels. 1994. Annual flux of dissolved organic carbon from the euphotic zone in the northwestern Sargasso Sea. *Nature* 371 (6496):405-408.

Carpenter, Edward J., Joseph P. Montoya, James Burns, Margaret R. Mulholland, Ajit Subramaniam, and Douglas G. Capone. 1999. Extensive bloom of a N_2-fixing diatom/cyanobacterial association in the tropical Atlantic Ocean. *Marine Ecology Progress Series* 185:273-283.

Chaloner, D. T., K. M. Martin, M. S. Wipfli, P. H. Ostrom, and G. A. Lamberti. 2002. Marine carbon and nitrogen in southeastern Alaska stream food webs: evidence from artificial and natural streams. *Canadian Journal of Fisheries and Aquatic Sciences* 59:1257-1256.

Chaloner, D. T., G. A. Lamberti, A. D. Cak, N. L. Blair, and R. T. Edwards. 2007. Inter-annual variation in responses of water chemistry and epilithon to Pacific salmon spawners in an Alaskan stream. *Freshwater Biology* 52:478-490.

Chao, M. A., W. U. Dexing, and LIN Xiaopei. 2009. Variability of surface velocity in the Kuroshio Current and adjacent waters derived from Argos drifter buoys and satellite altimeter data. *Chinese Journal of Oceanology and Limnology* 27 (2):208-217.

Chassot, Emmanuel, Sylvain Bonhommeau, Nicholas K. Dulvy, Frederic Melin, Reg Watson, Didier Gascuel, and Olivier Le Pape. 2010. Global marine primary production constrains fisheries catches. *Ecology Letters* 13:495-505.

Chen, Yi-Bu, Jonathan P. Zehr, and Mark Mellon. 1996. Growth and nitrogen fixation of the diazotrophic filamentous nonheterocystous cyanobacterium *Trichodesmium* sp. IMS101 in defined media: evidence for a circadian rhythm. *Journal of Phycology* 32:916-932.

Childers, Amy Ruehs. 2005. Nutrient dynamics in the Northern Gulf of Alaska and Prince William Sound: 1998-2001. Dissertation, Marine Science and Limnology, University of Alaska Fairbanks, Fairbanks, Alaska.

Church, M. J., C. M. Short, B. D. Jenkins, D. M. Karl, and J. P. Zehr. 2005. Temporal patterns of nitrogenase gene (*nifH*) expression in the oligotrophic North Pacific Ocean. *Applied and Environmental Microbiology* 71 (9):5362-5370.

Corredor, Jorge E., Boris Warwik, John H. Paul, Hiep Tran, Lee Kerkhof, Jose M. Lopez, Angel Dieppa, and Oswaldo Cardenas. 2004. Geochemical rate-RNA integration study: Ribulose-1,5-Bisphosphate Carboxylase/Oxygenase gene transcription and photosynthetic capacity of planktonic photoautotrophs. *Applied and Environmental Microbiology* 70 (9):5459-5468.

De La Rocha, C. L., and U. Passow. 2007. Factors influencing the sinking of POC and the efficiency of the biological carbon pump. *Deep-Sea Research Part II-Topical Studies in Oceanography* 54 (5-7):639-658.

del Giorgio, Paul A., Johnathan J. Cole, and Andre Cimbleris. 1997. Respiration rates in bacteria exceed phytoplankton production in unproductive aquatic systems. *Nature* 385:148-151.

Deuser, W. G., F. E. Muller-Karger, and C. Hemleben. 1988. Temporal variations of particle fluxes in the deep subtropical and tropical North Atlantic: eulerian versus lagrangian effects. *Journal of Geophysical Research* 93 (C6):6857-6862.

Dorado, Sam, Jay R. Rooker, Bjorn Wissel, and A. Quigg. 2012. Isotope baseline shifts in pelagic food webs of the Gulf of Mexico. *Marine Ecology Progress Series* 464:37-49.

Dortch, Quay, and Terry E. Whitledge. 1992. Does nitrogen or silicon limit phytoplankton production in the Mississippi River plume and nearby regions? *Continental Shelf Research* 12 (11):1293-1309.

Dugdale, R. C., and J. J. Goering. 1967. Uptake of new and regenerated forms of nitrogen in primary productivity. *Limnology and Oceanography* 12 (2):196-206.

Dunne, John P., Robert A. Armstrong, Anand Gnanadesikan, and Jorge L. Sarmiento. 2005. Empirical and mechanistic models for the particle export ratio. *Global Biogeochemical Cycles* 19:1-16.

Eppley, R. W., R. W. Holmes, and J. D. H. Strickland. 1967. Sinking rates of marine phytoplankton measured with a fluorometer. *Journal of Experimental Marine Biology and Ecology* 1:191-208.

Eppley, Richard W., and Bruce J. Peterson. 1979. Particulate organic matter flux and planktonic new production in the deep ocean. *Nature* 282 (5740):677-680.

Emerson, S., and J. Hedges. 2008. *Chemical Oceanography and the Marine Carbon Cycle* : Cambridge University Press.

Eslinger, D. L., R. T. Cooney, C. P. McRoy, A. Ward, T. C. Kline, E. P. Simpson, J. Wang, and J. R. Allen. 2001. Plankton dynamics: observed and modelled responses to physical conditions in Prince William Sound, Alaska. *Fisheries Oceanography* 10:81-96.

Eyre, B. D., R. N. Flud, and N. Patten. 2008. Mass coral spawning: A natural large-scale nutrient addition experiment. *Limnology and Oceanography* 53 (3):997-1013.

Falcón, Luisa I., Edward J. Carpenter, Frank Cipriano, Birgitta Bergman, and Douglas G. Capone. 2004. N_2 Fixation by unicellular bacterioplankton from the Atlantic and Pacific Oceans:phylogeny and *in situ* rates. *Applied and Environmental Microbiology* 70 (2):765-770.

Falkowski, Paul G., Edward A. Laws, Richard T. Barber, and James W. Murray. 2003. Phytoplankton and their role in primary, new and export production. In *Ocean Biogeochemistry The Role of the Ocean Carbon Cycle in Global Change*, edited by M. J. R. Fasham. Verlag Berlin Heidelberg: Springer-Verlag Berlin Heidelberg New York.

Falkowski, Paul G., and John A. Raven. 2007. *Aquatic Photosynthesis*: Princeton University Press.

Falkowski, Paul G., and Andrew H. Knoll. 2011. *Evolution of Primary Producers in the Sea*. Burlington, MA: Elsevier Academic Press.

Fawcett, Sarah E., Michael W. Lomas, John R. Casey, Bess B. Ward, and Daniel M. Sigman. 2011. Assimilation of upwelled nitrate by small eukaryotes in the Sargasso Sea. *Nature Geoscience* 4:717-722.

Febres-Ortega, G., and L. E. Herrera. 1976. Caribbean sea circulation and water mass transports near the Lesser Antilles. *Boletin del Instituto Oceanografico* 15:83-96.

Feely, Richard A., Christopher L. Sabine, Kitack Lee, Will Berelson, Joanie Kleypas, Victoria J. Fabry, and Frank J. Millero. 2004. Impact of anthropogenic CO_2 on the $CaCO_3$ system in the oceans. *Science* 305:362-366.

Fernández, E., E. Marañón, X. A. G. Morán, and P. Serret. 2003. Potential causes for the unequal contribution of picophytoplankton to total biomass and productivity in oligotrophic waters. *Marine Ecology Progress Series* 254:101-109.

Field, Chrispother B., Michael J. Behrenfeld, James T. Randerson, and Paul Falkowski. 1998. Primary production of the biosphere: integrating terrestrial and oceanic components. *Science* 281:237-240.

Finkel, Z. V. 2007. Does phytoplankton cell size matter? The evolution of modern marine food webs. In *Evolution of Primary Producers in the Sea*, edited by P. Falkowski and A. Knoll. Burlington, MA: Elsevier.

Flagg, Charles N., and Hyun-Sook Kim. 1998. Upper ocean currents in the northern Arabian Sea from a shipboard ADCP measurements collected during the 1994-1996 U.S. JGOFS and ONR programs. *Deep Sea Research II* 45:1917-1959.

Francois, R., S. Honjo, R. Krishfield, and S. Manganini. 2002. Factors controlling the flux of organic carbon to the bathypelagic zone of the ocean. *Global Biogeochemical Cycles* 16 (4).

Fry, Brian. 2006. *Stable Isotope Ecology*. Vol. 521. New York: Springer.

Fuenzalida, Rosalino, Wolfgang Schneider, Jose Garces-Vargas, and Luis Bravo. 2008. Satellite altimetry data reveal jet-like dynamics of the Humboldt Current. *Journal of Geophysical Research* 113:1-11.

Gaarder, T., and H. H. Gran. 1927 Investigation of the production of plankton in the Oslo Fjord. *Rapp. P-v. Réun. Cons. Perm. Int. Explor. Mer.* 42:1-48.

Gardner, Wilford D. 1980. Sediment trap dynamics and calibration: a laboratory evaluation. *Journal of Marine Research* 38 (1):17-39.

Gardner, W. D. 1997. The flux of particles to the deep sea: methods, measurements, and mechanisms. *Oceanography* 10 (3):116-121.

Gehlen, M., L. Bopp, N. Emprin, O. Aumont, C. Heinze, and O. Ragueneau. 2006. Reconciling surface ocean productivity, export fluxes and sediment composition in a global biogeochemical ocean model. *Biogeosciences* 3:521-537.

Groβkopf, Tobias, Weibke Mohr, Tina Baustian, Harald Schunck, Diana Gill, Marcell M. M. Kuypers, Gaute Lavik, Ruth A. Schmitz, Douglas W. R. Wallave, and

Julie LaRoche. 2012. Doubling of marine dinitorgen-fixation rates based on direct measurements. *Nature* 488:361-364.

Gruber, N., and J. L. Sarmiento. 1997. Global patterns of marine nitrogen fixation and denitrification. *Global Biogeochemical Cycles* 11 (2):235-266.

Gruber, Nocholas. 2005. A bigger nitrogen fix. *Nature* 436:786-787.

Gruber, N. 2008. The marine nitrogen cycle: overview and challenges. In *Nitrogen in the marine environment*, edited by D. G. Capone, D. A. Bronk, M. R. Mulholland and E. J. Carpenter. Amsterdam, The Netherlands: Elsevier.

Guidi, Lionel, Lars Stemmann, George A. Jackson, Frederic Ibanez, Herve Claustre, Louis Legendre, Marc Picheral, and Gabriel Gorsky. 2009. Effects of phytplankton community on production, size and export of large aggregates: A world-ocean analysis. *Limnology and Oceanography* 54 (6):1951-1963.

Guld, R. N., B. D. Eyre, and N. Patten. 2008. Biogeochemical response to mass coral spawning at the Great Barrier Reef: effects on respiration and primary production. *Limnology and Oceanography* 53 (3):1014-1024.

Guillard, R., and J. Ryther. 1962. Studies of marine planktonic diatoms. I. Cyclotella nana Hustedt, and Detonula confervacea (cleve) Gran. *Canadian Journal of Microbiology* 8:229-239.

Hales, B., J. N. Moum, P. Covert, and A. Perlin. 2005. Irreversible nitrate fluxes due to turbulent mixing in a coastal upwelling system. *Journal of Geophysical Research* 110:C10S11.

Harding Jr., L. W., B. W. Meeson, B. B. Prezelin, and B. M. Sweeney. 1981. Diel periodicity of photosynthesis in marine phytoplankton. *Marine Biology* 61:95-105.

Harding Jr., L. W., B. B. Prezelin, B. M. Sweeney, and J. L. Cox. 1982. Primary production as influenced by diel periodicity of phytoplankton photosynthesis. *Marine Biology* 67:179-186.

Hardy, R. W. F., R. D. Holsten, E. K. Jackson, and R. C. Burns. 1968. The acetylene-ethylene assay for N_2 fixation: laboratory and field evaluation. *Plant Physiology* 43:1185-1207.

Helfield, J. M., and R. J. Naiman. 2001. Effects of salmon-derived nitrogen on riparian forest growth and implications for stream productivity. *Ecology* 82 (9):2403-2409.

Hicks, B. J., M. S. Wipfli, D. W. Lang, and M. E. Lang. 2005. Marine-derived nitrogen and carbon in freshwater-riparian food webs of the Copper River Delta, southcentral Alaska. *Oecologia* 144:558-569.

Hobson, Keith A., John F. Piatt, and Jay Pitocchelli. 1994. Using stable isotopes to determine seabird trophic relationships. *Journal of Animal Ecology* 63:786-789.

Holl, Carolyn M., Tracy A. Villareal, Christopher D. Payne, Tonya D. Clayton, Cassandra Hart, and Joseph P. Montoya. 2007. Trichodesmium in the western Gulf of Mexico: $^{15}N_2$-fixation and natural abundance stable isotope evidence. *Limnology and Oceanography* 52 (5):2249-2259.

Honjo, Susumu, Steven J. Manganini, Richard A. Krishfield, and Roger Francois. 2008. Particulate organic carbon fluxes to the ocean interior and factors controlling the biological pump: a synthesis of global sediment trap programs since 1983. *Progress In Oceanography* 76 (3):217-285.

Hougaard, David Michael, Henrik Hansen, and Lars-Inge Larsson. 1997. Non-radioactive in situ hybridization for mRNA with emphasis on the use of oligodeoxynucleotide probes. *Histochem Cell Biol* 108:335-344.

Howarth, Robert W., and Roxanne Marino. 2006. Nitrogen as the limiting nutrient for eutrophication in coastal marine ecosystems: evolving views over three decades. *Limnology and Oceanography* 51 (1 part 2):364-376.

Hyka, P., S. Lickova, P. Pribyl, K. Melzoch, and K. Kovar. 2012. Flow cytometry for the development of biotechnological processes with microalgae. *Biotechnology Advances*.

Irwin, Andrew J., Zoe V. Finkel, Oscar M. E. Schofield, and Paul G. Falkowski. 2006. Scaling-up from nutrient physiology to the size-structure of phytoplankton communities. *Journal of Plankton Research* 28 (5):459-471.

Jeffrey, S. W., R. F. C. Mantoura, and S. W. Wright. 1997. *Monographs on Oceanographic Methodology*. 2nd ed, *Phytoplankton Pigments in Oceanography Guidelines to Modern Methods*: UNESCO.

Jackson, George A., and Adrian B. Burd. 2002. A model for the distribution of particle flux in the mid-water column controlled by subsurface biotic interactions. *Deep Sea Research II* 49:193-217.

Jenkins, W. J. 1988. Nitrate flux into the euphotic zone near Bermuda. *Nature* 331:521-532.

Jiao, Nianzhi, Gerhard J. Herndl, Dennis A. Hansell, Ronald Benner, Gerhard Kattner, Steven W. Wilhelm, David L. Kirchman, Markus G. Weinbauer, Tingwei Luo, Feng Chen, and Farooq Azam. 2010. Microbial production of recalcitrant dissolved organic matter: long term carbon storage in the global ocean. *Nature Reviews Microbiology* 8:593-599.

John, David E., Stacey S. Patterson, and John H. Paul. 2007. Phytoplankton-group specific quantitative polymerase chain reaction assays for RuBisCO mRNA transcripts in seawater. *Marine Biotechnology* 9:747-759.

John, David E., Jose M. Lopez-Diaz, Alvaro Cabrera, and Nelson A. Santiago. 2012. A day in the life in the dynamic marine environment: how nutrients shape diel patterns of phytoplankton photosynthesis and carbon fixation gene expression in the Mississippi and Orinoco River plumes. *Hydrobiologia* 679:155-173.

Johnson, Gregory C., Michael J. McPhaden, and Eric Firing. 2001. Equatorial Pacific Ocean horizontal velocity, divergence and upwelling. *American Meterological Society* 31:839-849.

Karl, D., R. Letelier, L. Tupas, J. Dore, J. Christian, and D. Hebel. 1997. The role of nitrogen fixation in biogeochemical cycling in the subtropical North Pacific Ocean. *Nature* 388.

Karl, David M., Matthew J. Church, John E. Dore, Ricardo M. Letelier, and Claire Mahaffey. 2012. Predictable and efficient carbon sequestration in the North

Pacific Ocean supported by symbiotic nitrogen fixation. *Proc. Natl. Acad. Sci. USA* 109 (6):1842-1849.

Karner, Markus B., Edward F. DeLong, and David M. Karl. 2001. Archaeal dominance in the mesopelagic zone of the Pacific Ocean. *Nature* 409:507-509.

Kirchman, David L. 2008. *Microbial Ecology of the Oceans*. Edited by D. L. Kirchman. 2nd Edition ed: John Wiley & Sons, Inc.

Kline Jr., Thomas C. 1999. Temporal and spatial variability of $^{13}C/^{12}C$ and $^{15}N/^{14}N$ in pelagic biota of Prince William Sound Alaska. *Canadian Journal of Fisheries and Aquatic Sciences* 56 (1):94-117.

Kline Jr., Thomas C. 2009. Characterization of carbon and nitrogen stable isotope gradients in the northern Gulf of Alaska using terminal feed stage copeopdite-V *Neocalanus cristatus*. *Deep Sea Research II* 56:2537-2552.

Kline Jr., Thomas C. 2010. Stable carbon and nitrogen isotope variation in the northern lampfish and *Neocalanus*, marine survival rates of pink salmon, and meso-scale eddies in the Gulf of Alaska. *Progress In Oceanography*.

Knap, A. H., A. Michaels, A. Close, H. W. Ducklow, and A. Dickson. "Protocols for the joint global flux study (JGOFS) core measurements." *JGOFS, Reprint of the IOC Manuals and Guides No. 29, UNESCO 1994* 19 (1996).

Kolber, Zbigniew S., and Paul G. Falkowski. 1993. Use of active fluorescence to estimate phytoplankton photosynthesis *in situ*. *Limnology and Oceanography* 38 (8):1646-1665.

Kolber, Zbigniew S., Ondrej Pra¨sil, and Paul G. Falkowski. 1998. Measurements of variable chlorophyll fluorescence using fast repetition rate techniques: defining methodology and experimental protocols. *Biochimica et Biophysica Acta* 1367:88-106.

Laws, Edward A., Paul G. Falkowski, Walker O. Smith Jr., Hugh Ducklow, and James J. McCarthy. 2000. Temperature effects on export production in the open ocean. *Global Biogeochemical Cycles* 14 (4):1231-1246.

Laws, Edward A., Eurico D'Sa, and Puneeta Naik. 2011. Simple equations to estimate ratios of new or export production to total production from satellite-derived estimates of sea surface temperature and primary production. *Limnology and Oceanography: Methods* 9:593-601.

Lee, O. A., P. Olivier, R. Wolt, R. W. Davis, and F. Weltz. 2009. Aggregations of Sea Otters (*Enhydra litris kenyoni*) feeding of fish eggs and kelp in Prince William Sound, Alaska. *American Midland Naturalist* 161 (2):401-405.

Lee, J. H. W., T. Katano, M. Chang, and M-S Han. 2012. Application of tyramide signal amplification-fluorescence in situ hybridization and flow cytometry to detection of *Heterosigma akashiwo* (Raphidophyceae) in natural waters. *New Zealand Journal of Marine and Freshwater Research* 46 (1):137-148.

Lefort, Thomas, and Josep M. Gasol. 2013. Global-scale distributions of marine surface bacterioplankton groups along gradients of salinity, temperature, and chlorophyll: a meta-analysis of fluorescence in situ hybridization studies. *Aquatic Microbial Ecology* 70 (2):111-130.

Legendre, Louis, and Richard B. Rivkin. 2002. Fluxes of carbon in the upper ocean: regulation by food-web control nodes. *Marine Ecology Progress Series* 242:95-109.

Leroux, Shawn J., and Michael Loreau. 2008. Subsidy hypothesis and strength of trophic cascades across ecosystems. *Ecology Letters* 11:1147-1156.

Lewis, Marlon R., and John C. Smith. 1983. A small volume, short-incubation-time method for measurement of photosynthesis as a function of incident irradiance. *Marine Ecology Progress Series* 13:99-102.

Longhurst, Alan R., and W. Glen Harrison. 1989. The biological pump: Profiles of plankton production and consumption in the upper ocean. *Progress In Oceanography* 22 (1):47-123.

Lomas, M. W., D. K. Steinberg, T. D. Dickey, C. A. Carlson, Nelson N. B., R. H. Condon, and N. R. Bates. 2010. Increased ocean carbon export in the Sargasso Sea linked to climate variability is countered by its enhanced mesopelagic attenuation. *Biogeosciences* 7:57-70.

Lomas, Michael W., Deborah Bronk, A., and Ger van den Engh. 2011. Use of flow cytometry to measure biogeochemical rates and processes in the ocean. *Annual Review of Marine Science* 3:537-566.

Lumpkin, Rick, and Gregory C. Johnson. 2013. Global ocean surface velocities from drifters: mean, variance El Niño-Southern Oscillation response, and seasonal cycle. *Journal of Geophysical Research* 118:2992-3006.

Luz, Boaz, and Eugeni Barkan. 2000. Assessment of oceanic productivity with the triple-isotope composition of dissolved oxygen. *Science* 288:2028-2031.

Lynn, Ronald J., and James J. Simpson. 1987. The California Current system: the seasonal variability of its physical characteristics. *Journal of Geophysical Research* 92 (C12):12947-12966.

Marie, Dominique, Frederic Partensky, Stephan Jacquet, and Daniel Vaulot. 1997. Enumeration and cell cycle analysis of natural populations of marine picoplankton by flow cytometry using the nucleic acid stain SYBR Green I. *Applied and Environmental Microbiology* 63 (1):186-193.

Martin, J. H., G. A. Knauer, D. M. Karl, and W. W. Broenkow. 1987. VERTEX: carbon cycling in the northeast Pacific. *Deep Sea Research I* 34 (2):267-285.

Martin-Nieto, Jose, Antonia Herrero, and Enrique Flores. 1991. Control of nitrogenase mRNA levels by products of nitrate assimilation in the cyanobacterium *Anabena* sp. Strain PCC 7120. Plant Physiology 97:825-828.

McDonnell, Andrew M. P., and Ken O. Buesseler. 2010. Variability in the average sinking velocity of marine particles *Limnology and Oceanography* 55 (5):2085-2096.

Michaels, A. F., N. R. Bates, K. O. Buesseler, C. A. Carlson, and A. H. Knap. 1994. Carbon-cycle imbalances in the Sargasso Sea. *Nature* 372 (6506):537-539.

Millero, F. J. 1996. *Chemical Oceanography*. Second ed: CRC Press LLC.

Mohr, Wiebke, Tobias Grobkopf, Douglas W. R. Wallace, and Julie LaRoache. 2010. Methodological underestimation of oceanic nitrogen fixation rates. *PLoS One* 5 (9):1-7.

Monteiro, F. M., S. Dutkiewicz, and M. J. Follows. 2011. Biogeographical controls on the marine nitrogen fixers. *Global Biogeochemical Cycles* 25:1-8.

Montoya, J. P., M. Voss, P. Kahler, and D. Capone. 1996. A simple, high-precision, high-sensitivity tracer assay for N_2 fixation. *Applied and Environmental Microbiology* 62 (3):986-993.

Montoya, Joseph P., Carolyn M. Holl, Jonathan P. Zehr, Andrew Hansen, Tracy A. Villareal, and Douglas G. Capone. 2004. High rates of N_2 fixation by unicellular diazotrophs in the oligotrophic Pacific Ocean. *Nature* 430.

Moore, C. M., M. M. Mills, K. R. Arrigo, I. Berman-Frank, L. Bopp, P. W. Boyd, E. D. Galbraith, R. J. Geider, C. Guieu, S. L. Jaccard, T. D. Jickells, J. LaRoache, T.M. Lenton, N. M. Mahowald, E. Maranon, I. Marinov, J. K. Moore, T. Nakatsuka, A. Oschlies, M. A. Saito, T. F. Thingstad, A. Tsuda, and O. Ulloa. 2013. Processes and patterns of oceanic nutrient limitation. *Nature geoscience* 6:701-710.

Murray, James W., Jennifer Young, Jan Newton, John Dunne, Thomas Chapin, Barbara Paul, and James J. MacCarthy. 1996. Export flux of particulate organic carbon from the central equatorial Pacific determined using a combined drifting trap-^{234}Th approach. *Deep Sea Research II* 43 (4-6):1095-1132.

Murrell, Michael C., and Emile M. Lores. 2004. Phytoplankton and zooplankton seasonal dynamics in a subtropical estuary: importance of cyanobacteria. *Journal of Plankton Research* 26 (3):371-382.

NASA Ocean Motion (OM) 2011. Last accessed *05 April 2011.* http://oceanmotion.org/html/help/credits.htm

Neess, John C., Richard C. Dugdale, Vera A. Dugdale, and John J. Goering. 1962. Nitrogen metabolism in lakes I. Measurement of nitrogen fixation with N^{15}. *Limnology and Oceanography* 7 (2):163-169.

Noll, Christian J., Timothy M. Dellapenna, Andrea Gilkinson, and Randall W. Davis. 2009. A high-resolution geophisical investigation of sediment distribution controlled by catchment size and tides in a multi-basin turbid outwash fjord: Simpson Bay, Prince William Sound, Alaska. *Geo-Marine Letters* 29 (1):1-16.

Nonaka, Masami, Hideharu Sasaki, Bunmei Taguchi, and Hisashi Nakamura. 2012. Potential predictability of interannual variability in the Kuroshio Extension Jet speed in an eddy-resolving OGCM. *American Meterological Society* 25:3645-3652.

Norcross, B. L., E. D. Brown, R. J. Foy, M. Frandsen, S. M. Gay, Jr. Kline, T. C., D. M. Mason, E. V. Patrick, A. J. Paul, and K. D. E. Stokesbury. 2001. A synthesis of the life history and ecology of juvenile Pacific herring in Prince William Sound, Alaska. *Fisheries Oceanography* 10 (1):42-57.

Okasanen, J., F. G. Blanchet, R. Kindt, Legendre P., Minchin P. R. O'Hara R. B., G. L. Simpson, Solymos P., M. H. H. Stevens, and H. Wagner. 2011. Vegan:

Community Ecology Package. R package version 2.0-2.http://CRAN.R-project.org/package=vegan.

Paul, J. H. 1996. Carbon cycling: molecular regulation of photosynthetic carbon fixation. *Microbial Ecology* 32:231-245.

Paul, John H., Jordan B. Kang, and F. Robert Tabita. 2000. Diel patterns of regulation of *rbcL* transcription in a cyanobacterium and a prymnesiophyte. *Marine Biotechnology* 2:429-436.

Partensky, F., J. Blanchot, and D. Vaulot. 1999. Differential distribution and ecology of *Prochlorococcus* and *Synechococcus* in oceanic waters: a review. *Bulletin de l'Institut Oceanographique* special 19:457-475.

Pernthaler, Jakob, Frank Oliver Glockner, Wilhelm Schonhuber, and Rudolf Amann. 2001. Fluorescence *in situ* hybridization In *Methods in Microbiology:Marine Microbiology*, edited by J. Paul: Academic Press Ltd, London.

Pernthaler, Annelie, Jakob Pernthaler, and Rudolf Amann. 2002. Fluorescence *in situ* hybridization and catalyzed reporter deposition for the identification of marine bacteria. *Applied and Environmental Microbiology* 68 (6):3094-3101.

Pernthaler, A., and R. Amann. 2004. Simultaneous fluorescence *in situ* hybridization of mRNA and rRNA in environmental bacteria. *Applied and Environmental Microbiology* 70 (9):5426-5433.

Pernthaler, Annelie, Jakob Perenthaler, and Rudolf Amann. 2004. Sensitive multi-color fluorescence in situ hybridization for the identification of environmental

microorganisms. In *Molecular Microbial Ecology Manual*: Kluwer Academic Publishers.

Pershing, Andrew J., Line B. Christensen, Nicholas R. Record, Graham D. Sherwood, and Peter B. Stetson. 2010. The impact of whaling on the ocean carbon cycle: why bigger was better. *PloS One* 5 (8).

Petticrew, Ellen L., John F. Rex, and Sam J. Albers. 2011. Bidirectional delivery of organic matter between freshwater and marine systems: the role of flocculation in Pacific salmon streams. *Journal North American Benthological Society* 30 (3):779-786.

Pickard, George L., and William J. Emery. 1990. *Descriptive Physical Oceanography: An Introduction*. Woburn, MA: Butterworth-Heinemann.

Pilhofer, Martin, Marko Pavlekovic, Natuschka M. Lee, Wolfgang Ludwig, and Karl-Heinz Schleifer. 2009. Fluorescence *in situ* hybridization for intracellular localization of *nifH* mRNA. *Systematic and Applied Microbiology*.

Pilskaln, Cynthia H., Charlotte Lehmann, Jennifer B. Paduan, and Mary W. Silver. 1998. Spatial and temporal dynamics in marine aggregate abundance, sinking rate and flux: Monterey Bay, central California. *Deep Sea Research Part II: Topical Studies in Oceanography* 45 (8-9):1803-1837.

Polis, Gary A., Wendy B. Anderson, and Robert D. Holt. 1997. Toward an integration of landscape and food web ecology: the dynamics of spatially subsidized food webs. *Annual Review of Ecology and Systematics* 28:289-316.

Polovina, Jeffrey J., Evan A. Howell, and Melanie Abecassis. 2008. Ocean's least productive waters are expanding. *Geophysical Research Letters* 35:1-5.

Pomeroy, Lawrence R., and Don Deibel. 1986. Temperature regulation of bacterial activity during the spring bloom in Newfoundland coastal waters. *Science* 233 (4761):356-361.

Powers, Sean P., Mary Anne Bishop, and Erika Clesceri. 2005. Characterization of energy and potential contaminant pathways in subarctic estuarine habitats: ecology of tidal flat communities of the Copper River Delta, Alaska. In *Final Report to the Prince William Sound Regional Citizens Advisory Council*. Prince William sound Science Center.

Pickard, George L., and William J. Emery. 1990. *Descriptive Physical Oceanography: An Introduction*. Woburn, MA: Butterworth-Heinemann.

Prichard, S. L., L. Campbell, Kendall L. Carder, J. B. Kang, J. Patch, F. Robert Tabita, and John Paul, H. 1997. Analysis of ribulose bisphosphate carboxylase gene expression in natural phytoplankton communities by group-specific gene probing. *Marine Ecology Progress Series* 149:239-253.

Quigg, Antonietta, J. B. Sylvan, A. B. Gustafson, T. R. Fisher, S. Tozzi, and J. W. Ammerman. 2011. Going west: phosphorus limitation of primary production in the northern Gulf of Mexico and the importance of the Atchafalaya River. *Aquatic Geochemistry* 17:519-544.

Quigg, Antonietta, Clifton C. Nunnally, Allison S. McInnes, Shelton Gay, Gilbert T. Towe, Timpthy M. Dellapenna, and Randall W. Davis. 2013. Hydrographic and

biological controls in two subarctic fjords: an environmental case study of how climate change could impact phytoplankton communities. *Marine Ecology Progress Series* 480:21-37.

Quigg, Antonietta, Mohsin Al-Ansi, Nehad Nour Al Din, Chih-Lin Wei, Clifton C. Nunnally, Ibrahim S. Al-Ansari, Gilbert T. Rowe, Yousria Soliman, Ibrahim Al-Maslamani, Ismail Mahmoud, Nabiha Youssef, and Mohamed A. Abdel-Moati. 2013b. Phytoplankton along the coastal shelf of an oligotrophic hypersaline environment in a semi-enclosed marginal sea: Qatar (Arabian Gulf). *continental Shelf Research* 60 (1):1-16.

Redfield, A. C. 1958. The biological control of chemical factors in the environment. *American Scientist* 46:205-221.

Reisinger, Alexander J., Dominic T. Chaoner, Jeanine Ruegg, Scott D. Tiegs, and Gary A. Lamberti. 2013. Effects of spawning Pacific salmon on the isotopic composition of biota differ among southeast Alaska streams. *Freshwater Biology* 58:938-950.

Richardson, P. L., and G. Reverdin. 1987. Seasonal cycle of velocity in the Atlantic North Equatorial Countercurrent as measured by surface drifters, current meters, and ship drifts. *Journal of Geophysical Research* 92 (C4):3691-3708.

Richardson, T. L., and G. A. Jackson. 2007. Small phytoplankton and carbon export from the surface ocean. *Science* 315:838-840.

Robinson, Carol, Deborah K. Steinberg, Thomas R. Anderson, Javier Aristegui, Craig A. Carlson, Jessica R. Frost, Jean-Francois Ghiglione, Santiago Hernandez-Leon,

George A. Jackson, Rolf Koppelmann, Bernard Queguiner, Olivier Ragueneau, Fereidoun Rassoulzadegan, Bruce H. Robinson, Christian Tamburini, Tsuneo Tanaka, Karen F. Wishner, and Jing Xhang. 2010. Mesopelagic zone ecology and biogeochemistry - a synthesis. *Deep Sea Research II* 57:1504-1518.

Roper, Christopher N., Lewis J. Haldorson, and Terrance J. Quinn II. 1999. Habitat factors controlling Pacific herring (*clupea pallasi*) egg loss in Prince William Sound, Alaska. *Canadian Journal of Fisheries and Aquatic Sciences* 56:1133-1142.

Sabine, Christopher L., Richard A. Feely, Nicolas Gruber, Robert M. Key, Kitack Lee, John L. Bullister, Rik Wanninkhof, C. S. Wong, Douglas W. R. Wallace, Bronte Tilbrook, Frank J. Millero, Tsung-Hung Peng, Alexander Kozyr, Tsueno Ono, and Aida F. Rios. 2004. The oceanic sink for anthropogenic CO_2. *Science* 305:367-371.

Sakamoto, Kei, Hiroyuki Tsujino, Shiro Nishikawa, Hideyuki Nakano, and Tatsuo Motoi. 2010. Dynamics of the coastal Oyashio and its seasonal variation in a high-resolution Western North Pacific Ocean model. *American Meterological Society* 40:1283-1301.

Santschi, P. H., J. W. Murray, M. Baskaran, C. R. Benitez-Nelson, L. D. Guo, C.-C. Hung, C. H. Lamborg, S. B. Moran, U. Passow, and M. Roy-Barman. 2006. Thorium speciation in seawater. *Marine Chemistry* 100:250-268.

Sarmiento, J. L., R. Murnane, and C. Le Quere. 1995. Air-sea CO_2 transfer and the carbon budget of the North Atlantic. *Phil. Trans. R. Soc. Lond.* 348:211-219.

Shannon, L. V. 1985. The Benguela Ecosystem, I. Evolution of the Benguela, physical features and processes. *Oceanography and Marine Biology* 23:105-182.

Sekar, Raju, Bernhard M. Fuchs, Rudolf Amann, and Jakob Pernthaler. 2004. Flow sorting of marine bacterioplankton after fluorescence *in situ* hybridization. *Applied and Environmental Microbiology* 70 (10):6210-6219.

Siegel, David A., Timothy C. Granata, Anthony F. Michaels, and Tommy D. Dickey. 1990. Mesoscale eddy diffusion, particle sinking, and the interpretation of sediment trap data. *Journal of Geophysical Research* 95 (C4):5305-5311.

Siegel, D. A., and W. G. Deuser. 1997. Trajectories of sinking particles in the Sargasso Sea: modeling of statistical funnels above deep-ocean sediment traps. *Deep Sea Research Part I: Oceanographic Research Papers* 44 (9-10):1519-1541.

Siegel, D. A., E. Fields, and K. O. Buesseler. 2008. A bottom-up view of the biological pump: Modeling source funnels above ocean sediment traps. *Deep Sea Research I* 55:108-127.

Smayda, Theodore J. 1971. Normal and accelerated sinking of phytoplankton in the sea. *Marine Geology* 11 (2):105-122.

Steeman-Nielsen, E. 1952. Use of radioactive carbon (C^{14}) for measuring organic production in the sea. *Journal du Consiel* 18:117-140.

Subramaniam, Ajit, Christopher W. Brown, Raleigh R. Hood, Edward J. Carpenter, and Douglas G. Capone. 2002. Detecting *Trichodesmium* blooms in SeaWiFS imagery. *Deep Sea Research Part II: Topical Studies in Oceanography* 49 (1-3):107-121.

Sweeney, Erin, N., Dennis J. McGillicuddy Jr., and Ken O. Buesseler. 2003. Biogeochemical impacts due to mesoscale eddy activity in the Sargasso Sea as measured at the Bermuda Atlantic Time-series Study (BATS). *Deep Sea Research II* 50:3017-3039.

Sylvan, J. B., Quay Dortch, D. M. Nelson, A. F. Maier Brown, W. Morrison, and J. W. Ammerman. 2006. Phosphorus limits phytoplankton growth on the Louisiana Shelf during the period of hypoxia formation. *Environmental Science and Technology* 40:7548-7553.

Trull, T. W., S. G. Bray, K. O. Buesseler, C. H. Lamborg, S. Manganini, C. Moy, and J. Valdes. 2008. *In situ* measurement of mesopelagic particle sinking rates and the control of carbon transfer to the ocean interior during the Vertical Flux in the Global Ocean (VERTIGO) voyages in the North Pacific. *Deep Sea Research II* 55:1684-1695.

Turner, Jefferson T. 2002. Zooplankton fecal pellets, marine snow and sinking phytoplankton blooms. *Aquatic Microbial Ecology* 27:57-102.

Tyrell, Toby. 1999. The relative influences of nitrogen and phosphorus on oceanic primary production. *Nature* 400:525-531.

Varpe, Oystein, Oyvind Filksen, and Aril Slotte. 2005. Meta-ecosystems and biological energy transport from ocean to coast: the ecological importance of herring migration. *Oecologia* 146:443-451.

van de Corput, Mariette P.C., Roeland W. Dirks, Rob P. M. vanGijlswijk, Erca van Binnendijk, Claudia M. Hattinger, Roelof A. de Paus, Jim E. Landegent, and

Anton K. Raap. 1998. Sensitive mRNA detection by fluorescence *in situ* hybridization using horseradish peroxidase-labeled oligonucleotides and tyramide signal amplification. *Journal of Histochemistry and Cytochemistry* 46 (11):1249-1259.

Vitousek, Peter M., and Robert W. Howarth. 1991. Nitrogen limitation on land and in the sea: How can it occur? *Biogeochemistry* 13:87-115.

Volk, T., and M. I. Hoffert. 1985. *Ocean carbon pumps-Analysis of relative strengths and efficiencies in ocean-driven atmospheric CO2 changes*.

von Bodungen, B., A. Antia, E. Bauerfeind, O. Haupt, W. Koeve, E. Machado, I. Peeken, R. Peinert, S. Reitmeier, C. Thomsen, M. Voss, M. Wunsch, U. Zeller, and B. Zeitzschel. 1995. Pelagic processes and vertical flux of particles: an overview of a long-term comparative study in the Norwegian Sea and Greenland Sea. *Geol Rundsch* 84:11-27.

Waite, Anya M., and Paul S. Hill. 2006. Flocculation and phytoplankton cell size can alter ^{234}Th-based estimates of the vertical flux of particulate organic carbon in the sea. *Marine Chemistry* 100:366-375.

Waite, A. M., B. A. Muhling, C. M. Holl, L. E. Beckley, J. P. Montoya, J. Strzelecki, P. A. Thompson, and S. Pesant. 2007. Food web structure in two counter-rotating eddies based on δ^{15}N and δ^{13}C isotopic analyses. *Deep Sea Research II* 54:1055-1075.

Waite, Anya M., Lars Stemmann, Andrew McC. Hogg, Ming Feng, Lionel Guidi, Peter A. Thompson, Marc Piceral, and Gaby Gorsky. In Review. The Wine-Glass

Effect concentrates particle export and biogeochemical fluxes in an ocean vortex. *Proc. Natl. Acad. Sci. USA*.

Wallner, Gunter, Rudolf Amann, and Wolfgang Beisker. 1993. Optimizing fluorescent *in situ* hybridization with rRNA-targeted oligonucleotide probes for flow cytometric identification of microorganisms. *Cytometry* 14:136-143.

Warwrik, B., J. H. Paul, and F. R. Tabita. 2002. Real-time PCR quantification of *rbcL* (Ribulose-1,5-Bisphosphate Carboxylase/Oxygenase) mRNA in diatoms and pelagophytes. *Applied and Environmental Microbiology* 68 (8):3771-3779.

Weber, Michael J., and Michael L. Brown. 2013. Continuous, pulsed and disrupted nutrient subsidy effects on ecosystem productivity, stability, and energy flow. *Ecosphere* 4 (2):1-13.

Whitaker D, Christman M (2010) Clustsig: Significant Cluster Analysis. R package version 1.0. http://CRAN.R-project.org/package=clustsig.

Wild, C., C. Jantzen, U. Struck, O. Hoegh-Guldberg, and M. Huettel. 2008. Biogeochemical responses following coral mass spawning on the Great Barrier Reef: pelagic-benthic coupling. *Coral Reefs* 27:123-132.

Willson, Mary F., and Jamie N. Womble. 2006. Vertebrate exploitation of pulsed marine prey: a review and the example of spawning herring. *Rev Fish Biol Fisheries* 16:183-200.

Wilson, S. E., D. K. Steinberg, and K. O. Buesseler. 2008. Changes in fecal pellet characteristics with depth as indicators of zooplankton repackaging of particles in the mesopelagic zone of the subtropical and subarctic North Pacific Ocean.

Deep-Sea Research Part II-Topical Studies in Oceanography 55 (14-15):1636-1647.

Wipfli, M. S., J. Hudson, and J. Caouette. 1998. Influence of salmon carcasses on stream productivity: response of biofilm and benthic macroinvertebrates in southeastern Alaska, U.S.A. *Canadian Journal of Fisheries and Aquatic Sciences* 55:1503-1511.

Wyman, Michael. 1999. Diel Rhythms in Ribulose-1,5-Bisphosphate Carboxylase/Oxygenase and glutamine synthetase gene expression in a natural population of marine picoplanktonic cyanobacteria (*Synechococcus* spp.). *Applied and Environmental Microbiology* 65 (8):3651-3659.

Yan, Fengting, Xin Wu, Melissa Crawford, Wenrui Duan, Emily E. Wilding, Li Gao, Nana-Sinkam, Miguel A. Villalona-Calero, Robert A. Baiocchi, and Gregory A. Otterson. 2010. The search for an optimal DNA, RNA, and protein detection by *in situ* hybridization, immunohistochemistry, and solution-based methods. *Methods* 52:281-286.

Yang, Louie H., Justin L. Bastow, Kenneth O. Spence, and Amber N. Wright. 2008. What can we learn from resource pulses? *Ecology* 89 (3):621-634.

Yang, Louie H., Kyle F. Edwards, Jarrett E. Byrnes, Justin L. Bastow, Amber N. Wright, and Kenneth O. Spence. 2010. A meta-analysis of resource pulse-consumer interactions. *Ecological Monographs* 80 (1):125-151.

Yoshikawa, Takashi, and Ken Furuya. 2006. Effects of diurnal variations in phytoplankton photosynthesis obtained from natural fluorescence. *Marine Biology* 150:299-311.

Zehr, Jonathan P., Edward J. Carpenter, and Tracey A. Villareal. 2000. New perspectives on nitrogen-fixing microorganisms in tropical and subtropical oceans. *Trends in Microbiology* 8 (2):68-73.

Zehr, Jonathan P. , John B. Waterbury, Patricia J. Turner, Joseph P. Montoya, Enoma Omoregie, Grieg F. Steward, Andrew Hansen, and David M. Karl. 2001. Unicellular cyanobacteria fix N_2 in the subtropical North Pacific Ocean. *Nature* 412:635-638.

Zehr, Jonathan P., Bethany D. Jenkins, Steven M. Short, and Grieg F. Steward. 2003. Nitrogenase gene diversity and microbial community structure: a cross-system comparison. *Environmental Microbiology* 5 (7):539-554.

APPENDIX A

TABLES

Table A1: Literature values of size and settling velocities for various particles with calculated theoretical horizontal distance carried (2000 m depth) under two different current velocities (CV).

Species/Group	Size (μm)	Settling Velocity (m day^{-1})	Horizontal distance carried (km) CV 21600 m day^{-1}	CV 48000 m day^{-1}	Reference
Monochrystis lutherii	2.95	0.18	239628	533331	Eppley et al. 1967
Cyclotella nana	3.35	0.16	269419	599987	
Dunallelia teritiolecta	4.3	0.39	110761	246153	
Coccolithus huxleyi, bald	5.2	0.28	153835	342852	
Coccolithus huxleyi	6.5	1.30	33228	73844	
Cricosphaera elongata	8	0.25	171871	383994	
Rhizosolenia setigera	123	0.18	239628	533331	
Thalassiosira rotula	15	0.43	100287	223258	
Ditylum brightwellii	42.5	0.60	71716	159999	
Rhizosolenia stolterfohii	63	1.01	42968	95049	
Coscinodiscus sp. Clone AD	21.5	1.96	22054	48980	
Gonyaulax polyedra	23.5	2.81	15384	34164	
Coscinodiscus sp. empty cell wall	35	14.43	2994	6653	
Ditylum resting spore	63.8	8.02	5388	11970	
Coscinodiscus wailesii	70	7.02	6153	13675	
Chaetoceros didymus	8.5	0.53	81253	181132	
Thalassiosira fulviatilis	18	0.60	71773	159999	
Skrletonema costatum	18	0.33	130497	290908	
Chaetoceros lauderii	35	0.50	86128	192000	
Bacteriastrum hyalinum	25	0.43	100149	223258	
Fecal Pellets	90	194.22	222	494	Smayda, 1971
	100	239.92	180	400	
	135	111.96	386	857	
	150	82.26	525	1167	
	150	102.82	420	934	
	170	111.96	386	857	
	210	84.54	511	1136	
Aggregates	750	17.25	2505	5565	Pilskaln et al. 1998
	1500	29.44	1468	3261	
	2500	36.42	1186	2636	
	3500	26.71	1617	3594	
	4500	31.65	1365	3033	

FIGURES

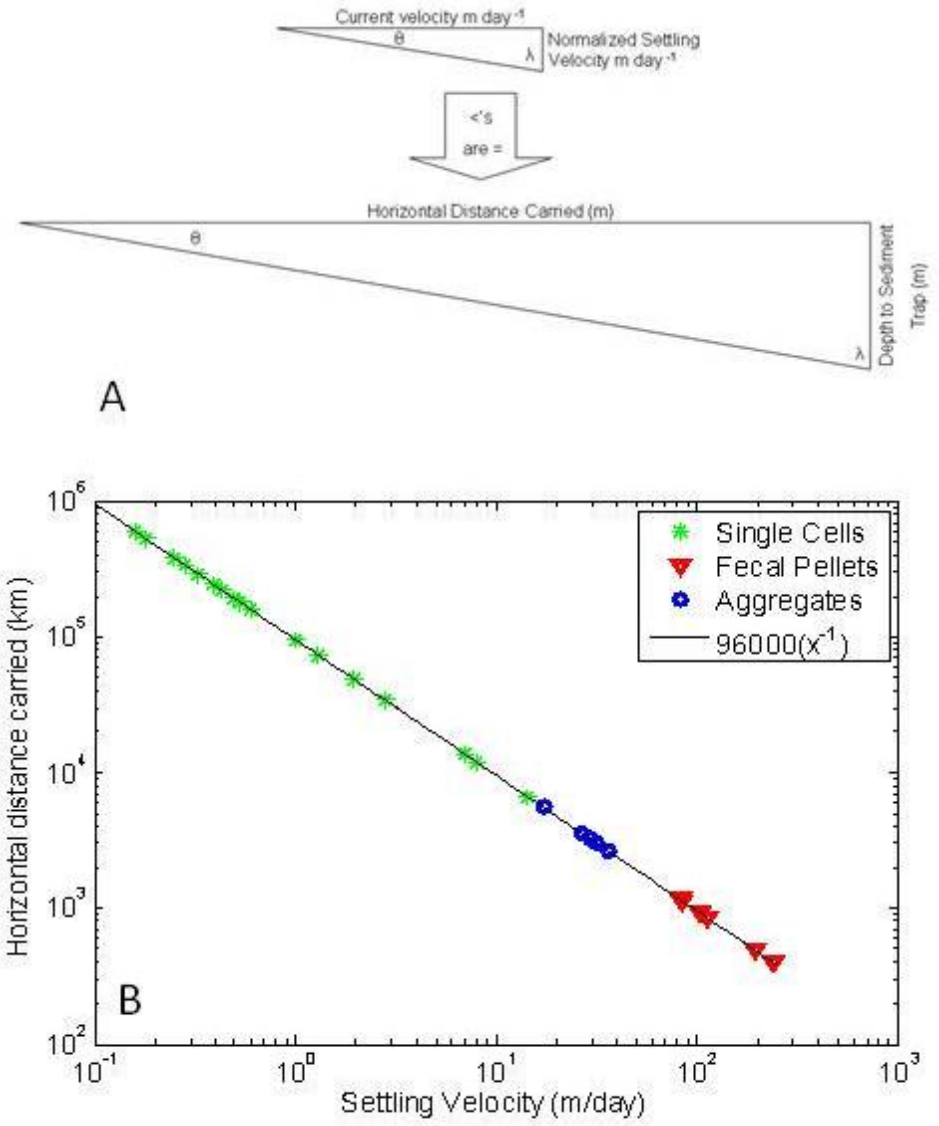

Figure A1: Regression of calculated horizontal distance carried versus the settling velocity of single cells, fecal pellets and aggregates. Horizontal distance carried was calculated using the laws of similar triangles and vector addition (A); by relating the two vectors: current velocity (m day^{-1}) and normalized settling velocity (m day^{-1}) the second set of horizontal distance carried (km) relates in the same way to the depth of the sediment trap (km). Log log plot of this calculated horizontal distance carried versus settling velocity (B) yields a simplified model generated from the regression (B).

APPENDIX B

TABLES

Table B1. Target sequences *rbcL* probe. Conserved regions of *rbcL* were chosen targets of oligonucleotide probes and corresponding probe sequences. Below is a compilation of conserved region of *rbcL* gene for an array of target species. Dashes represent matched bases, if there is a mismatch between the target and the probe the base present in the target sequence is displayed; % refers to the mismatch percentage, # is the number of sequences for each species. Horseradish peroxidase was attached directly to the 5‘ end of the oligonucleotide probe to reduce potential background fluorescence.

Probe	3' CTR	CTR	CTT	TTR	YAD	TTG	AG 5' HRP		
Target	5' GAY	GAY	GAA	AAY	RTH	AAC	TC 3'	%	#
Amphora sp	- - -	- - -	- - -	- - -	- - -	- - -	- -		6
Chaetoceros sp	- - -	- - -	- - -	- - -	- - -	- - -	- -		11
Chlamydomonas sp	- - -	- - -	- - -	- - -	- - -	- - -	- -		
Chlorella vulgaris	- - -	- - -	- - -	- - -	- - -	- - -	- -		
Cryptomonas paramecium	- - -	- - -	- - -	- - -	- - -	- - T	- -	5	
Cyanothece sp	- - -	- - -	- - -	- - -	- - -	- - -	- -		3
Dunaliella sp	- - -	- - -	- - -	- - -	- - -	- - -	- -		18
Emiliania huxleyi	- - -	- - -	- - G	- - -	- - -	- - -	- -	5	3
Gracilaria sp	- - -	- - -	- - -	- - -	- - -	- - -	- -		
Heterosigma akashiwo	- - -	- - -	- - G	- - -	- - -	- - -	- -	5	2
Microcystis aeruginosa	- - -	- - -	- - -	- - -	- - -	- - -	- -		
Navicula sp	- - -	- - -	- - -	- - -	- - -	- - -	- -		2
Odontella sp	- - -	- - -	- - -	- - -	- - -	- - -	- -		12
Phaeodactylum tricomutum	- - -	- - -	- - G	- - -	- - -	- - -	- -	5	4
Prochlorococcus marinus	- - -	- - -	- - G	- - -	- - -	- - -	- -	5	6
Pycnococcus provasolii	- - -	- - -	- - G	- - -	- - -	- - -	- -	5	
Pyramimonas parkeae	- - -	- - -	- - -	- - -	- - -	- - T	- -	5	
Rhodomonas salina	- - -	- - -	- - -	- - -	- - -	- - -	- -		
Skeletonema sp	- - -	- - -	- - -	- - -	- - -	- - -	- -		12
Scenedesmus obliquus	- - -	- - -	- - -	- - -	- - -	- - -	- -		
Synechococcus sp	- - -	- - -	- - -	- - -	- - -	- - -	- -		14
Thalassiosira sp	- - -	- - -	- - -	- - -	- - -	- - -	- -		8
Thermosynechococcus elongatus	- - -	- - -	- - -	- - -	- - -	- - -	- -		
Trichodesmium sp	- - -	- - -	- - -	- - -	- - -	- - -	- -		3

Table B2. Target sequences *nifH* probe. Conserved regions of *nifH* were chosen targets of oligonucleotide probes and corresponding probe sequences. Below is a compilation of conserved region of *nifH* gene for an array of target species. Dashes represent matched bases, if there is a mismatch between the target and the probe the base present in the target sequence is displayed; % refers to the mismatch percentage, # is the number of sequences for each species. Horseradish peroxidase was attached directly to the 5‘ end of the oligonucleotide probe to reduce potential background fluorescence.

Probe	3' CCA	CCA	GGA	GCC	GGA	CCA	5' HRP	
Target	5' GGT	GGT	CCT	GAG	CCT	GGT	3' %	#
Anabaena sp.	- - -	- - -	- - A	- - A	- - C	- - -	17	4
Pseudoanabaena PCC7403	- - -	- - -	- - C	- - A	- - A	- - G	22	1
Calothrix brevissima	- - -	- - -	- - A	- - A	- - -	- - -	11	12
Chlorogloeopsis	- - -	- - G	- - A	- - A	- - A	- - C	28	1
Cyanothece	- - -	- - -	- - -	- - -	- - -	- - -	0	13
UCYN-A	- - -	- - -	- - -	- - -	- - -	- - A	6	1
Dermocarpa	- - C	- - -	- - C	- - A	- - A	- - -	22	1
Fisherella UTEX1903	- - -	- - -	- - C	- - -	- - -	- - -	6	2
Lyngbya sp.	- - -	- - -	- - A	- - A	- - C	- - -	17	3
Leptolyngbya	- - C	- - C	- - A	- - A	- - C	- - -	28	1
Myxosarcina sp.	- - -	- - -	- - C	- - A	- - -	- - -	11	1
Nostoc sp.	- - -	- - C	- - -	- - A	- - C	- - C	22	9
Phormidium sp.	- - -	- - -	- - -	- - -	- - C	- - C	11	1
Richelia sp.	- - -	- - -	- - -	- - -	- - -	- - -	0	14
Scytonema	- - -	- - -	- - A	- - A	- - C	- - -	17	1
Synechocystis sp	- - -	- - -	- - -	- - -	- - -	- - A	6	4
Xenococcus sp.	- - -	- - -	- - C	- - A	- - -	- - -	11	1
Trichodesmium erythraeum	- - -	- - -	- - -	- - -	- - -	- - -	0	28
Azoarcus sp	- - C	- - -	- - G	- - A	- - C	- - C	28	1
Pectobacterium atrosepticm	- - -	- - C	- - A	- - -	- - G	- - C	22	1
Desulfitobacterium hafniense	- - C	- - C	- - G	- - A	- - G	- - -	28	1
Pseudomona stutzeri	- - C	- - -	- - G	- - -	- - G	- - C	22	1
Clostridium acetobutylicum	- - -	- - A	- - A	- - A	- - -	- - -	17	1
Rhodobacter sphaeroides	- - C	- - G	- - G	- - -	- - G	- - C	28	1
Rhodospirillum centenum	- - C	- - -	- - C	- - -	- - G	- - C	22	1
Azotobacter vinelandii	- - C	- - C	- - C	- - -	- - G	- - C	28	2
Clostridium kluyveri	- - A	- - A	- - -	- - -	- - -	- - C	17	1
Rhizobium etli	- - C	- - -	- - G	- - A	- - G	- - C	28	1
Methanococcus maripaludis	- - A	- - A	- - -	- - -	- - A	- - A	22	2
Rhodobacter sphaeroides	- - C	- - G	- - A	- - -	- - G	- - C	28	3
Rhodospirillum rubrum	- - -	- - -	- - G	- - -	- - C	- - C	17	2
Geobacter sulfurreducens	- - -	- - -	- - C	- - -	- - G	- - C	17	1
Gluconacetobacter diazotrophicus	- - C	- - G	- - G	- - -	- - C	- - C	28	1
Azospirillum sp	- - C	- - C	- - G	- - -	- - G	- - G	28	1
Desulfatibacillum alkenivorans	- - C	- - C	- - -	- - A	- - A	- - G	28	1

FIGURES

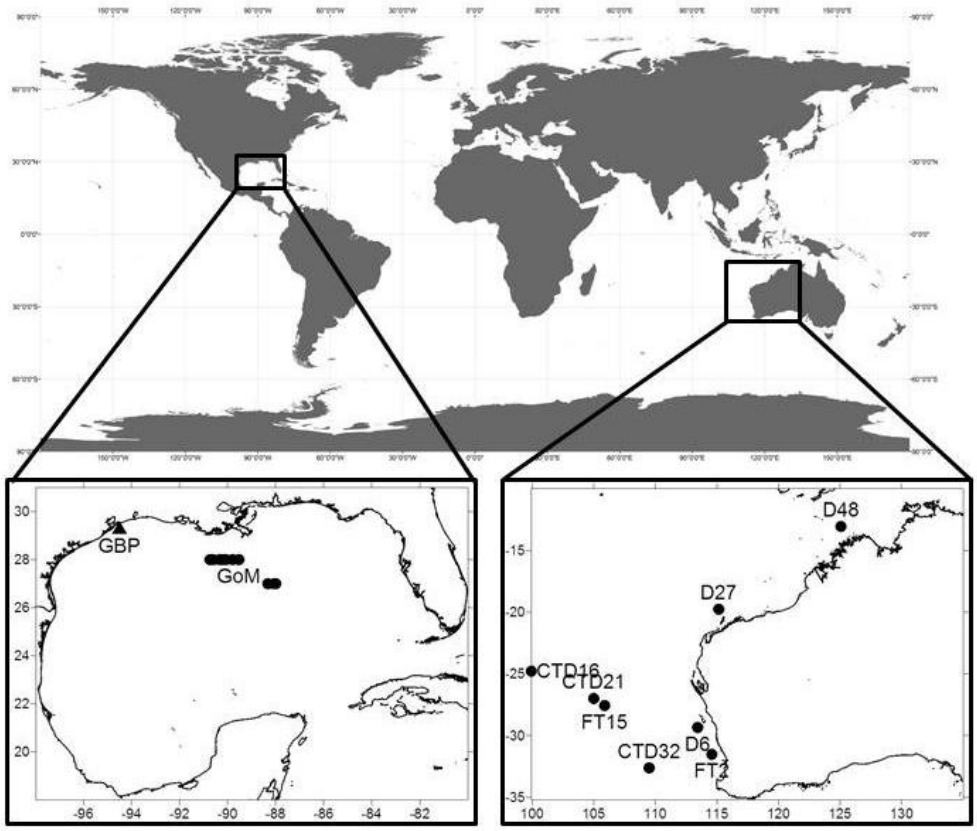

Figure B1: Locations of all environmental samples collected. Samples from the Gulf of Mexico (GoM) were combined into one homogeneous sample for optimization of *rbcL* and *nifH* assays. Coastal samples were collected from Galveston Bay (NW corner of GoM).Environmental samples for analysis of *nifH* mRNA expression versus ^{15}N uptake were collected in the eastern Indian Ocean during two cruises in August and September of 2012